Republic of Iraq

Ministry of Higher Education & Scientific Research

University of Kerbala

College of Engineering

Civil Engineering Department

Characteristics of Sustainable Reinforced Concrete Circular Columns Exposed to Sea Water

A Thesis Submitted to the College of Engineering/University of Kerbala in Partial Fulfillment of the Requirements for the Degree of Doctor of Philosophy in Civil Engineering/Infrastructure

By:

Abdulrasool Thamer Abdulrasool Qandeel

Supervised By:

Prof. Dr. Laith Shakir Rasheed Alqarawee

Assist Prof. Dr. Aymen Jameel Kadhim Al-Saad

July 2025 Muharram 1447

Republic of Iraq

Ministry of Higher Education & Scientific Research

University of Kerbala

College of Engineering

Civil Engineering Department

Characteristics of Sustainable Reinforced Concrete Circular Columns Exposed to Sea Water

A Thesis Submitted to the College of Engineering/University of Kerbala in Partial Fulfillment of the Requirements for the Degree of Doctor of Philosophy in Civil Engineering/Infrastructure

By:

Abdulrasool Thamer Abdulrasool Qandeel

Supervised By:

Prof. Dr. Laith Shakir Rasheed Alqarawee

Assist Prof. Dr. Aymen Jameel Kadhim Al-Saad

July 2025 Muharram 1447

بِسْمِ اللَّهِ الرَّحْمَٰنِ الرَّحِيمِ

﴿يَرْفَعِ اللَّهُ الَّذِينَ آمَنُوا مِنكُمْ وَالَّذِينَ أُوتُوا الْعِلْمَ دَرَجَاتٍ﴾

صدقَ اللهُ العليُّ العظيم

(المجادلة: من الآية 11)

Examination committee certification

We certify that we have read the thesis entitled "**Characteristics of Sustainable Reinforced Concrete Circular Columns Exposed to Sea Water**" and as an examining committee, we examined the student "**Abdulrasool Thamer Abdulrasool Qandeel**" in its content and in what is connected with it and that in our opinion it is adequate as a thesis for the degree of doctor of philosophy in civil engineering/infrastructure.

Supervisor

Signature:
Name :. Prof. Dr. Laith Shakir Rasheed
Date: / / 2025

Supervisor

Signature:
Name :. Assist. Prof. Dr. Aymen Jameel Kadhim
Date: / / 2025

Member

Signature:
Name :. Prof. Dr. Ali Hamid Nasser
Date: / / 2025

Member

Signature:
Name :. Prof Dr. Shatha Sadiq Hasan
Date: / / 2025

Member

Signature:
Name :. Assist. Prof. Dr. Ali Ghanim Abbas
Date: / / 2025

Member

Signature:
Name :. Assist. Prof. Dr. Wail Asim M. Hussain
Date: / / 2025

Chairman

Signature:
Name :. Prof. Dr. Adel A. Al-Azzawi
Date: / / 2025

Head of Civil Engineering Department

Signature:
Name : Assist. Prof. Dr. Aysar Tuama Al-Awadi
Date: / / 2025

Dean of the Engineering College

Signature:
Name :. Prof. Dr. Haider N. Azziz
Date: / / 2025

Supervisor certificate

I certify that the thesis entitled **"Characteristics of Sustainable Reinforced Concrete Circular Columns Exposed to Sea Water"** was prepared by **Abdulrasool Thamer Abdulrasool Qandeel** under our supervision at the Department of Civil Engineering, Faculty of Engineering, University of Kerbala as a partial of fulfilment of the requirements for the degree of doctor of philosophy in civil engineering/infrastructure.

Signature:

Prof. Dr. Laith Shakir Rasheed Alqarawee

Date: / / 2025

Signature:

Assist Prof. Dr. Aymen Jameel Kadhim Al-Saad

Date: / / 2025

Linguistic certificate

I certify that the thesis entitled " **Characteristics of Sustainable Reinforced Concrete Circular Columns Exposed to Sea Water** " which has been submitted by **Abdulrasool Thamer Abdulrasool Qandeel** has been proofread and its language has been amended to meet the English style.

Signature:

Assist. Prof. Dr. Hawra Mohamed Ali M.Taher

Date: / / 2025

Abstract

Reinforced concrete structures in marine environments face severe environmental challenges due to constant exposure to chloride and sulfate ions present in seawater, which contribute to concrete deterioration and accelerate the corrosion of reinforcing steel, reducing service life and increasing maintenance costs. To address this problem, research is directed toward developing sustainable concrete mixes using fine admixtures such as mineral powders and pozzolanic materials, which improve density, reduce permeability, and resist harmful chemical reactions.

This study aims to evaluate the performance of reinforced concrete columns made from mixes containing secondary materials that partially replace cement, such as glass powder, ceramic powder, and marble powder, as well as cement additives such as carbon black powder and graphite powder.

These materials were incorporated in the concrete mixes either as additives specifically carbon black and graphite powders at ratios of 0.5%, 1%, and 1.5% by weight of cement or as partial cement replacements, including glass, ceramic, and marble powders at replacement levels of 5%, 10%, and 15%. A total of sixteen concrete mixes were investigated in this study, comprising five different powder-based cement replacement materials, each tested at three replacement or additive ratios, in addition to a reference mix without any supplementary materials.

The tested specimens were subjected to a comprehensive experimental program that included mechanical, structural, and durability evaluations. Mechanical tests involved measuring compressive strength, splitting tensile strength, and density. Structural behavior was assessed through ultimate load capacity, ductility, and toughness indices. For durability assessment, the

specimens underwent chloride ion penetration testing, water permeability under pressure, and half-cell potential measurements to evaluate the likelihood of reinforcement corrosion. The structural tests were conducted on two groups of specimens: the first group was unexposed to corrosion, while the second group underwent accelerated corrosion through the application of an electric current.

The enhanced mixtures incorporating fine powders demonstrated a notable improvement in the structural capacity of concrete columns. The mixture containing 15% ceramic powder recorded the highest increase in ultimate load, with an improvement of 19.16% compared to the reference mix. This was followed by the glass powder mixture 10% with a 17.69% increase, graphite powder 0.5% with 11.69%, marble powder 10% with 11.36%, and finally carbon black 0.5% with an 8.93% increase. These results reflect the positive influence of the added powders in enhancing axial load resistance and improving the internal cohesion of concrete.

Under accelerated corrosion conditions, several modified mixtures exhibited a smaller reduction in ultimate load compared to the reference mix, which lost 19.6% of its structural capacity. The best performance in terms of durability was achieved by the graphite powder mix 0.5%, with only a 3.6% decrease in load capacity, followed by 0.5 % carbon black 3.73%, 10% marble powder 12.39%, 10% glass 16.69%, and 15% ceramic 18.64%. These findings highlight the effectiveness of certain powders, particularly graphite and carbon black, in mitigating the adverse effects of corrosion on structural behavior.

Several modified mixtures also showed reduced water permeability under pressure relative to the reference mix, indicating improved resistance to fluid and contaminant ingress. The 10% glass powder mixture exhibited the

highest reduction at 76.92%, followed by 15% ceramic powder 68.46%, 0.5% graphite powder 33%, 10% marble powder 31.54%, and 0.5% carbon black 24.62%. This improvement is attributed to both the physical and chemical roles of the powders in reducing porosity and enhancing particle packing.

Regarding chloride ion penetration resistance, all mixtures outperformed the reference mix, reflecting a positive impact on corrosion resistance. The graphite powder mix 0.5% achieved the greatest reduction in chloride ingress at 76.27%, followed by 0.5% carbon black 45.76%, 15% ceramic powder 34.58%, 10% marble powder 33.05%, and 10% glass powder 30.51%. These outcomes indicate that the powders, especially graphite powder, enhance reinforcement protection in chloride-rich environments.

The non-presentation of the remaining mixes does not imply poor performance; rather, the highlighted mixes demonstrated improvements across all tests, unlike the others, which showed either slight decreases or marginal improvements in certain aspects.

The study recommends selecting precise and well-thought-out additive ratios based on the physical and chemical properties of the materials while avoiding excessive use of highly conductive materials until their homogeneous distribution is ensured. It also emphasizes the importance of conducting a comprehensive assessment of mechanical and structural properties when designing concrete mixes intended for aggressive environments to ensure long-term performance sustainability.

Undertaking

I certify that research work titled "**Characteristics of Sustainable Reinforced Concrete Circular Columns Exposed to Sea Water**" is my own work. The work has not been presented elsewhere for assessment. Where material has been used from other sources it has been properly acknowledged / referred.

Signature:

Abdulrasool Thamer Abdulrasool

Date: / / 2025

Dedication

To those who instilled in my heart the love of knowledge and nourished my spirit with patience and faith, to those who have been my support and guide along the path of learning…

To my dear parents, the source of generosity and the beacon of wisdom, who provided me with endless support and were my companions throughout this journey…

To my dear sisters and brother, who have been my pillars of strength and support with their encouraging silence and constant presence, I am deeply grateful.

To my esteemed professors, who shared their knowledge and guidance with me, you have been the guiding lights that illuminated my path…

To my friends and colleagues, who have been my assistance and support throughout the research and the challenge…

To everyone who had an impact on my academic journey, I dedicate the fruits of this effort in gratitude and appreciation.

Signature: 

Abdulrasool Th. Abdulrasool

Date: / / 2025

Acknowledgements

First and foremost, I would like to express my deep gratitude and appreciation to **God** Almighty for granting me the blessings of health and strength, enabling me to conduct and successfully complete this research.

I would like to express my deep thanks to my supervisors, **Prof. Dr. Laith Sh. Rasheed** and **Assist. Prof. Dr. Aymen J. Kadhim**, for their encouragement, valuable guidance, helpful advice, and dedicated efforts throughout the preparation of this work.

I would like to express special thanks to my family (**my parents**, **sisters**, **and brother**) and all my friends for their constant encouragement and unwavering support at all times.

I extend my sincere gratitude to **Kerbala University, College of Engineering, and the Department of Civil Engineering** for providing the academic and research environment that made this work possible. Their resources, facilities, and continuous support played an essential role in my academic journey and the completion of this research.

Finally, I would like to express my sincere gratitude and deep appreciation to my supervisor, **Professor Dr. Laith Shakier Rasheed**, who played the most crucial role in guiding and supporting me throughout all stages of my academic journey, from my bachelor's to my master's and then to my doctoral studies. His vast expertise, insightful guidance, and constant attention to my work have been invaluable sources of motivation and inspiration. His unwavering belief in my abilities and his continuous support have enabled me to overcome academic challenges with determination and strength. Words cannot fully express my gratitude, but this work is a small token of my deep appreciation for everything he has contributed throughout this academic journey.

Signature: ✍

Abdulrasool Thamer Abdulrasool Qandeel

Date: / / 2025

Table of Contents

Chapter Three: The Experimental Work

Chapter Four: Experimental Results and Discussion

Chapter Five: Finite Element Analysis

List of Tables

List of Figures

List of Equations

List of Abbreviations

ACI	American Concrete Institute
ASTM	American Society for Testing and Materials
BS	British Standards
IQS	Iraqi Quality Standards

List of Symbols

SW	Seawater
IC	Impressed current
CID	Chloride ion diffusion
ACE	Artificial climate environment
RC	Reinforcement concrete
DC	Direct current
ACID	Accelerated chloride ion diffusion
PC	Portland cement
WMP	Waste marble powder
GEG	Ground expanded graphite
CB	Carbon black
w/b	Water-to-binder ratio

Chapter One: Introduction

1.1 General

Due to the effects of environmental factors such as corrosion from seawater, the actual life of marine concrete structures is often less than their designed life (Val et al., 2003). It is acknowledged that concrete cover is enough to protect reinforcement from corrosion when a reinforced concrete structure is intended for an urban or coastal environment. However, since concrete is a porous material that hostile ions like carbon dioxide and chlorides can pass through to reach reinforcements and initiate the corrosion process, merely covering them with concrete is insufficient to safeguard reinforcement. Many studies have been conducted on this topic because this design premise does not accurately reflect the harsh conditions that a structure is subjected to. Thus, it is widely acknowledged that the primary degradation process associated with actual reinforced concrete structures is reinforcement corrosion, particularly in marine environments where chloride action can cause a significant reduction in the bearing capacity of the structure, affecting not only the structure's service life but also increasing the risk of structural collapse (Balestra c 2019).

Due to the overuse of natural material sources, the use of waste materials as a feasible substitute for conventional materials in concrete has grown in favor in recent years (Hamada et al., 2020). Utilizing garbage in concrete has two benefits: it allows waste to be disposed of environmentally and enhances the concrete's strength and durability (Tayeh et al., 2019).

Global technological advancements have demonstrated that unprocessed or treated industrial waste materials can be included in concrete to provide a sustainable solution. This alternate option creates a cleaner and greener environment in addition to helping with waste material recycling (Azmi et al., 2017).

1.2 Deterioration of R.C. Structures

Reinforced concrete (RC) infrastructure placed in maritime environments should not fail too soon because it may have serious consequences for the economy, the environment, and sustainability. The exact mechanisms underlying the onset and progression of reinforced corrosion in marine environments, as well as the potential structural damage that follows, are still unknown despite decades of investigation. This is not good enough. It hinders long-term durability through sound design (Melchers, 2020).

Under ideal circumstances, concrete can prevent reinforcement corrosion by either offering physical shielding, such as a sufficient layer of concrete cover or by inhibiting the corrosion caused by the often-high pH of the concrete surrounding the bars. Excellent resistance to reinforcement corrosion has already been demonstrated by a sizable body of data from real RC structures in a range of marine and other settings, such as the splash zone, tidal zone, immersion zone, or a marine, salt-laden atmosphere (Melchers et al., 2017).

Chloride-induced reinforcement corrosion in a marine environment causes a localized decrease in the cross-section of reinforcement, which gets deeper as the corrosion process goes on. This is accompanied by a localized decrease in cross-section and a concentration of tension in the area of corroded bars, which reduces the bearing capacity of reinforced concrete buildings even at low corrosion levels (Balestra et al., 2016). Assessing the corrosion process dynamic, the alkaline environment in which the reinforcements are embedded in concrete prevents corrosion by forming a passivating layer made of iron hydroxides. This is because the concrete pores contain an alkaline solution. Nevertheless, chlorides found in the marine environment can enter the network of pores in concrete, and this passivating layer is locally destroyed

when concentrations exceeding 0.4% of cement mass (0.05% of concrete mass) reach the surface of reinforcements (Standard, 2011). In this manner, chlorides, in conjunction with oxygen and moisture found in the pores of the concrete, initiate a progressive pitting corrosion process, resulting in expansive corrosion products that accumulate near the reinforcement. This causes radial tensions along the bars' axis, which causes the concrete cover to crack and spall (Balestra et al., 2016). The reactions involved are found in the following two equations:

$Fe^{2+} + 2Cl^{-} \rightarrow FeCl_2$

$FeCl_2 + 2H_2O \rightarrow Fe(OH)_2 + 2HCl$

The reactions in above equations break both ferric oxide and magnetite (Fe_3O_4) layers on the steel (Popov, 2015). Chlorides in concrete that are soluble in nitric acid (sometimes referred as total chlorides) include bound chlorides which can be chemically bound with cement hydration products such as the C_3A or C_4AF or loosely bound chlorides with the C–S–H. It is only the remaining chlorides, namely free or water-soluble chlorides which react with steel and are responsible for its corrosion(S. Ahmad, 2003).

1.3 Columns in a marine structure

The reinforced concrete (RC) structures have been extensively employed globally. The efficacy of this structural system, especially in civil engineering contexts, can be ascribed to its attributes, including sufficient mechanical strength, cost-effectiveness, adaptability, chemical and heat resistance of steel, durability, and financial considerations. Nonetheless, pathological issues diminish the longevity of such structures. The issues identified include sulphate expansion, alkali-aggregate interaction, leaching, and corrosion of reinforcements (Goncalves et al., 2018). Furthermore, it is

important to emphasise that the corrosion of reinforcements has resulted in significant economic losses globally. It is projected that the expenses associated with inspection, maintenance, and repair due to corrosion of reinforcements amount to 4% of the Gross Domestic Product (Ueda et al., 2007).

The corrosion of reinforcements transpires by chemical and/or electrochemical processes. In reinforced concrete constructions, the reinforcements are safeguarded against such reactions by the passivating layer. The thin layer encasing the reinforcements exhibits chemical stability due to the alkalinity of the aqueous solutions within the concrete pores. Nonetheless, the chemical interactions of Cl- ions within the concrete pores compromise the chemical stability of this layer (Shaikh, 2018). The corrosion process commences when the Cl- concentration at the passivating layer attains the critical threshold. The phenomenon of depassivation transpires in this instance. The corrosion products occupy a greater volume than the original arrangement, resulting in internal tensions that produce cracking and spalling, as illustrated in Figure 1-1. The precise prediction and modelling of the initiation period are crucial for structural engineering applications to avert and prevent complex and accelerated mechanical deterioration events.

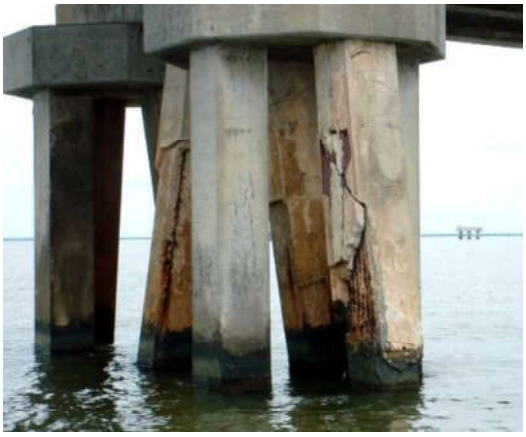

Figure 1-1. Column in sea water (Moser et al., 2011).

1.4 Concrete Performance Enhancement through Alternative Materials

Improving concrete performance and increasing its durability are key goals in developing sustainable building materials. In this context, recent studies have shown that the use of alternative materials such as marble powder, glass, ceramics, graphite, and carbon can have a positive impact on concrete's mechanical properties and durability. Using ceramic waste powder as a partial replacement for cement is a promising approach to sustainable concrete, addressing both environmental and resource conservation concerns. Incorporating ceramic waste powder into cement has the potential to improve the microstructure of concrete, as well as enhance its mechanical, structural, and durability properties. Ceramic waste powder can be obtained from a variety of products, such as pottery, household items, electrical insulation, tiles, and sanitary ware. Results have demonstrated the promising potential of ceramic waste powder as an effective alternative to cement (Ikotun et al., 2025).

The reactivity of glass powder, which is a pozzolanic substance, is mostly determined by its size; smaller sizes react more. Glass is a ubiquitous material that is used in windows, windshields, cathode ray tubes, bottles, jars, and other products. These products have a short lifespan and need to be recycled to prevent landfilling or stockpiling, which can harm the environment. To create environmentally friendly concrete from glass waste, glass powder must be used in the building industry. The results showed that using glass powder as a substitute for cement significantly improves the properties of fresh and hardened concrete (Elaqra et al., 2019).

Marble powder waste, which has a lot of potential for use with concrete materials, is produced in huge quantities during the production and processing of marble. A significant environmental issue arises from waste marble

powder, an inert substance that is produced as an industrial by-product of the sawing, shaping, and polishing of marble. The impact of various marble powder varieties and their replacement ratio on the mechanical characteristics of concrete has been the subject of numerous investigations. The findings demonstrated that the filler effect of marble dust greatly enhanced the mechanical behavior of concrete (Aliabdo et al., 2014a).

Black carbon with different sizes, shapes, microstructures, and surface areas can be used to develop cement-based materials for deformation monitoring and damage detection in concrete structures. Black carbon holds promising prospects for the production of multifunctional building materials. However, the current literature mainly focuses on electrical properties. Limited studies have been conducted to demonstrate the effect of black coal on fluidity, strength, hydration, porosity, and microstructure. These results indicate that it improves the mechanical properties of concrete (Q. Zhang et al., 2022).

The material particles that make up fresh concrete are widely distributed in size inside the water. It has been demonstrated that adding graphite particles broadens the range of particle sizes to include nanoscale dimensions. This could improve the packing of particles in freshly mixed concrete as well as the characteristics of concrete materials once they have hardened. One study examined five different packing density classes of concrete (normal-strength, high-strength, ultra-high-performance, normal-strength self-compacting, and ultra-high-performance self-compacting) in order to test this idea. The results showed that ultra-high-performance concrete had the maximum packing density and normal-strength concrete had the lowest. Fine particles were found to have a stronger impact on raising the

packing density with increased compressive strength in the case of self-compacting concrete (Ahmed Sbia et al., 2015a).

1.5 Research Significance

This study aims to analyze the impact of seawater corrosion on concrete columns using the electrical conductivity method. It then explores the potential of utilizing local materials, including some construction waste, as part of a sustainability approach by reusing them to improve the behavior of concrete mixes. The effect of adding ceramic powders, marble, glass, carbon, and graphite on the properties of concrete mixes was studied, improving their durability and mechanical behavior, given the chemical and physical effects of these materials. In addition, Abaqus software was used to simulate the concrete column models studied.

1.6 The Objective of Research

This research aims to comprehensively investigate the effect of incorporating alternative sustainable materials on the mechanical, structural, and durability properties of reinforced concrete, with a particular focus on their behaviour under accelerated corrosion conditions. The specific objectives are as follows:

1. To identify the optimal replacement ratios of ceramic and glass powders originating from construction and demolition waste, as sustainable pozzolanic materials partially substituting cement and to assess their influence on the properties of concrete.
2. To determine the most effective ratios of marble powder originating from construction and demolition waste, as a sustainable filler replacement, and to assess its influence on the properties of concrete.

3. To evaluate the incorporation of graphite and carbon powders, considered sustainable by-products of industrial manufacturing processes, as filler additives, and to investigate their effect on the properties of the concrete.
4. To evaluate the mechanical properties of modified concrete mixes incorporating the above-mentioned materials through standardized tests, including compressive strength, splitting tensile strength, and density.
5. To assess the durability properties of the modified concrete, including water permeability under pressure, half-cell potential, and chloride ion penetration, in order to determine the resistance of the mixes to aggressive environmental conditions.
6. To analyze the structural behaviour of reinforced concrete columns cast with selected optimal mixes by subjecting them to axial loading until failure, focusing on parameters such as ultimate load capacity, toughness, and ductility.
7. To simulate the degradation process of reinforced concrete columns by applying an accelerated corrosion technique using impressed electric current, and subsequently evaluating the residual structural performance after corrosion.
8. To develop a finite element model using ABAQUS software that accurately represents the mechanical response of both uncorroded and corroded reinforced concrete columns incorporating the alternative materials, and to validate the model with experimental results.

9. To provide a comparative analysis between traditional and modified concrete mixes in terms of sustainability, long-term performance, and resilience under corrosive environments, offering practical insights for future use in marine or aggressive exposure conditions.

1.7 Dissertation Outline

Chapter One: This chapter provides an introduction to the effect of salts on concrete columns, in addition to reviewing the main objectives of the study.

Chapter Two: This chapter presents a detailed study of the effect of seawater on sustainable concrete columns, in addition to reviewing previous studies on practical applications and case studies with a similar topic.

Chapter Three: This chapter reviews the general plan of the study, the method of work, and the tests of the materials necessary for the purpose of achieving the study case.

Chapter Four: In this chapter presented the practical results with explanations that show the general behavior of each case study with it is discussions.

Chapter Five: This chapter shows the results of the analytical study using the Abacus program.

Chapter Six: The last chapter includes the most important conclusions and recommendations reached through the study as a whole.

Chapter Two: Literature Review

2.1 General

The corrosion of reinforcing steel in concrete presents a considerable difficulty because to its prevalence in specific constructions and the high costs linked to repairs. Among the earliest thoroughly documented instances were noted in marine constructions and chemical production facilities (Biczok et al., 1964). Numerous investigations have consistently demonstrated the frequency of this issue in bridge decks, parking structures, and other concrete components exposed to chlorides, thereby emphasizing the seriousness of the problem (Litvan et al., 1987).

Corrosion cannot be fully understood or described without considering the surrounding environment, as every exposure condition possesses a certain level of corrosiveness (Z. Ahmad, 2006).

Therefore, it can be seen that corrosion is a powerful force that depletes resources, undermines the economy, and results in expensive and premature plant, equipment, and component failures.

As a harsh and complicated natural environment, the ocean presents serious obstacles to the longevity of construction, a problem that many nations encounter. In marine engineering, steel corrosion is the main cause of durability failure. Corrosion reduces the effective cross-sectional area of the steel bars and causes concrete to crack due to rust expansion, which lowers the safety performance and load-bearing capacity of concrete structures. Concrete degradation and corrosion caused by chloride are hazards for both prestressed and conventionally reinforced concrete piles in seawater (Whitmore, 2018):

Concrete reinforcement steel corrosion and chloride penetration can be stopped or postponed using a variety of techniques, including organic coatings and inhibitors. Reinforced concrete structures have also been protected by

electrochemical techniques that result in cathodic protection or chloride extraction. To prevent chloride attack, concrete porosity and permeability should be reduced in coastal and submerged areas. Utilizing waste materials or industrial by-products as a substitute for cement during the concreting process is a reasonably priced way to lower the porosity and permeability of concrete, thereby shielding reinforced concrete against chloride attack (Chousidis et al., 2016).

2.2 Corrosion of Reinforcing Steel in Marine Concrete Structures

Chlorides accumulate on the concrete surface via direct contact with adjacent water bodies, polluted runoff across the surface, or exposure to salt-laden airborne spray. The existence and concentration of chlorides at the surface facilitate entrance by a variety of intricate transport mechanisms, including absorption, convection, diffusion, migration, penetration, and thermodiffusion (Nguyen et al., 2017). The chloride ingress process is further complicated by chloride binding, ionic interactions, ageing variables, temperature, humidity, and submerged pressure effects (Bastidas-Arteaga et al., 2011). The subsequent durability modelling is complicated by the existence of cracks in the concrete, the sustained or fatigue stress in the internal reinforcement, and the properties of the reinforcing alloy and its microstructure (Bastidas-Arteaga et al., 2011). Under ideal conditions, the reinforcement in concrete remains in a passivated form, stabilized by the concrete's high alkalinity. When the chloride concentration surpasses a critical threshold at the reinforcement level, the passivation coating becomes destabilized, leading to the onset of localized corrosion. Moreover, carbonation diminishes the alkalinity of concrete and impedes passivation, hence accelerating corrosion in the presence of chlorides (Bastidas-Arteaga et

al., 2011). Carbonation typically promotes corrosion across a broader area of the reinforcement, but chloride-induced corrosion can be very localized in high-performance concrete, particularly in the presence of fissures. Recent research on the interaction between carbonation and chloride-induced corrosion has demonstrated enhanced effects. Corrosion deteriorates the reinforcement, leading to section loss and/or debonding from the adjacent concrete. The corrosion is exacerbated by the development of expansive oxidation products, leading to cracks and surface splitting of the concrete, which subsequently promotes chloride ingress. The enhanced chloride penetration ultimately results in the delamination of the concrete cover and subsequent deterioration of structural integrity. Chloride diffusion is expedited, and the onset of corrosion is more probable in the presence of carbonation compared to only chloride ingress, possibly due to carbonation liberating a fraction of the bound chlorides into the pore solution (Bastidas-Arteaga et al., 2011). A considerable amount of experimental research on chloride penetration and corrosion under many settings has been conducted, and more recently, modelling techniques, particularly artificial neural networks, have illuminated this subject. Various mitigation strategies are acknowledged and presently employed to diminish chloride penetration into concrete, including: 1) the utilization of less permeable concrete mixtures, predominantly incorporating supplemental pozzolans (such as granulated blast furnace slag, fly ash, silica fume, and metakaolin); 2) enhanced concrete cover; and 3) surface treatments or barriers to seal the concrete surface (for instance, silanes and methyl methacrylate). Nonetheless, these mitigating measures merely postpone the initiation of corrosion. Ultimately, the chloride ions infiltrate the concrete cover and amass to the critical concentration level, so instigating corrosion of the internal steel reinforcement bars.

Figure 2-1. Corrosion in columns in marine structure (Moser et al., 2011).

2.3 Reinforced Concrete Marine Structures

Many concrete buildings around the world were either directly or indirectly exposed to seawater. The impact of seawater on concrete warrants particular consideration for a number of reasons. Numerous physical, chemical, and mechanical deterioration processes work simultaneously on the coastal, onshore, and offshore structures (Ahn, 2005).

Depending on their characteristics and impact on the exposed structure, the sea environment, sometimes referred to as the marine environment, is typically separated into three zones. According to Table 2-1, concrete is vulnerable to several kinds of attacks in each environmental zone. The structural concrete in the splash zone is subject to physical and chemical reactions, which is why deterioration is typically seen to be more severe four. Additionally, the structure in the splash zone has alternating cycles of wetting and drying, which speeds up the chemical reaction of water and salts on the nearby concrete and steel reinforcement (M. S. Islam et al., 2005).

Table 2-1. Different attack zones of the marine environment (M. Islam et al., 2012).

Zone descriptions	Type of attack
Atmospheric zone - where structural components are above the spray zone or the highest point of high tide.	Chemical and Physical
Splash zone - The area above high tide, where it is not submerged but is exposed to constant spray from waves and wind.	Chemical, Physical, and Electrochemical
Tidal zone - The parts between the highest and lowest points of high tide.	Chemical, Physical, and Mechanical
Submerged zone - Where structural components are constantly submerged in seawater.	Chemical and Physical

Structures in splash and tidal zones are more susceptible to the violent action of seawater than those that are completely and constantly submerged in water for the reasons listed below (M. Islam et al., 2012):

1. Since the rate of corrosion is dependent on the availability of oxygen, the presence of O_2 in sufficient quantities causes steel to corrode in concrete significantly more quickly.
2. The water in the concrete structure's above-sea level section rises due to capillary action, leaving behind salts and crystals when it evaporates. Tensile stresses are caused by the progressive wetting and drying cycles, which cause this crystalline development to rise steadily. When the tensile strength is exceeded, the concrete surface disintegrates.
3. The varying sea level causes erosion of the concrete, which leads to the loss of concrete mass, as well as the washing away of corroded concrete fragments and leached salts.

4. Concrete wears down more quickly in active tidal zones due to the mechanical force of sea waves.

Experience has demonstrated that the splash zone, which is directly above the high-water level, is where seawater attacks concrete the most severely. The areas below the water level that are consistently submerged are least damaged, as is the area between low and high water marks (O'Neill Iqbal et al., 2009). Continuous contact with highly aerated seawater, the erosive effect of salt water spray, temperature gradient, and wave action in the presence of ambient O_2 and CO_2 gas are the characteristics that define the splash zone (Gupta, 1988).

Some of the dissolved salts are left behind as crystals, primarily sulfate, in the tidal/splash zone, where concrete is frequently wetted by sea water and alternately dried during periods of pure water evaporation. After further wetting, these crystals rehydrate and expand, applying an expanding force to the surrounding hardened concrete. High temperatures are especially conducive to salt weathering, a gradual surface weathering process. Additionally, salt water can rise by sorption, or capillary action, in which pure water evaporates from the surface and leaves behind salt crystals that, when rewetted, can create disturbance (M. Islam & et al., 2012).

Concrete deterioration is not characterized by expansion brought on by a significant amount of ettrengite generated as a result of sulfate attack in structures that are constantly submerged in seawater after a steady condition of saturation and salt concentration is achieved. Rather, it primarily manifests as erosion or the removal of solid components from the bulk (Wee et al., 2000). Both gypsum and ettringite dissolve in the presence of chloride and can be removed by seawater.

According to (Thangavel et al., 2000), the ionic radii of sulfate and chloride ions are 2.30 Å and 1.81 Å, respectively. Additionally, according to (Tumidajski et al., 1995), the diffusion coefficients for sulfate and chloride are $2*10^{-8}$ cm^2 S^{-1} and $3*10^{-7}$ cm^2 S^{-1}, respectively. Chloride ions penetrate more quickly than sulfate ions because of their larger diffusion coefficient. However, sulfate's effect on degradation is more hazardous because it contains two negative ions, whereas chloride just contains one. Therefore, concrete exposed to a maritime environment may suffer from both sulfate and chloride penetration.

2.3.1 Chloride Attack

Since chloride attack largely results in the corrosion of concrete reinforcement, it is one of the most significant factors affecting the durability of concrete. According to statistics, corrosion of reinforcement accounts for more than 40% of structural failures. Cement, water, aggregate, admixtures, and environmental dispersion are the main sources of chloride in concrete. About 89% of the total dissolved salts in SW are composed of chloride compounds, which make up the largest amount. It contributes roughly 55% of the overall concentration of salt ions in terms of ionic composition. Calcium chloroaluminate and calcium chloride are produced when the hydrated cement products react with the chloride salts found in seawater (M. M. Islam et al., 2009). Friedel salts, another name for calcium chloroaluminate, have a low to medium growth rate. Because calcium chloride is liquid, it leaches out of concrete, causing material loss and a decrease in strength.

Metha (Mehta, 1980) states that $MgCl_2$ reacts with the hydrated cement's $Ca(OH)_2$ to generate calcium chloride, which is soluble and leaches away, causing material loss and weakening.

2.3.2 Sulfate Attack

The second most abundant of the anionic components found in SW is sulfate. Sulfate of calcium, sodium, and magnesium makes up between 3.5 and 3.75 % of the total salts in SW, or roughly 10 to 11 %. According to Nevile (A. M. Neville, 1995), white look is a property of concrete that has been damaged by sulfates. The buildings' edges and corners are where the deterioration is first noticed, and then there is increasing cracking and spalling.

After reacting with hydrated C_3A and $Ca(OH)_2$, a hydrated cement product, the sea salt magnesium sulfate produces calcium aluminate sulfate hydrate (ettringite) and calcium sulfate (gypsum). Following crystallization, the volumes of gypsum and ettringite in concrete pores are larger than those of the compounds they replace. Bogue (Bogue, 1955) believes that gypsum formation results in a 17.7% increase in volume. The formation of $Mg(OH)_2$ causes a volume increase of roughly 20% in the presence of magnesium ions.

The softening form of fracture is caused by the pressure exerted by expanding etringite crystals. Expansion can also happen from gypsum formation brought on by cation exchange processes (Bogue, 1955). According to reports, the process by which gypsum formation deteriorates hardened Portland cement paste results in a decrease in stiffness and strength, followed by expansion, cracking, and finally, the materials becoming mushy or noncohesive. Therefore, a steady loss of structural concrete's mass and strength is linked to sulfate assault in seawater.

2.4 The Effect of Sea Water on Reinforced Concrete

For many years, concrete has been regarded as an essential building element (Mangi et al., 2019). It has had such a compelling effect that no structure can be put together today without it (Ali et al., 2019). All of this is due to its qualities, which include strength, durability, moldability, affordability, and lightweight (Jatoi et al., 2019). By 2050, it is expected that the yearly demand for concrete for buildings will reach 18 billion tons (Mangi et al., 2018). Concrete is utilized to build maritime onshore and offshore constructions because of its wide range of applications and capabilities. The Romans built the first concrete structure on the Mediterranean Sea shore, demonstrating the relationship between seawater and concrete (Mh et al., 2020). Furthermore, its use has greatly increased because of the tremendous economic progress that has occurred globally over the past century. Every building in existence today is either directly or indirectly exposed to seawater. Examining how seawater affects concrete's qualities is therefore essential for a number of reasons (M. M. Islam et al., 2009). However, seawater is a complex mixture of substances that are harsh on structures, especially salts. The strength and longevity of concrete exposed to marine water can be compromised by the presence of salts in varying amounts. According to some estimates, the typical salt content of saltwater is 3.5% (M. S. Islam et al., 2010). In addition, salts have three different effects on concrete: mechanical, chemical, and physical (M. S. Islam et al., 2010). The physical effects of seawater include temperature gradients, ocean currents, tides, sea waves, and freeze-thaw cycles. While mechanical effects include cyclic drag, abrasions, strength loss, etc., chemical impacts include corrosion of steel reinforcement and deterioration of the cement matrix (M. M. Islam et al., 2009).

Furthermore, it is typical for buildings affected by seawater to experience alternating wet and dry tides, which hasten the deteriorating process (M. S. Islam et al., 2005). Additionally, concrete that is in use develops cracks in the cold sea environment, which could lead to its failure (Diao et al., 2011). Figure 2-2 shows the degradation of the concrete matrix exposed to seawater. According to Table 2-2, the salts that primarily harm concrete are sulfate and chloride, which are found in the sea as ions.

Table 2-2. The main ions are found in natural saltwater (Lindahl, 2009).

Ions	Na	Cl	SO_4	Mg	Ca	K
Quantity (grams)	10,360	29.353	2.712	1.294	0.413	0.387

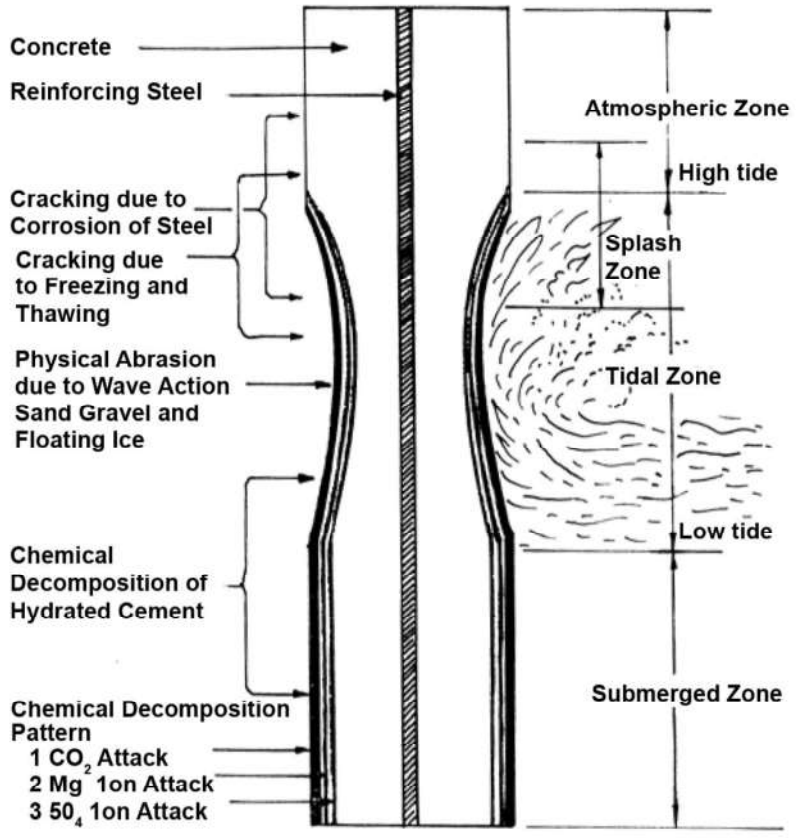

Figure 2-2. Type of concrete marine building assault under various exposure circumstances (Mehta et al., 2006).

The most frequent way that reinforced concrete infrastructure deteriorates is through corrosion of the steel reinforcement. While carbonation is the primary cause of corrosion in buildings, chloride is typically what causes corrosion in bridges, parking lots, and maritime constructions (Jones, 1997). There are two possible issues with reinforcement corrosion: first, the loss of the reinforcement's cross-section, which reduces the structure's ability to support loads and, consequently, its safety; and second, the possibility of cracking or spalling under specific corrosion conditions. In addition to being unsightly, the latter will hasten the spread of damage because the protective concrete cover will be gone, and it may even pose a direct safety risk, as in the event that fragments of spalled concrete fall on oncoming cars. Cracking and spalling are caused by the corrosion process's reaction products, which are formed along with a volume expansion. The volume of the corrosion product is usually 1.5 to 6.5 times that of pure iron, depending on the type of reaction product (Tuutti, 1982).

Due to chemical reactions that cause iron to decompose and transform into oxides larger than its initial size, employment is one of the most detrimental factors that affect the safety of facilities, particularly reinforced concrete columns. As a result, the area of the armament's cross-section decreases. Concrete experiences internal pressure as a result of this size expansion, which leads to surface and deep fissures. These flaws allow more damaging environmental elements, including moisture and aggressive ions, to enter the concrete, hastening the rate of degradation. Furthermore, erosion-induced weakening of the concrete-reinforcement connection lowers the column's capacity to transfer loads efficiently, which may result in a reduction in its resistance and deformation capacity and, ultimately, a loss of structural stability. In hostile settings like coastal regions, where chloride ions combine

with the armor iron's protective surface layer to speed up the rusting process, the effect of corrosion is amplified. Long-term erosion issues are made worse by the fact that facilities that are subjected to frequent episodes of moisture and dehydration are more susceptible to this kind of degradation because of variations in temperature and moisture levels (Mehta et al., 2005).

2.5 Corrosion Definition

The general definition of corrosion is the deterioration of materials as a result of a reaction between the material and its surroundings. The type of degradation-causing processes varies depending on the material class: corrosion in metals is an electrochemical process, while merely chemical dissolution can cause failure in ceramics (Virtanen, 2009). Nonetheless, a broader definition encompasses the deterioration of a material due to interaction with its surroundings. Corrosion can encompass non-metallic materials, including concrete and plastics, as well as mechanisms such as cracking, in addition to material loss(Virtanen, 2009).

The corrosion of reinforcing steel and other embedded metals is the primary cause of concrete deterioration. Corrosion of steel results in rust that occupies a larger volume than the original steel. This expansion induces tensile stresses in the concrete, potentially leading to cracking, delamination, and spalling. The alkaline nature of concrete creates a strongly adhering layer on the reinforcing steel, which typically safeguards it against significant corrosion. Consequently, the corrosion of reinforcing steel is not a major issue in the majority of concrete elements or structures (Mehta et al., 2005). Corrosion of steel may pose an issue if:

a) The concrete is not resistant to the penetration of corrosion-inducing agents.

b) The structure is inadequately designed for the service environment.

c) The surroundings do not meet expectations.

d) The structure undergoes modifications over its service life.

2.6 The Mechanisms of Steel Corrosion in Concrete

Durability concerns related to concrete structures are significant challenges for the global civil engineering community today. A major durability concern is the corrosion of steel reinforcement, resulting in rust formation, cracking, spalling, delamination, and structural damage. This is regarded as the primary element contributing to damage to bridges and other infrastructure (Michel et al., 2016). Atmospheric corrosion, galvanic corrosion, and stress corrosion cracking can adversely affect the functionality and aesthetics of concrete structures. Consequently, global research is focused on devising ways or materials to mitigate the corrosion of steel in concrete.

Generally, when metals and alloys chemically, biochemically, or electrochemically interact with their environment, surface degradation occurs, resulting in their transformation into more thermodynamically stable oxides, hydroxides, or carbonates. This phenomenon is referred to as corrosion (Popov, 2015).

When there is a difference in electrical potential along the surface of an embedded steel bar, the concrete functions as an electrochemical cell, comprising anodic and cathodic regions on the steel, with the pore water in the hardened cement paste serving as an electrolyte (Razaqpur et al., 2009). This induces a current flow within the system, resulting in an attack on the metal with the higher negative electrode potential, namely the anode, while the cathode stays unscathed(Michel et al., 2016).

Corrosion transpires in the presence of carbonation, chloride ions, or substandard concrete alongside water and oxygen(Ebell et al., 2016). Upon

the initiation of cement hydration, steel embedded in concrete forms a protective passive layer on its surface, comprised of γ-Fe_2O_3 (Kurdowski, 2002). This layer inhibits ion transfer between the steel and adjacent concrete, thereby diminishing the corrosion rate(Berrocal et al., 2016). This oxide coating protects the steel from harm, as shown in Figure 2-3. It remains stable solely at elevated pH levels, specifically between 12 and 14 (Popov, 2015).

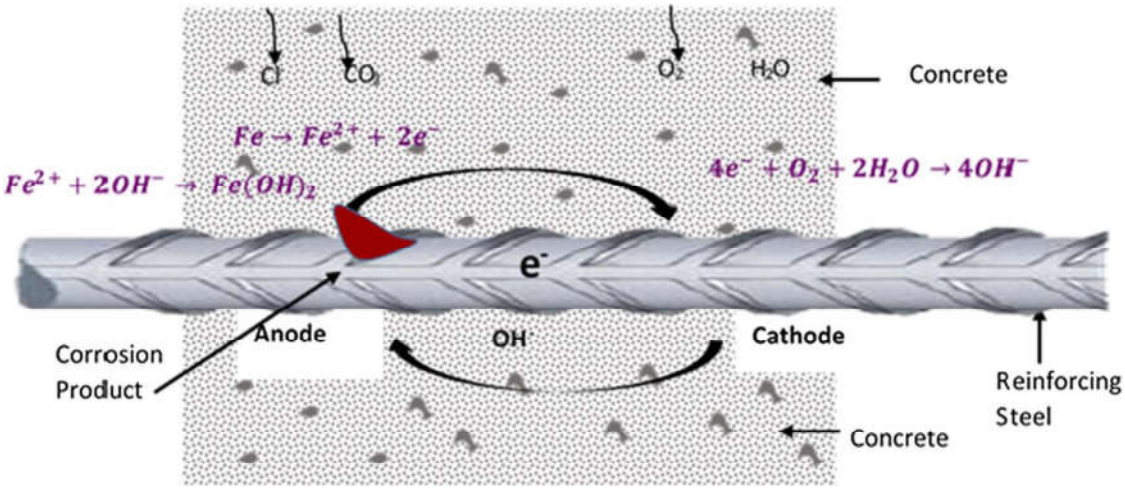

Figure 2-3. Diagrams illustrating the corrosion process in concrete (Virtanen, 2009).

Hydrated ferric oxide, commonly known as rust, is produced from these reactions and is characterized by significant porosity, possessing a volume 6–10 times greater than that of steel, which leads to cracking and spalling (Broomfield, 2023).

2.7 The factors affecting corrosion

The factors affecting corrosion of steel in concrete may be classified into two major categories, as follows:

a) External factors;
b) Internal factors.

2.7.1 Internal Factors Affecting Corrosion of Steel in Concrete

They include mostly the environmental parameters, as follows:

2.7.1.1 Availability of oxygen and moisture at rebar level

The presence of moisture and oxygen supports the corrosion. Moisture fulfills the electrolytic requirement of the corrosion cell, and moisture and oxygen together help in the formation of more OH^- thereby producing more rust components, i.e., $Fe(OH)_2$. Oxygen also affects the progress of cathodic reactions. In the absence of enough oxygen, even in a situation of depassivation, corrosion will not progress due to cathodic polarization (S. Ahmad, 2003).

2.7.1.2 Relative humidity and temperature:

The relative humidity mainly affects the carbonation of concrete. Within 50–100% RH, the increase of environmental relative humidity decreases the carbonation of concrete. Based on their calculation, Cahyadi and Uomoto(Cahyadi et al., 1993) have found that, within 50–30% RH, a decrease in environmental RH may not cause a decrease in the carbonation of concrete especially in normal concentrations of CO_2 even after a long period of exposure. A rise in temperature may result in a twofold effect:

1. The electrode reaction rates are generally increased, and
2. The oxygen solubility is decreased resulting in a reduction in the rate of corrosion (Mozer et al., 1965).

If the situation is conducive for corrosion to take place, the corrosion rate is increased by high temperature and high humidity(Uhlig et al., 1985).

2.7.1.3 Carbonation and entry of acidic gaseous pollutants to rebar level

The effect of carbonation and other acidic gases, such as SO_2 and NO_2, is due to their tendency to reduce the pH of the concrete. The fall in the pH to certain levels may cause the commencement of reinforcement corrosion, loss of passivity of concrete against reinforcement corrosion, and catastrophic reinforcement corrosion (Berkeley et al., 1990).

2.7.1.4 Aggressive anions

Aggressive anions, mostly chloride ions, reaching to the rebar level, either through the concrete ingredients or from the external environment: Chloride in concrete may be present in either of the following forms:

1. Acid-soluble chloride which is equal to the total amount of chloride present in the concrete or that is soluble in nitric acid (ASTM C1152/C1152M-20, 2020),
2. Bound chloride which is the sum of chemically bound chloride with hydration products of the cement, such as the C_3A (tricalcium aluminate) or C_4AF (tetracalcium aluminoferrite) phases, and loosely bound chloride with C–S–H gel, and
3. Free or water-soluble chloride which is the concentration of free chloride ions (Cl^-) within the pore solution of concrete, and is extractable in water under defined conditions.

It is generally recognized that only the ‘‘free chloride’’ ions influence the corrosion process (Arya et al., 1987). It is reported that the resistivity decreases and corrosion rate increases with an increase in the chloride content. However, the change in pH is found to be insignificant due to a change in the chloride content of concrete (Ip & C., 1987).

2.7.1.5 Stray currents:

Stray currents from the various sources, e.g., building power supply systems, cathodic protection systems, locomotive power supply systems, etc. cause the electrolytic corrosion (Revie, 2008).

2.7.1.6 Bacterial action

Bacterial action is found to be effective in three ways:

1. The bacteria decrease the amount of cover by disintegration of the cementitious materials.
2. The anaerobic bacteria produce iron sulfides in the oxygen deficit conditions, such as concrete sewers, which enables the corrosion reaction to proceed even in the absence of oxygen (Berkeley et al, 1990), and
3. Aerobic bacteria may also aid in the formation of differential aeration cells, which can lead to corrosion.

2.7.2 Internal Factors Affecting Reinforcement Corrosion

They include concrete and steel quality parameters, as discussed below:

2.7.2.1 Cement composition

The cement in the concrete provides protection to the reinforcing steel against corrosion in the following ways:

1. By maintaining a high pH in the order of 12.5–13 owing to the presence of $Ca(OH)_2$ and other alkaline materials in the hydration product of cement, and
2. By binding a significant amount of total chlorides as a result of chemical reaction between C_3A and C_4AF content of cement in concrete. Thus the threshold chloride value shifts to the higher side with

an increase in the C_3A content of cement (Rasheeduzzafar, 1992). The use of blended cement, such as microsilica blended high-C_3A cement, is found to be concomitantly resistant to sulfate attack and chloride corrosion of reinforcement (Dakhil et al., 1990).

2.7.2.2 Impurities in aggregates

Aggregates containing chloride salts cause serious corrosion problems, particularly those associated with sea-water and those whose natural sites are in ground water containing high concentration of chloride ions (Butler et al., 2001).

2.7.2.3 Impurities in mixing and curing water

Mixing and curing water, either contaminated with sufficient quantity of chloride or being highly acidified due to any undesirable substance present in water, may prove to be detrimental as for as corrosion of rebar is concerned.

2.7.2.4 Admixtures:

The addition of calcium chloride in concrete, as a common admixture for accelerating the hydration of cement is perhaps the most significant reason for the presence of chloride in concrete in the RC structures exposed to normal weather conditions. Some water reducing admixtures also contain chlorides (Butler et al., 2001).

2.7.2.5 W/C ratio

The w/c ratio, known to control principally strength, durability and impermeability of concrete, does not itself control the rate of corrosion of reinforcement. When RC structures are immersed in some aggressive solution, it is the permeability of concrete, which is a function of w/c ratio, affects the corrosion of rebar. The depth of penetration of a particular chloride

threshold value increases with an increase in the w/c ratio (Jaegermann, 1990). Carbonation depth has been found to be linearly increasing with an increase in the w/c ratio (Ho et al., 1987). The oxygen diffusion coefficient is also found to be increasing with an increase in the w/c ratio (Kobayashi et al., 1991).

2.7.2.6 Cement content

The cement content in concrete does not only affect the strength but it also has a significant effect on durability. Due to the inadequate amount of cement in the mix, the concrete is not consolidated properly leading to the formation of honeycombs and other surface defects. These honeycombs and surface defects help in the penetration and diffusion of corrosion-causing agents, such as Cl^-, H_2O, O_2, CO_2, etc., in concrete. This results in the initiation of reinforcement corrosion due to the formation of differential cells. Further, concrete with low cement content has a lack of plastic consistency due to which it does not form a uniform passive layer on the surface of the steel bars (S. Ahmad, 2003).

2.7.2.7 Aggregate size and grading

Since the size of aggregates has a bearing upon the consistency of concrete, it may have an effect upon reinforcement corrosion. Aggregate grading is another factor, which should be considered for high-quality impermeable concrete. It has been observed that for a given w/c ratio, the coefficient of permeability of concrete increases considerably with increasing size of aggregates. Keeping this in view, Cordon and Gillespie (Cordon et al., 1963) have recommended the maximum size of aggregate as $1^1/_2$ in. for 5000 psi concrete, $^3/_4$ in. for 6000 psi concrete, and $^3/_8$ to $^1/_2$ in. for concrete with a compressive strength of more than 6000 psi.

2.7.2.8 Construction practices

Serious corrosion problems may occur if enough care, such as listed below, is not taken at the construction stage (Rasheeduzzafar et al., 1989):

1. Aggregate washing for deleterious materials, if any;
2. Control of chloride in almost all ingredients of concrete, i.e., water, cement, aggregate, and admixtures;
3. Strict enforcement of designed and recommended levels of w/c ratio, cement content, cover thickness, etc.;
4. Proper consolidation of freshly placed concrete; and
5. Proper curing of concrete.

2.7.2.9 Cover over reinforcing steel

Cover depth has a significant effect in case of corrosion due to penetration of either chloride or carbonation (Beeby, 1978). This effect of cover is limited within the time of casting to the time at which the rebar is depassivated and corrosion is initiated. The rate of corrosion, once it has started, is independent of the cover thickness (Schiessl, 1975).

2.7.2.10 Chemical composition and structure of the reinforcing steel

The differences in the chemical composition and structure of reinforcing steel and the presence of stress in the reinforcement, either static or cyclic, create different potentials at different locations on the surface of reinforcement, causing the formation of differential corrosion cells, which leads to its corrosion (Mozer et al., 1965).

2.8 Corrosion Initiated by Chloride

When steel is immersed in a solid layer of concrete, it stays in the passive state, meaning it is not corroded; however, when the concrete around

it deteriorates, steel undergoes an active state, where corrosion starts. Chloride ions can enter the reinforcement by internal mixing or environmental penetration. The alkalinity close to the reinforcement rises when chloride seeps into the concrete. The Cl^- and OH^- ions diffuse to the contact in order to preserve electroneutrality. The concentration of chloride ions will accumulate on the surface due to their increased mobility, saturating the interface with (Fe^{2+}) and (Cl^-). As a result, less $Fe(OH)^+$ will develop, moving the potential in a more cathodic direction (Popov, 2015).

Critical chloride content is the amount of chloride necessary for steel de-passivation and corrosion commencement. The passive layer is locally damaged, and causes localized pitting corrosion if the concentration of chloride ions rises over this threshold value (Bertolini et al., 2013). According to A. Neville (A. Neville, 1995), the passivated surface becomes a cathode, and the steel surface that is attacked by chloride ions becomes an anode.

Concrete chlorides that dissolve in nitric acid, also known as total chlorides, comprise bonded chlorides, which can be loosely bound with the C–S–H or chemically bound with cement hydration products like the C_3A or C_4AF. Only the residual chlorides, specifically those that are free or soluble in water, react with steel and cause corrosion (S. Ahmad, 2003).

The amount of chlorine in steel determines its passivity. As the amount of chloride in steel increases, its pitting potential decreases. If a structure becomes contaminated with chloride, its pitting potential (Epit) decreases from 500 to −500 mV. The required total chloride content for a typical corrosion potential ranges from 0.4 to 1% of the cement's weight (Angst et al., 2009). The chloride concentration limit for prestressed and reinforced concrete structures is 0.1% and 0.4, respectively, in accordance with BS 1504-9:2008 (Ann et al., 2007).

Even at highly basic pH values, such as about 12, corrosion can occur in the presence of chlorides. Recent studies, however, have demonstrated that, depending on exposure and environmental factors, this threshold limit may be as low as 0.2% or less or even more than 1%. As a result, scientists cannot agree on a threshold level for corrosion. Therefore, without assuming any acceptable limitations, the corrosion risk for each structure should be assessed based on the site's real conditions. According to the author's real-world experience, the danger of corrosion should not only be determined by half-cell or chloride values but also by the actual state of the structures. When evaluating corrosion risk, it is important to take into account how temperature and humidity affect the transport of chloride ions, the resistivity of concrete, and the rate of corrosion. Varying sections or components of a building may have varying threshold levels for chloride ion contamination (Goyal et al., 2018).

2.9 Performance of Corroded Columns

In maritime environments, it is inevitable that dangerous compounds like chloride ions may seep into reinforced concrete (RC) structures. This compromises the safety and durability of marine concrete structures, resulting in resource waste, economic loss, and even casualties. According to research, the primary cause of maritime concrete structures' performance degradation during their entire service life is rebar corrosion (Balestra, et al., 2019). The yield strength and cross-sectional area of the original rebar are reduced as a result of rebar corrosion, which consumes original materials and produces much lighter rust products (Chen, 2018). The rust products from rebar corrosion continue to spread outward and cause a hoop tensile stress on the surrounding concrete, which causes the concrete to crack and the bond

strength between the rebar and the concrete to weaken (K. Zhang et al., 2019). The concrete cover peels off once cracks link with one another (H. Yu et al., 2017), thus weakening the rebar bond and reducing the RC constructions' bearing capacity. In addition to decreasing RC structures' dependability and safety, reinforcement corrosion also shortens the structures' service life.

Comprehensive studies have been conducted over the past decade on the impact of reinforcement corrosion on the performance of reinforced concrete structures (L. Yu et al., 2015). Numerous experimental investigations were undertaken to evaluate the impact of rebar corrosion on concrete cracking, revealing that fracture width increases with the advancement of rebar corrosion (Khan et al., 2014). The phenomenon of corrosion-induced concrete cracking can be categorized into three stages: crack initiation, crack propagation, and complete loss of concrete cover (Chen et al., 2013). Research indicates that the bond strength of rebar may first increase during the early stages of corrosion, thereafter declining sharply to a low value once fractures develop on the concrete cover surface (F. Li et al., 2013). The simultaneous occurrence of rebar corrosion and concrete cracking may lead to a discordance in the stress-strain connection between the rebar and the adjacent concrete (Coccia et al., 2016). Furthermore, as the unrestrained length of the corroded rebar within the reinforced concrete columns rises, the squeezed steel bars are susceptible to premature buckling(Tapan et al., 2011). To compensate for the reduction in rebar bearing capacity and the diminution of the concrete cross-section, the height of the compression zone within the concrete cross-section may be altered.

2.10 Accelerated Corrosion Regimes

The detrimental impact of reinforced concrete corrosion on the longevity of concrete structures is extensively documented. Accelerated laboratory modeling is typically necessary to enhance comprehension of reinforcement corrosion and its impacts (Berke, 1990). The methods for accelerating chloride-induced steel corrosion are mostly founded on the thermodynamic process of chloride penetration. This process transpires when chloride ions penetrate the concrete layer to reach the steel surface. The alkaline conditions of concrete can facilitate the formation of a passive layer on the reinforcement surface, safeguarding steel against corrosion. This passive layer is compromised or "depassivated" when chloride content exceeds a specific threshold or when the underlying concrete undergoes acidification owing to carbonation (Malumbela et al., 2012). Various electrochemical reactions may transpire on the surface of steel as a result of chloride corrosion. In these instances, the concrete pore solution serves as an electrolyte, while the steel surface functions as an electrode linked by a steel body (Hansson, 1984). Figure 2-4 depicts the electrochemical mechanism of steel corrosion within concrete. The techniques for accelerating chloride-induced corrosion can be classified into three categories: the IC method, the CID method, and the ACE approach. The specifics of each strategy are elucidated and examined in the subsequent sub-sections.

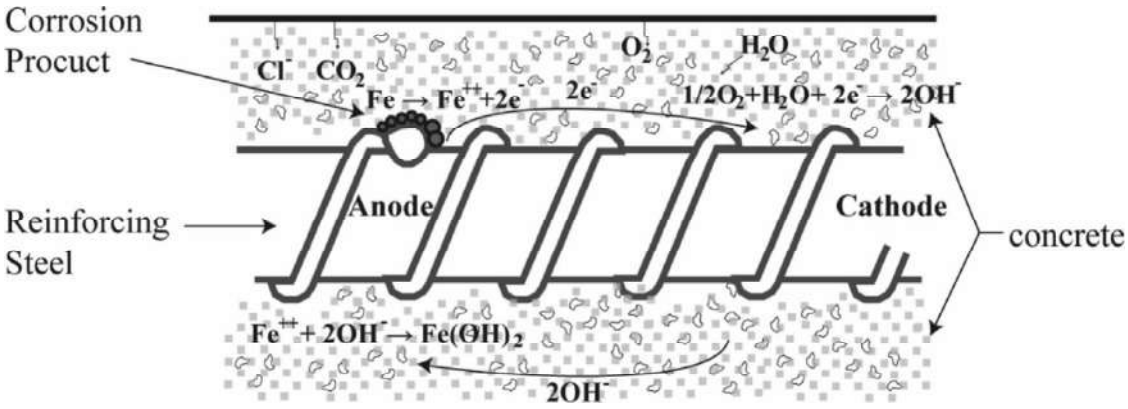

Figure 2-4. Schematic representation of electrochemical reactions occurring during the corrosion of reinforcing steel (Hansson, 1984).

2.10.1 Impressed current (IC) method

The IC approach is extensively employed to expedite corrosion in RC corrosion studies. Corrosion occurs when an electrochemical potential is applied between the anode (steel reinforcement) and the cathode. The potential is adjusted to maintain a consistent current density. The natural corrosion current density ranges from 0.1 to 10 μA/cm² (Malumbela et al., 2012). In a conventional IC approach, the applied current may reach up to 100 times more than the natural current flow from a direct current (DC) power supply, resulting in significant mass loss of the anode throughout the testing period. This procedure is efficacious when the specimen is submerged in chloride-containing solutions (S. Ahmad, 2009) as, in these instances, the corrosion of steel specimens under impressed current adheres to Faraday's law, hence optimizing efficiency. Figure 2-5 illustrates the schematic diagram of the experimental configuration for a standard IC corrosion method, which comprises a DC power supply, a data logger, a tank filled with NaCl solution, two stainless steel plates linked to the negative terminal of the DC power supply, and an RC specimen connected to the positive terminal.

Electrochemical reactions will occur as long as voltage is applied to the system. The data logger records the applied current intensity.

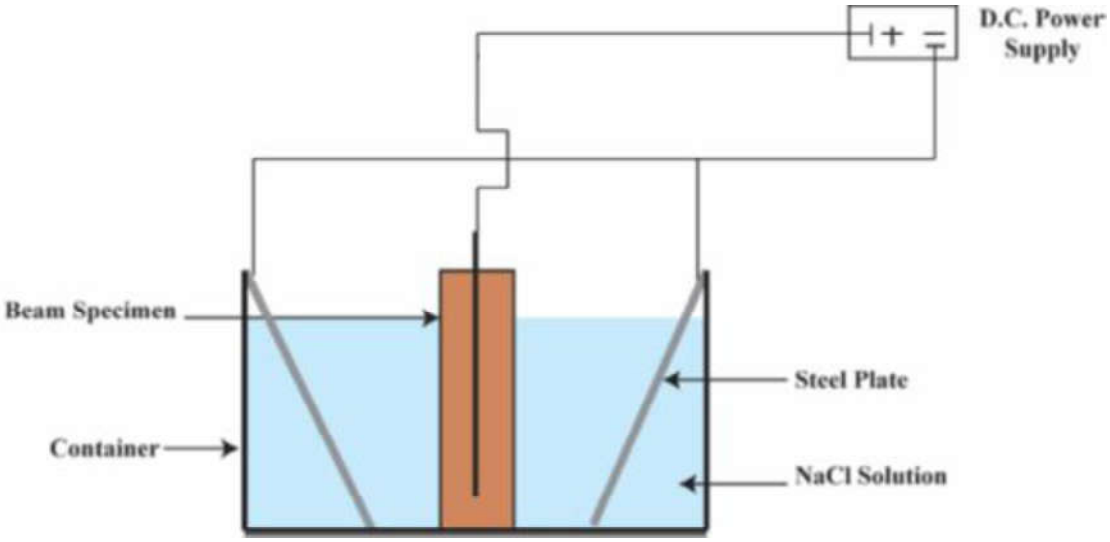

Figure 2-5. Schematic representation of the experimental configuration for the accelerated corrosion technique (Feng et al., 2021).

In scenarios where an impressed current induces corrosion, the mass loss correlates with the electrical energy expended when passivity is breached and can be represented by Faraday's equation, Equation (2-1):

$$Mass\ loss\ = {}^{Mit}/_{zF} \quad \text{... Equation 2-1}$$

Where:

M is the molar mass (55.847 g/mol for iron);

i is the current (A);

t is the time (s);

z is the number of electrons transferred;

F is Faraday's constant (96,487 Coulombs/mole).

2.10.2 Accelerated Chloride ion diffusion (ACID) method

Tuutti's model (Fakhri et al., 2020), posits that the deterioration of reinforced concrete occurs in two stages: the initiation phase and the corrosion

propagation phase. Upon the commencement of the initiation phase, the corrosion propagation phase will occur autonomously. Stanish et al.'s study(Stanish et al., 2000), identified three transport pathways for chloride ion penetration::

1. Capillary absorption,
2. Hydrostatic pressure, and
3. Diffusion.

Among the three methods, diffusion is a recognized process in which chloride ions (Cl^-) migrate in response to the concentration gradient. The CID approach primarily aims to reduce the migration time of chloride ions from the concrete surface to the steel surface, as chloride ions are essential in the start phase. Nonetheless, the migration of chloride ions typically requires time under standard conditions. An efficient method involves the application of an electric field to facilitate the accelerated movement of chloride ions toward the anode. Chunlei et al. (Geng et al., 2008) employed an accelerated chloride ion diffusion (ACID) device (refer to Fig. 2-6) to expedite the diffusion of chloride ions in concrete. This gadget may erode steel reinforcement within a few days, enabling researchers to expedite the evaluation of corrosion inhibitor efficacy. They asserted that the ACID approach augmented chloride ingress through concrete cover via electro-osmosis, hence reducing the corrosion duration.

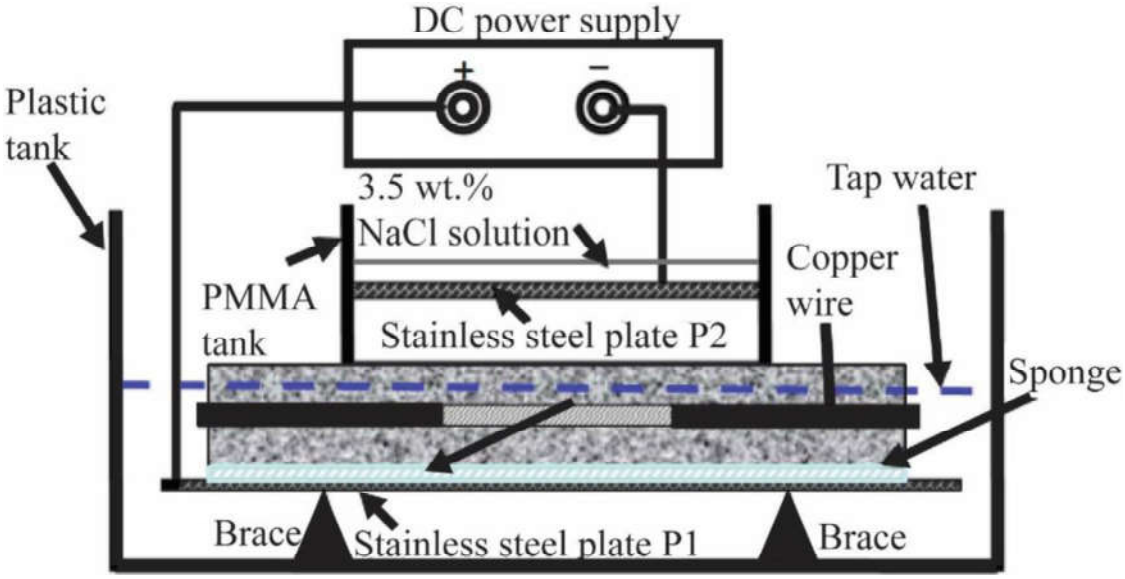

Figure 2-6. Schematic representation of the accelerated corrosion test for steel in concrete utilizing the ACID method (Feng et al., 2021).

2.10.3 Artificial Climate Environment (ACE) method

Enhancing the corrosion process through splashes, saltwater spraying, and modifying climatic conditions without the use of electricity can likely replicate the natural ion transport mechanism. The two aforementioned strategies for expediting the corrosion of reinforcing steel were devised by electrochemical methods utilizing a DC power source and submerging reinforced concrete samples in a NaCl solution. The primary elements influencing the corrosion of reinforced concrete structures in the natural environment are humidity, temperature, and oxygen availability. The artificial climate environment (ACE) approach is typically formulated by considering the influencing factors and aims to establish a conducive condition for enhancing corrosion rates. The ACE technique is generally executed by positioning specimens within an environmental chamber equipped with temperature and relative humidity monitoring capabilities, adjustable spray nozzles, and loading jigs (Feng et al., 2021).

2.11 Transportation and Accumulation Process of Chloride Ions and Major Influential Factors

Chloride ions are transported from the marine atmosphere to bulk concrete via wind-driven ingress from sea air to the concrete surface. The chloride ions subsequently infiltrate, distribute, and accumulate within the concrete mass due to concentration gradients and capillary absorption. (Yang et al., 2017). The subsequent sections examine the transit method, accumulation regulations, and variables influencing chloride ions in concrete within the marine atmospheric environment.

2.11.1 Chloride Ion Transport in Marine Atmosphere

Biological, physical, and chemical interactions in the seabed frequently produce air bubbles that detonate and ascend to the sea surface, resulting in the formation of marine whitecaps and breaking surf, which create marine aerosols. The sea wind, which agitates and carries saltwater, is the force responsible for marine whitecaps and breaking surf in the marine atmospheric zone. Ascending air currents enable marine aerosols to climb thousands of meters into the atmosphere and be transported several kilometers inland by prevailing winds. These particles inherently create a chloride environment (i.e., a marine aerosol environment) as a result of wind interacting with the saltwater surface. The marine aerosol generated by breaking surf possesses a high chloride concentration and larger particles, while the marine aerosol produced by whitecaps contains a low chloride concentration and smaller particles. A study (Xu & Zhao, 1994) demonstrated that the concentration of marine aerosols generated by breaking surf is approximately 40 times more than that produced by whitecaps. Consequently, the sea spray generated by breaking waves significantly contributes to the chloride-induced corrosion of

marine reinforced concrete structures. Nevertheless, marine aerosols comprising larger particles generated by breaking surf have a limited airborne travel distance, resulting in a significant decrease in concentration with increasing distance from the coastline. The distance from the coast significantly affects both chloride salt deposition and the surface chloride concentration in concrete (Morcillo et al., 2000). Field data documented in the literature (Safehian et al., 2013) were gathered to examine the correlation between the surface chloride concentration of concrete and the proximsity to the coast. A nonlinear regression analysis (Equation 2-2) indicated that an exponential function was utilized to characterize the correlation between surface chloride concentration and distance from the coast:

$$C_{S,air}^{1}(d) = 1.16e^{-0.01d} \ldots \textit{Equation 2-2}$$

Where:

$C_{S,air}^{1}(d)$: the apparent surface chloride concentration (% by mass of the binder) of concrete as a function of the distance from the shore,

d: distance from the coast (m).

2.11.2 Transportation Process of Chloride Ions within Concrete

Chloride ions in salt sprays accumulate on the surface layer of unsaturated concrete in a maritime environment and infiltrate the concrete through pore water, influenced by parameters such as concentration gradient, wetting and drying cycles, and capillary action (C. Li et al., 2010). The aforementioned critical elements indicate that wetting and drying cycles considerably impact the deposition of chloride salts and the distribution of chloride ions in concrete. When external conditions are arid, water evaporates from the exposed extremities of capillary pores that are accessible to the surrounding air. Consequently, the salinity of the residual water escalates

adjacent to the concrete surface, as only pure water undergoes evaporation, leaving the salt behind. If environmental conditions become moist, the dry concrete absorbs chloride salt water. The concentration gradient caused by diffusion propels salts in the water adjacent to the concrete surface towards areas of lower concentration. It is evident that water migrates outward while salts migrate inward during this process. The subsequent cycle of wetting with saline solution introduces additional salt solution into the capillary pores. The concentration gradient now diminishes outward from a maximum value at a specific depth beneath the surface. Internal chloride ions penetrate more as additional external chloride ions are introduced into the concrete via pore water. As wetting and drying occur, chloride ions from external sources are continually transported and deposited on the surface layer of concrete, leading to an increased concentration within the bulk concrete. It is important to recognize that there are two types of chloride ions in concrete: binding chloride ions, which are absorbed by the solid matrix, and free chloride ions, which exist in the pore solution of the concrete (A. Neville, 1995).

The concentration of surface chlorides in concrete depends on environmental conditions, exposure time, and the water-to-binder ratio. As the hydration process continues, the porosity and pore structure of the concrete improve, slowing the rate of increase in surface chloride concentration over time until it reaches a plateau.

An exponential mathematical relationship has been formulated to describe the evolution of surface chloride concentration over time:

$$C^{3}_{S,air}(t) = 2.30(1 - e)^{-0.97t} \text{ ...Equation 2-3}$$

Where:

$C_{S,air}^{3}(t)$: the apparent surface concentration of chlorides (%) in the concrete according to exposure time.

t: denotes the exposure duration (in years).

The water-to-binder ratio also significantly affects concrete density, pore structure, and the concrete's ability to bind chloride ions. Studies have shown a linear relationship between surface chloride concentration and the water-to-binder ratio, represented by the following equation:

$$C_{S,air}^{4}(R_{W/B}) = 3.01R_{W/B} \ldots \textit{Equation 2-4}$$

Where:

$C_{S,air}^{4}(R_{W/B})$: the ratio of water to the total mass of cement and mineral additives, and expresses the apparent surface concentration of chlorides (%) accordingly.

$R_{W/B}$: is the water-to-binder ratio,

These results indicate that increasing the water-to-binder ratio leads to a linear increase in surface chloride concentration, which enhances the potential for reinforcement corrosion in concrete exposed to the marine atmosphere (Wang et al., 2015).

2.12 Pozzolanic Materials

Pozzolan is characterized as a siliceous or siliceous-aluminous substance that, on its own, exhibits minimal or negligible cementitious value; however, when finely divided and in the presence of water, it can react with calcium hydroxide at ambient temperature to produce compounds with cementitious properties (Sánchez de et al., 2013). The definition of pozzolan is determined by its capacity to react with lime and water rather than its source material. When pozzolan interacts with lime in aqueous conditions, hydroxide ions are liberated, resulting in an elevation in the pH level (about 12.4). At

that juncture, pozzolanic processes transpire, wherein silicon and aluminum amalgamate with the available calcium, producing cementitious compounds known as calcium silicate hydrates (CSH) and calcium aluminate hydrates (CAH). One benefit of these chemicals is their enha ncement of the mixture's mechanical characteristics through the ongoing progression of pozzolanic reactions (Pourakbar et al., 2016).

2.12.1 Effect of Pozzolanic Materials on Concrete

The majority of concrete manufactured today is ordinary concrete, exhibiting suboptimal corrosion resistance indices. Concrete corrosion refers to the deterioration of the concrete matrix resulting from the impact of environmental physical-chemical processes(Aïtcin, 2007). The degradation of concrete structural elements subjected to soils and groundwater tainted with sulfate salts poses a significant challenge to concrete durability. Sulfate ions interact with the hydration products of cement, specifically C_3A and $Ca(OH)_2$, resulting in expansive and softening forms of degradation (Z. Ahmad, 2006).

Today, supplementary cementitious materials (SCMs) are commonly employed in concrete, either in blended cement or added individually in the concrete mixer. The use of SCMs such as blast-furnace slag, a byproduct from pig iron production, or fly ash from coal combustion, is a possible method to partially substitute Portland cement (PC). The use of such materials, where no additional clinkering process is involved, leads to a significant reduction in CO_2 emissions per ton of cementitious materials (grinding, mixing, and transportation of concrete use very little energy compared to the clinkering process) and is also a means to utilize by-products of industrial manufacturing processes.

The development of hydration products and the subsequent microstructural evolution are influenced by various parameters, including the characteristics of the Portland cement and pozzolanic material, the materials' fineness, the water-to-cement ratio, and temperature. Consequently, it is infeasible to accurately delineate the processes of clinker hydration and pozzolanic reaction. Nonetheless, the hydration of cement using pozzolanic elements exhibits a consistent pattern that allows for the identification of general behavior.

Pozzolanic activity dictates the velocity of the pozzolanic reaction, facilitating the production and augmentation of bond strength with calcium hydroxide (CH) in the presence of moisture. This activity encompasses all reactions between the active constituents of pozzolans and lime (Zeyad et al., 2017). Consequently, pozzolanic activity denotes the capacity of calcium ions (Ca^{2+}) from calcium hydroxide (CH) to interact with siliceous or aluminous substances, resulting in the formation of stable compounds possessing cementitious characteristics.

The incorporation of pozzolanic mineral additives in blended cement enhances the quality of concrete paste. Both physical aspects, including tiny particle size and chemical effects related to the pozzolanic reaction are essential.

Physical effects largely influence the composition of the mixture, its fluidity, and the extent of hydration. The primary advantages of pozzolanic activity encompass enhanced resistance to thermal cracking, diminished alkali-aggregate expansion, and decreased permeability to deleterious fluids, hence augmenting the strength and durability of cement (Jokhio et al., 2020).

The short-term pozzolanic activity is contingent upon specific surface area, whereas the long-term activity is influenced by chemical and mineral

composition (Aprianti et al., 2015). Active pozzolans facilitate the forward chemical reaction by engaging with CH in the hydrated concrete. The pozzolanic reaction serves as a secondary catalyst for the primary reaction between cement and water.

Research indicates that amorphous silicon dioxide (SiO_2) and aluminum oxide (Al_2O_3) found in pozzolanic materials undergo a chemical reaction with calcium hydroxide (CH) generated by the hydration of ordinary Portland cement (OPC), leading to the synthesis of calcium silicate hydrate (CSH) and calcium aluminate hydrate (CAH), recognized as cement hardening products. This process is referred to as the pozzolanic reaction (A. M. Neville, 1995).

The combination of lime and pozzolan with water results in the decomposition of calcium hydroxide, elevating the pH to 12.5. At this elevated pH, calcium (Ca^+), potassium (K^+), and sodium (Na^+) ions solubilize, thereby commencing the pozzolanic reaction.

Calcium hydroxide (CH) generated from cement hydration serves as the principal source of lime that interacts with pozzolans. This is contingent upon the ratio of C_3S and C_2S that interact with water to produce CSH and CH. Research demonstrates that about 25% of calcium hydroxide (CH) interacts with pozzolans, but the remaining 75% has a role in enhancing the strength and durability of concrete (Ayub et al., 2021).

2.12.2 Effect of Filler Materials on Concrete

The incorporation of fillers is an effective method to enhance the microstructural and mechanical scharacteristics of concrete, as evidenced by certain research (Awoyera et al., 2019). Fillers are often finely pulverized substances employed to occupy spaces in concrete, hence achieving a more

compact microstructure that enhances mechanical qualities. The advantage of utilizing fillers lies in their diminutive size and form, which allows them to effectively occupy the pores in concrete and aggregates. The inclusion of fillers enhances the compactness and parking density of the cemented paste (Awoyera, et al., 2017). During the mixing stage, fillers help reduce the friction between aggregate particles, thereby enhancing the packing density of the fresh concrete mixture(Awoyera, et al., 2017). Fillers can enhance both the hardened and fresh characteristics of concrete. Fillers may be naturally occurring, synthetically produced, or byproducts of various industrial processes. Although fillers are typically chemically stable, they may interact with hydrated cement paste and, in certain instances, display hydraulic qualities. Nonetheless, these features do not adversely affect the concrete but rather improve the characteristics of the cement paste.

The incorporation of fillers in concrete enhances its qualities and provides environmental advantages, as many fillers are byproducts of other industrial processes, and their utilization mitigates environmental deposition. Fillers diminish the quantity of cement needed, hence decreasing the total embodied energy and carbon footprint of the concrete. Microstructural studies indicate that the use of fillers results in a more homogeneous structure and enhances the particle packing of aggregates in concrete (Moosberg-Bustnes et al., 2004).

2.13 Sustainable aspects of the use of wastes in concrete

Due to exponential population expansion, nations worldwide are confronted with the persistent increase of various types of trash. In 2016/17, developed nations such as Australia produced approximately 67 million tons of garbage, of which only 37 million tons (55%) were recycled (Sandanayake,

et al., 2020). Conversely, it has been stated that Beijing, one of China's largest cities, processes 25,000 tons of waste daily (Guo et al., 2020). The waste materials primarily originate from residential garbage, commercial and industrial waste, as well as construction and demolition waste (Sandanayake, et al., 2020). Although these waste products might be repurposed, most are disposed of in landfills, resulting in detrimental environmental effects as well as social and economic consequences. Effective management, disposal, and reutilization are essential for tackling the principal challenge of waste generation. Despite the implementation of various ways to manage, reuse, or dispose of waste effectively, a modern solution that can complete the loop and foster a circular economy has yet to be realized. The building sector is a primary contributor to environmental degradation and a significant user of resources. built structure is accountable for considerable energy consumption and carbon emissions over its whole life cycle, from material acquisition to end-of-life (Luo et al., 2019). A significant portion of these results from the utilization of virgin resources in building. Research indicates that around 15% of a building's energy usage and carbon emissions derive from materials (Sandanayake, et al., 2020). The excessive utilization of virgin materials in construction leads to the consumption of natural resources and imposes further environmental difficulties (Sandanayake, et al., 2020). Consequently, substituting virgin resources with waste products tackles both critical concerns: the overproduction of trash and the consumption of virgin materials.

Numerous research investigations have concentrated on utilizing waste products to produce diverse construction materials(Lu et al., 2019). Concrete is unequivocally recognized as the primary construction material, utilizing the majority of raw resources and contributing to substantial energy usage (Sandanayake et al., 2019). In the last ten years, several studies have focused

on minimizing energy consumption and carbon emissions while lowering reliance on virgin materials in concrete (Callejas et al., 2017). The principal objective of most of these studies is to mitigate environmental impacts by substituting virgin resources with waste materials (Akadiri et al., 2013). Consequently, the utilization of waste in construction materials, such as concrete, as a sustainable resource that can promote environmental advantages has been thoroughly investigated. Before designating these as sustainable materials, it is essential to meticulously evaluate several more characteristics, including social benefits, practical implementation, appropriateness, and availability (Sandanayake, et al., 2020). The primary objective of prior research on incorporating waste materials into concrete was to substitute cement and thereby diminish the use of virgin resources (Ghahari et al., 2017). Furthermore, this also tackles the problem of producing substantial waste quantities in landfills. Nevertheless, numerous studies emphasize the challenges of utilizing waste materials in concrete, particularly regarding the substantial costs and energy expenditure required for converting these resources into a usable form (Sargam et al., 2020).

2.14 Effect of ceramic powder on concrete

Substituting cement in concrete with trash yields significant energy savings and offers substantial environmental advantages. Furthermore, it will significantly reduce concrete expenses, as cement constitutes about 45% of the total concrete expense. Some writers assert that the optimal approach for enhancing sustainability in the construction industry is to utilize trash from other industries as building materials (Meyer, 2009). Ceramic waste, characterized by its durability, hardness, and exceptional resistance to biological, chemical, and physical deterioration, is not amenable to recycling

through any current processes. The incorporation of inorganic industrial byproducts in concrete production will promote sustainable concrete design and an environmentally friendly approach (Hooton et al., 1995).

The utilization of ceramic waste in concrete production has garnered significant interest from scholars and practitioners over the past decade as a substitute for cement (Raval et al., 2013). The pozzolanic activity of the waste has been validated, resulting in the establishment of upper limits on the ceramic-to-cement replacement ratios (35%) to mitigate adverse impacts on strength development (Puertas et al., 2008). This results from the delayed hydration of the pozzolana and the diminished availability of calcium hydroxide required to initiate the pozzolanic process. The integration of ceramic waste into cement and concrete effectively reduced the leaching of harmful chemicals, including zinc, boron, and zirconium, typically used for surface glazing of tiles and ceramic artifacts. Furthermore, as both waste ceramic powder and fine aggregates often exhibit a broader grain-size distribution compared to cement and river sand, enhanced matrix compaction can be attained, resulting in diminished pore diameters(Gonzalez-Corominas et al., 2014). The reduced pore size also led to enhanced penetration resistance against chloride assault (Higashiyama et al., 2012).

2.15 Effect of glass powder on concrete

Utilizing solid waste materials or industrial by-products as a partial substitute for cement in concrete is an effective approach to diminish the reliance on Portland cement, hence mitigating the environmental and energy repercussions of concrete manufacturing (Gopalakrishnan et al., 2011). Federico and Chidiac, along with Jin et al (Federico et al., 2009), assert that mixed-color waste glass provides the requisite chemical composition and

reactivity for application as a supplemental cementitious material, enhancing the chemical stability, moisture resistance, and durability of concrete. To actualize this potential, waste glass must be pulverized to a micro-scale particle size to expedite its advantageous chemical interactions with concrete.

There are variations in the impact of glass powder on the compressive strength of cured concrete, specifically regarding the optimal glass powder content. Kumarappan and Khatib (Kumarappan, 2013) concluded that an enhancement in concrete compressive strength is observed with up to 10.0% glass powder cement substitution. Vandhiyan, Ramkumar, and Ramya (Vandhiyan et al., 2013) investigated the substitution of cement with waste glass powder and determined that a significant enhancement in early strength was observed, especially in specimens containing 15% glass powder, which exhibited a 29% increase in strength at 7 days compared to the control specimen. At 28 days, this disparity in strength diminishes to 23%. The optimal strength increase occurs at a 10% replacement level. Dali (Dali et al., 2012) examined the impact of glass powder filtered through a 600 μm screen and found that the compressive strength increased with up to 25% cement replacement, with the maximum enhancement occurring at 20% replacement. Patil (Patil et al., 2013) conducted experimental work utilizing glass powder with a particle size of less than 90 μm and determined that concrete compressive strength improves with up to 10.0% replacement of cement with glass powder. The test results of Vasudevan (Vasudevan et al., 2013) indicated that including glass powder up to 20.0% improved the compressive strength of concrete. Chikhalikar (Chikhalikar et al., 2012) noted that concrete compressive strength improves with glass powder cement replacement up to 20.0%, while Vijayakumar (Vijayakumar, 2013) determined that incorporating 75 μm sieved glass powder up to 40.0%

increases concrete compressive strength. The prior behavior of concrete compressive strength, when modified using glass powder as a cement substitute, was similarly noted in tensile and flexural strengths.

2.16 Effect of marble powder on concrete

The manufacturing of cement can be diminished by substituting a portion of the cement with waste elements that may enhance the properties of both fresh and hardened concrete. This would diminish the quantity of industrial operations, enhance cost and time efficiency while mitigate environmental contamination. Consequently, given the global demand for substantial quantities of cement, substituting cement with industrial and agricultural byproducts can yield economic and environmental advantages worldwide (Nagarajan et al., 2014). One ton of cement necessitates 1.5 tons of raw materials, 0.3 tons of air, and 6 gigajoules of fuel, resulting in the emission of 0.94 tons of CO_2 into the atmosphere (Şahan Arel, 2016). The incorporation of recycled industrial waste in concrete manufacturing can enhance economic efficiency and mitigate environmental impact (Topçu et al., 2007). Mining wastes, typically non-biodegradable and enduring in natural ecosystems, have been extensively utilized in concrete manufacturing (Levy et al., 2004). Marble dust is one of these byproducts. The incorporation of leftover marble in concrete manufacturing could be a significant advancement in sustainable development (Baboo et al., 2011).

Marble has been a highly favored material for construction and decoration since antiquity. It is employed for both structural and aesthetic purposes (Başaran et al., 2023). The utilization of waste materials to improve the characteristics of other substances, such as soil, has been documented in the literature (Arbili et al., 2022). The substantial energy consumption

involved in processing marble rocks is identified as a detrimental factor contributing to environmental contamination from waste marble powder (WMP) (Tugrul Tunc, 2019). A significant proportion of WMP is generated during the cutting and shaping of marble in various applications (Bostanci, 2020). This trash is projected to weigh 200 million tons worldwide (Ericsson, 2019).

Aliabdo et al. (Aliabdo et al., 2014b) examined the likelihood of employing WMP in the production of cement and concrete. The study initially assessed the properties of cement modified with WMP (cement with WMP additive), followed by an analysis of concrete, including WMP as a substitute for both cement and sand. The incorporation of WMP in concrete as a substitute for cement or sand enhanced both the mechanical and physical qualities of the concrete, especially with a reduced water-cement ratio. Ashish (Ashish, 2018) assessed the likelihood of WMP serving as a partial substitute for sand and cement. Concrete was mixed with WMP at weight proportions of 0%, 10%, and 15% for this purpose. The mechanical and durability properties may be achieved by utilizing 20% WMP. Seghir et al. (Toubal Seghir et al., 2019) also examined the feasibility of employing WMP as a partial replacement for cement in air-cured mortar. Three modified levels of cement substitution were evaluated: 5%, 10%, and 15% of the cement's weight. The findings indicated that substituting cement with WMP affected the physical and mechanical properties of air-cured mortar.

2.17 Effect of graphite powder on concrete

Enhancements in the mechanical performance of concrete are ascribed, though not only, to the incorporation of micro-level additional cementitious elements, including silica fume and fly ash. Alterations in the mechanical,

physical, and chemical qualities of concrete can be effectively attained and controlled by varying the quantities of its constituent components. The pore microstructure of concrete, including pore size, distribution, and interconnections, is crucial in influencing several properties of concrete, particularly conductivity (Medeiros-Junior et al., 2016).

Cement-based composites have been combined with various additives and admixtures to create a multifunctional material and enhance its mechanical, chemical, acoustical, thermal, and other qualities. Certain additions may originate from waste materials, thereby being revalorized as components of new composites, commonly referred to as eco-friendly composites. In recent years, numerous research studies have concentrated on the potential of carbon-derived additives in cement composites, including carbon black (Mingqing et al., 2008), natural graphite (Ahmed Sbia et al., 2015b), graphene nano-platelets(Du et al., 2016), Colloidal graphite(Chung, 2001), graphene nanotubes (Konsta-Gdoutos et al., 2010), Carbon nanofibers (Peyvandi et al., 2013), graphene oxide (X. Li et al., 2016), among others.

Graphite is a material frequently utilized by numerous industrial enterprises. It can be sourced from quarries or produced synthetically, and it serves as an excellent conductor of electricity and heat, particularly when high purity is attained (Rodrigues et al., 2013). The incorporation of graphite in cement-based composites is becoming increasingly important due to its enhancement of heat conductivity and piezo resistivity (He et al., 2014).

Ground expanded graphite (GEG) enhances the volumetric heat capacity and thermal conductivity of cement composites; nevertheless, with a GEG concentration of even 1%, thermal conductivity exhibits minimal variation while compressive strength increases by up to 16%. Conversely, an

increase in GEG by 15% resulted in a reduction of compressive strength by 30% (Yuan et al., 2012).

2.18 Effect of carbon black on concrete

Carbon black (CB) is a conductive material with a high surface area and low cost, making it a suitable option for enhancing the piezoresistive effect in smart cementitious composites (Monteiro et al., 2017). When subjected to compressive loads, CB contributes to the formation of a conductive network within the matrix, improving the ability to sense quasi-static and dynamic loads (Wen et al., 2007). However, its effect on mechanical properties is limited. Studies have shown that its addition to polymer-enhanced cementitious composites (ECCs) may improve sensing performance to a certain extent, but this depends on the loading conditions and curing age (Yıldırım et al., 2020) Regarding compressive and flexural strength(Ding et al., 2013) found that the addition of nanocarbon black (NCB) may result in a slight improvement in compressive strength due to an improved micro-filling effect, while its effect on flexural strength was negligible. Therefore, CB is an effective and low-cost conductive filler.

2.19 Concluding Remarks

A review of prior literature confirms that partially replacing cement with environmentally friendly alternative materials can significantly improve the mechanical and durability performance of concrete. However, while numerous studies have explored conventional pozzolanic materials such as fly ash, silica fume, and slag, limited research has focused on unconventional and sustainable materials derived from waste, such as ceramic, glass, marble, graphite, and carbon black—especially in the context of reinforced concrete structural elements exposed to aggressive environments.

Ceramic powder, typically originating from construction and demolition waste, possesses pozzolanic activity that allows it to react with calcium hydroxide, leading to the formation of additional calcium silicate hydrate (C-S-H). This reduces permeability and improves both strength and durability. Yet, studies on its optimal dosage and long-term behavior in structural elements remain scarce. Similarly, glass powder has shown potential to enhance later-age strength due to its amorphous silica content; however, its high alkali content raises the risk of alkali-silica reaction (ASR), particularly at elevated replacement levels. Comprehensive studies on its safe incorporation in structural concrete mixtures are still lacking.

Marble powder, another construction waste product, acts primarily as an inert filler that enhances particle packing and reduces the water demand. Despite its wide availability, few studies have evaluated its effectiveness as a sustainable additive in reinforced concrete exposed to chloride-laden environments. Likewise, graphite and carbon black, which are industrial by-products, contribute not only to filler effects but also introduce electrical conductivity within the cementitious matrix. However, their integration in conventional concrete systems—and their impact on both mechanical performance and corrosion resistance—remains an emerging area with insufficient experimental validation, particularly under accelerated corrosion conditions.

In addition, most previous investigations have been limited to small-scale specimens such as cubes or cylinders, without extending the evaluation to full-scale reinforced concrete columns subjected to realistic loading and deterioration scenarios. The interaction between these waste-derived materials and steel reinforcement under long-term environmental exposure,

including electrochemical corrosion, has not been comprehensively addressed.

Therefore, a significant research gap exists in experimentally and numerically assessing the individual effects of ceramic, glass, marble, graphite, and carbon black powders as cementitious replacements or filler additives in reinforced concrete. This includes investigating their influence on key mechanical properties such as compressive strength, splitting tensile strength, and density, as well as evaluating their impact on critical durability parameters including half-cell potential, chloride ion penetration, and pressurized water permeability. Moreover, the structural behavior of reinforced concrete columns incorporating these materials has not been sufficiently examined. In addition, the study includes the development of numerical models using advanced finite element software such as ABAQUS to simulate the mechanical behavior and deterioration of the tested concrete columns before and after corrosion. Addressing these gaps is essential for advancing sustainable concrete technology that combines durability, structural performance, and resilience in harsh environmental conditions.

Chapter Three: The Experimental Work

3.1 General

This chapter aims to identify and clarify the practical steps that will be followed to implement research based on replacing a portion of cement with alternative materials to improve the mechanical properties and durability of reinforced concrete columns. Based on a review of previous studies, it has been shown that the use of alternative materials such as ceramic powder, marble powder, glass powder, graphite, and carbon black can improve the properties of concrete columns and enhance their resistance to corrosion.

This chapter will detail the test program for conducting laboratory experiments aimed at studying the effect of these materials on concrete. Cement will be partially replaced by ceramic powder and glass powder at replacement levels of 5%, 10%, and 15% by weight of cement. In addition, marble powder will be incorporated at similar proportions of 5%, 10%, and 15%. Furthermore, graphite powder and carbon black will be introduced as additives at lower ratios of 0.5%, 1%, and 1.5% by weight of cement. The experiments will include testing the concrete's compressive strength, splitting strength, and density, as well as corrosion tests such as half-cell potential and chloride ion penetration, as shown in Figure 3-1.

These effects will be studied by comparing the performance of reinforced concrete columns replaced with these materials with conventional concrete without replacement, with a focus on improving their resistance to severe environmental influences such as corrosion resulting from the interaction of reinforcing steel with chloride ions.

These tests will be conducted according to established engineering standards to ensure the accuracy of the results. This chapter includes a detailed description of the procedures and methodology used to conduct these experiments.

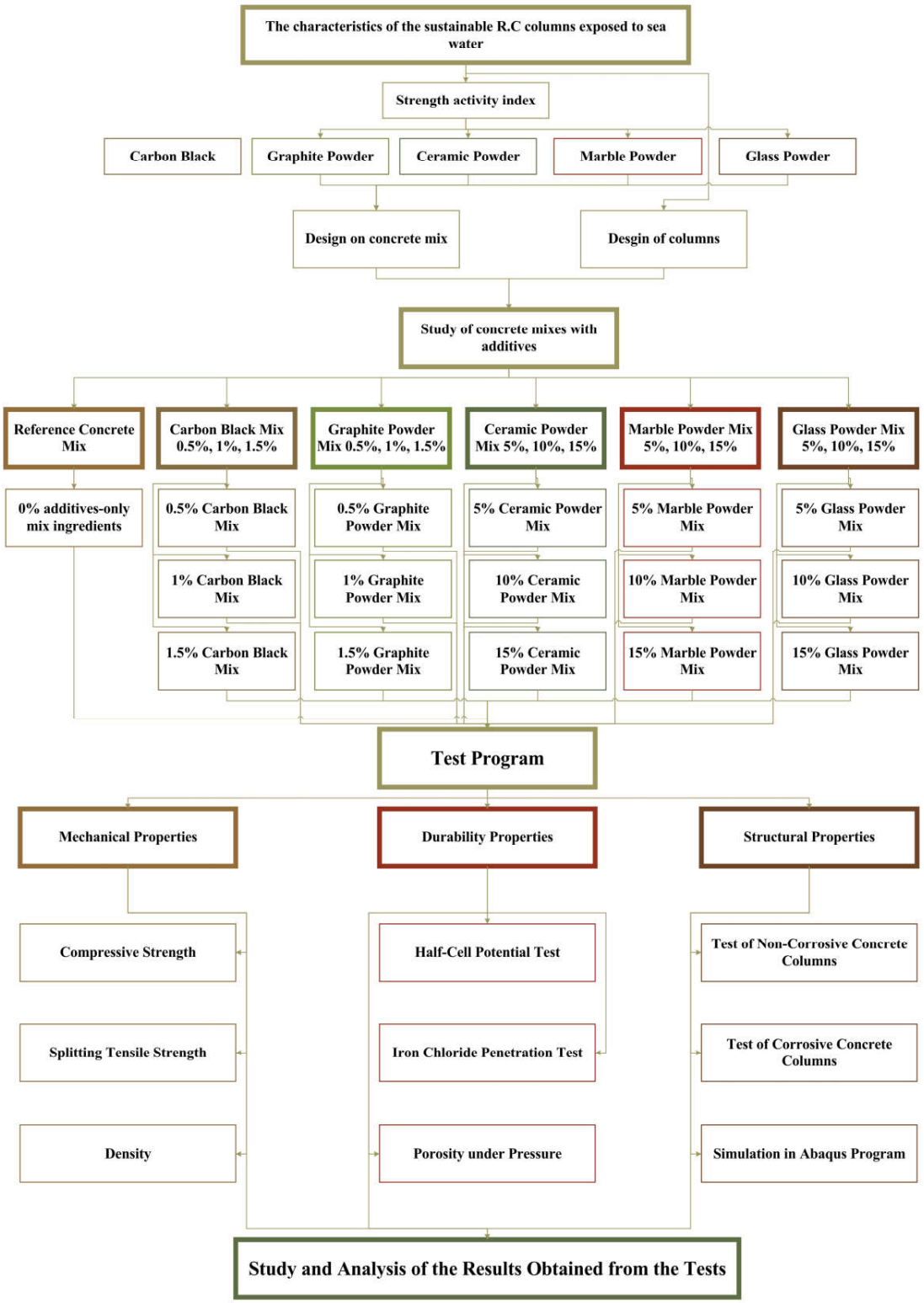

Figure 3-1. Detailed outline of the practical program followed in the study.

3.2 Materials

Concrete is a fundamental material in contemporary buildings owing to its versatility, durability, and structural integrity. Cement, aggregates, water, and often chemical and mineral admixtures are essential constituents for concrete to possess the requisite properties in both its fresh and hardened states. The meticulous selection and proportioning of these materials are crucial, since each component contributes uniquely to the combination, so enhancing the overall durability and performance of concrete.

Concrete mixtures must possess suitable mechanical strength, durability, and workability; thus, the materials must be meticulously selected and balanced. High-quality cement, aggregates, and water ensure robust structural performance, while the incorporation of chemical and mineral admixtures enhances specific properties according to the requirements of the mix. Consequently, it will review the fundamental materials utilized in the formulation of concrete mixtures.

3.2.1 Cement

Cement functions as the primary binding agent in concrete, bonding the other components and providing the necessary stability for many applications. The hydration process involves the combination of cement with water, resulting in a solid matrix that imparts strength and durability to concrete.

The quality of the cement significantly influences concrete's compressive strength, setting time, and long-term durability. Moreover, achieving the optimal water-to-cement ratio (w/c ratio), which affects both workability and strength, is fundamentally contingent upon the quantity of cement in the mixture relative to other components. Optimal cement selection and proportioning are essential for concrete to perform effectively and meet

the demands of both conventional and high-performance construction projects.

Iraqi sulfate-resisting Portland cement from the Karbala cement plant in Iraq was utilized in this study. This type adheres to IQS 5-2019 standards. The chemical and physical parameters of the utilized cement were conducted in the construction materials laboratory of Kerbala and are presented in Tables 3-1 and 3-2, respectively.

Table 3-1. Chemical composition and main compounds of sulfate-resisting Portland cement.

Properties	Chemical analysis of compounds		
Oxide	Chemical formula	Percentage % by weight	I.Q.S. 5: 2019 limits
Lime	CaO	57.5	/
Silica	SiO_2	18.9	/
Alumina	Al_2O_3	3.47	/
Iron oxide	Fe_2O_3	3.6	/
Sulfate	SO_3	2.75	2.5 (max)
Magnesia	MgO	3.72	5.0 (max)
Sodium oxide	Na_2O	0.25	/
Potassium oxide	K_2O	0.67	/
Insoluble residue	I.R	0.82	1.5 (max)
Loss on ignition	L.O.I	3.5	4.0 (max)
Lime saturation factor	L.S.F	0.95	0.66 – 1.02
Bogue potential compound composition		Percent by weight of cement	
Tricalcium silicate (C_3S)		61.98	/
Diacalcium silicate (C_2S)		7.45	/
Tricalcium aluminate (C_3A)		3.1	3.5 (max)
Tetra calcium aluminoferrite (C_4AE)		10.95	/

Table 3-2. Physical properties of cement.

Physical properties	Value	I.Q.S. 5:2019 limits
Fineness (Blaine specific surface (m^2/Kg))	285	230 (minimum)
Time of setting (Vicat test)		
Initial set (hrs.: min)	1:35	00:45 (minimum)
Final set (hrs.: min)	4:35	10:00 (maximum)
Compressive strength (MPa)		
2 days	18.9	10.00 (minimum)
28 days	33.5	32.50 (minimum)

3.2.2 Fine Aggregate

Sand is an essential component in concrete formulations, serving as a fine aggregate to equilibrate the proportions of cementitious materials and coarse aggregate. It is crucial to enhance the cohesion, stability, and density of the mixture during the processes of mixing and pouring. Sand contributes to minimizing voids in concrete, hence improving its compressive strength and resistance to external factors.

Sand selection must adhere to established criteria to ensure its purity and the absence of hazardous pollutants such as salts, clay, and organic matter. To enhance physical attributes such as workability and crack resistance, a uniform particle distribution within the mixture is attained by utilizing appropriately graded sand.

The properties of both fresh and cured concrete are directly influenced by the quality and particle size distribution of the sand. The particle size distribution and fineness modulus of the aggregates were determined according to the test methods outlined in IQS No. 45/1984. Table 3-3 shows

the physical properties of fine aggregate. Figure 3-2 illustrates the particle size distribution of the fine aggregate.

Table 3-3 Fine aggregate properties.

Fine aggregate properties	Value	Limits
Sulfates content	0.065 %	Max: 0.5%
The passing ratio of sieve No. 200	0.3 %	Max: 5%
Fineness modulus	2.34	2.3 – 3.1
Specific gravity	2.60	/

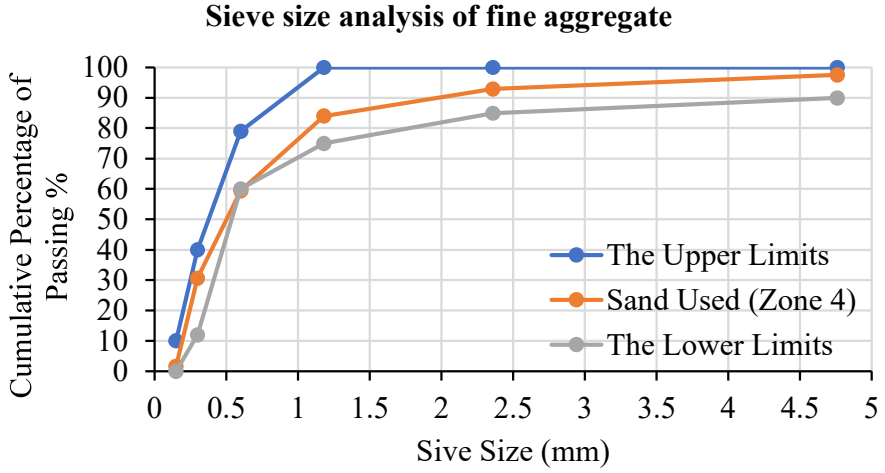

Figure 3-2. The particle size distribution of fine aggregate.

3.2.3 Coarse Aggregate

Coarse aggregate, or gravel, is a primary component of concrete mixtures, constituting the bulk of the concrete volume and being crucial for its strength and longevity. Gravel enhances the structural properties of concrete by providing internal support and reducing shrinkage and deformation caused by loads or environmental influences.

The performance of concrete is significantly influenced by the size, shape, and quality of the coarse aggregate. Well-graded aggregates are sought

to attain uniform particle distribution and minimize voids between particles. This enhances the compressive strength of the concrete.

It is essential to ensure that the aggregate is devoid of hazardous impurities such as sulfates, clay, and organic matter, as they may hinder chemical reactions or diminish the concrete's durability. The particle size distribution and nominal maximum size of the aggregates were determined in accordance with the test methods outlined in IQS No. 45/1984. Table 3-4 shows the physical properties of fine aggregate. Figure 3-3 illustrates the particle size distribution of coarse aggregate.

Table 3-4. Coarse aggregate properties.

Coarse aggregate properties	Value	Limits
Sulfates content	0.053%	Max: 0.1%
The passing ratio of sieve No. 200	0.06%	Max: 3%
Nominal maximum size	14	/
Specific gravity	2.65	/

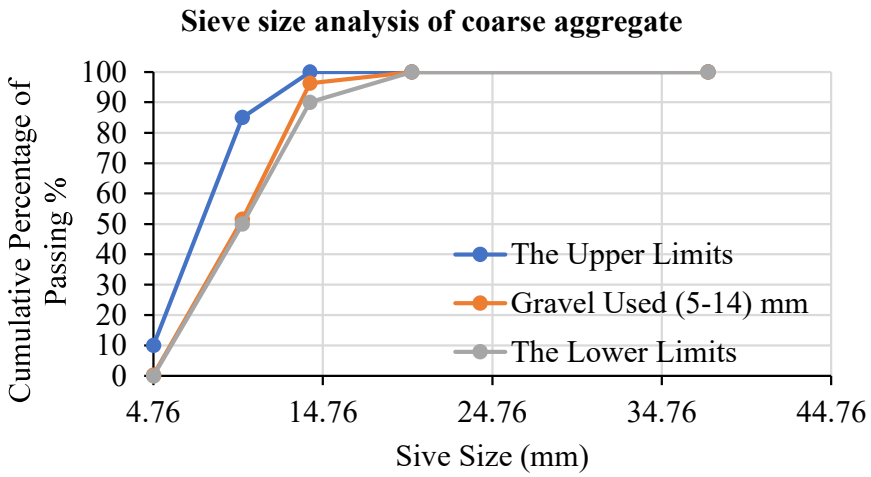

Figure 3-3. The particle size distribution of coarse aggregate.

3.2.4 Chemical Admixture (KUT PLAST SP 400)

In this study, KUT PLAST SP 400 complies with BS 5075, and ASTM C494 Type F is used for the purpose of improving the workability of concrete. KUT PLAST SP 400 is designed to improve the qualities of both fresh and hardened concrete. It is a high-performance concrete admixture that falls under the superplasticizer category. By reducing the mix's water-to-cement ratio, this ingredient increases the concrete's mechanical strength and density. Additionally, it improves fresh concrete's workability without adding more water.

Furthermore, KUT PLAST SP 400 increases the concrete's resistance to harsh environmental factors, including freeze-thaw cycles and exposure to sulfates and chlorides, while reducing the likelihood of cracks brought on by thermal shrinkage or drying.

Table 3-5 shows the physical properties and working requirements of superplasticizers KUT PLAST SP 400. According to the manufacturer's details listed in the data sheet.

Table 3-5. Physical properties and working requirements of superplasticizers KUT PLAST SP 400.

Properties	Values by manufacturer data sheet
Calcium chloride content	Nil
Specific gravity	1.24 – 1.26 @ 20°C
Air entrainment	Less than 1% additional air is entrained
Setting Time	3 – 4 hours
Dosage	2.5 liters / 100 kg cement
Chloride content	Nil to BS 5075

3.2.5 Water

The quality of water utilized in the mixtures significantly impacts the properties and longevity of concrete. The hydration process between cement and water, a chemical reaction that produces the binding agent responsible for concrete's strength and longevity, is significantly dependent on pure water. Organic substances, oils, acids, and alkalis are examples of contaminants that may disrupt this process or lead to the degradation of the concrete's chemical and physical properties over time. To ensure enough mechanical strength and minimize the risk of cracks or undesired reactions in the concrete construction, ACI 318 and ASTM C1602 recommend the use of clean, potable water during the mixing and curing procedures. Great attention was taken during the process of pouring the concrete mixtures utilized in the investigation.

3.2.6 Steel Bars Reinforcement

To enhance the mechanical properties of concrete, particularly its tensile strength and resistance to deformations caused by static or dynamic loads, the incorporation of reinforcement steel, or rebar, is crucial.

The selection of reinforcing steel is determined by attributes such as diameter, mechanical strength, and surface texture that enhance the steel-concrete bond.

The steel bars must conform with ASTM – A1064 specifications. The geometrical and mechanical properties were tested in the laboratory of Kerbala University. The properties of the steel bar used in reinforcement are shown in Table 3-6.

Table 3-6. Reinforcement steel properties.

Property	Nominal diameter (**mm**)		
Nominal diameter (**mm**)	8	6	4
Actual diameter (**mm**)	7.9	5.81	4
Cross-section area (**mm²**)	49	26.4	12.6
Yield stress (**MPa**)	373.5	405.3	475
Ultimate stress (**MPa**)	525.05	605.6	728.0
Elongation (**%**)	35	17.0	5.4
Nominal weight (**Kg/m**)	0.376	0.208	0.103
Grade	G 40	G 40	G 60

3.2.7 Materials Used in The Study

Cementitious, pozzolanic, and filler components are crucial for enhancing the mechanical and durability properties of concrete. Consequently, this study employed various materials to illustrate their impact on the mechanical, durability, and structural characteristics of concrete. These materials will be shown.

3.2.7.1 Silica Fume

Silica fume, a byproduct of the silicon and ferrosilicon alloy industry, is extensively utilized in concrete for its remarkable capacity to improve strength, durability, and performance. Silica fume primarily consists of exceedingly small particles that, when incorporated into concrete, occupy the voids between cement particles and reduce the overall porosity of the material. It reacts to generate more calcium silicate hydrate (C-S-H), so enhancing the concrete's density and microstructure and exhibits significant reactivity with

calcium hydroxide, a byproduct of cement hydration. The compressive strength, flexural strength, and resistance to severe environmental factors such as sulfate attack and chloride ingress all markedly improve as a consequence.

Silica fume used in the mixes is MegaAdd MS (D) densified micro-silica. The properties of the silica fume are presented in Table 3-7 at 25°C according to the manufacturer.

Table 3-7. Silica fume properties.

Property	Values by manufacturer data sheet
State	Sub-micron powder
Color	Grey to medium grey powder
Specific gravity	2.10 to 2.40
Bulk density	500 to 700 kg/m^3

3.2.7.2 Local Waste Materials

3.2.7.2.1 Ceramic Powder

The preparation of ceramic materials as a pozzolanic cement substitute via grinding is an innovative strategy for enhancing the sustainability of the construction industry. This technology seeks to utilize ceramic waste tiles by converting them into finely ground materials with pozzolanic activity. Utilizing advanced grinding apparatus such as ball mills or jet mills, ceramics are pulverized into fine particles, therefore augmenting the material's surface area and enhancing its chemical reactivity with calcium hydroxide produced during cement hydration. Ground ceramic materials enhance concrete performance through superior mechanical and chemical properties, such as increased compressive strength and reduced permeability, while simultaneously mitigating environmental effects by decreasing cement usage,

a significant contributor to carbon emissions. Thus, the construction sector's utilization of ground ceramic materials as a pozzolanic additive contributes to sustainability goals and minimizes waste.

Figure 3-4. Ceramic powder.

The local ceramics were refined using an industrial iron mill to obtain a powder with a sieve size of 200, i.e., smaller than 75 microns as shown in figure 3-4. Table 3-8 shows the chemical composition of ceramic powder.

Table 3-8. Chemical Composition of Ceramic Powder.

Constituents	**% by Mass**
Silicon dioxide (SiO_2)	66.57
Aluminum Oxide (Al_2O_3)	21.60
Iron Oxide (Fe_2O_3)	1.41
Calcium Oxide (CaO)	2.41
Sodium Oxide (Na_2O)	1.41
Potassium Oxide (K_2O)	2.79
Zirconium Oxide (ZrO_2)	1.49

3.2.7.2.2 Glass Powder

To mitigate the environmental effects of conventional cement production and enhance sustainability in the building sector, ground glass is regarded as a viable pozzolanic material that can serve as a partial substitute for cement in concrete manufacturing. The elevated amorphous silica content in ground glass imparts pozzolanic activity, enhancing the strength and durability of concrete by reacting with calcium hydroxide produced during the hydration of cementitious mixtures to generate supplementary cementitious compounds such as calcium silicate hydrate (C-S-H).

Moreover, the incorporation of ground glass improves concrete performance by reducing permeability and increasing resistance to chemical assaults, particularly from sulfates. Glass recycling reduces carbon emissions associated with cement production and diminishes the volume of waste directed to landfills.

Figure 3-5. Glass powder.

The waste glass was refined using an industrial iron mill to obtain a powder with a sieve size of 200, i.e., smaller than 75 microns as shown in figure 3-5. Table 3-9 shows the chemical composition of glass powder.

Table 3-9. Chemical Composition of Glass Powder.

Constituents	% by Mass
Silicon dioxide (SiO_2)	71.09
Aluminum Oxide (Al_2O_3)	3.52
Iron Oxide (Fe_2O_3)	1.77
Calcium Oxide (CaO)	10.59
Sodium Oxide (Na_2O)	10.46
Potassium Oxide (K_2O)	0.89
Magnesium Oxide (MgO)	1.56

3.2.7.2.3 Marble Powder

In concrete production, ground marble serves as a viable material that can partially substitute cement, reducing the reliance on conventional cement, which has a significant carbon impact, and fostering environmental sustainability. Calcium hydroxide generated during cement hydration can react with marble, mostly consisting of calcium carbonate along with varying amounts of silica and alumina, to form additional compounds that enhance the internal structure of concrete.

The utilization of ground marble has numerous benefits, such as enhancing the workability of concrete mixtures and increasing concrete density, hence reducing water permeability and augmenting resistance to external chemicals. Moreover, recycling marble trash conserves production expenses and natural resource use while also diminishing landfill waste.

Figure 3-6. Mable powder.

The waste marble was refined using an industrial iron mill to obtain a powder with a sieve size of 200, i.e., smaller than 75 microns as shown in figure 3-6. Table 3-10 shows the chemical composition of marble powder.

Table 3-10. Chemical Composition of Marble Powder.

Constituents	% by Mass
Silicon dioxide (SiO_2)	1.28
Aluminum Oxide (Al_2O_3)	1.38
Iron Oxide (Fe_2O_3)	0.54
Calcium Oxide (CaO)	50.10
Sodium Oxide (Na_2O)	0.29
Magnesium Oxide (MgO)	1.72

3.2.7.3 By-Product Materials

3.2.7.3.1 Black Carbon

The incorporation of carbon ash enhances concrete performance by augmenting both early and late compressive strength, diminishing

permeability, and bolstering concrete durability against environmental threats, including chemical corrosion and sulfate attacks.

Figure 3-7. Black carbon

The utilization of carbon ash is crucial in attaining sustainability objectives by diminishing the volume of solid waste directed to landfills, so alleviating the environmental impact linked to this waste. This procedure also aids in reducing greenhouse gas emissions associated with conventional cement production methods, hence supporting the attainment of carbon footprint reduction objectives in the building industry. The black carbon used in this study was nano-sized as shown in Figure 3-7.

3.2.7.3.2 Graphite Powder

Graphite powder is an advantageous filler element that can enhance concrete characteristics and promote environmental sustainability. This powder is generated as a byproduct of graphite production or the incineration of graphite in diverse sectors, with a distinctive chemical makeup with substantial carbon content, rendering it a useful additive in cementitious compositions.

Figure 3-8. Graphite powder.

Furthermore, the utilization of graphite powder diminishes the depletion of natural resources by repurposing industrial waste into a value-added material within the construction industry. Given these advantages, utilizing graphite powder as a filler in cement is a promising approach to enhance the environmental and mechanical properties of concrete in sustainable construction applications. The graphite powder used in this study was smaller than 75 microns as shown in Figure 3-8.

3.3 Strength activity index

The Strength Activity Index (SAI) is one of the primary indicators used to evaluate the effectiveness of cementitious additives, such as fly ash, silica fume, or natural pozzolanic materials. It measures their contribution to compressive strength when used as a partial replacement for Portland cement. According to ASTM C311, this index is calculated by comparing the compressive strength of a cement paste containing the additive at a specified replacement ratio (usually 20% by mass) with that of a reference mix containing no additives. The result is expressed as a percentage.

The reference mix is prepared using 500 grams of Portland cement, 1375 grams of standard sand, and 242 ml of water. The test mix consists of 400 grams of Portland cement, 100 grams of the material under evaluation, and 1375 grams of standard sand, with sufficient water to achieve workability (flow) that does not differ by more than ±5% from the reference mix. The test can be performed at 7 or 28 days, and the strength is determined based on the average of three 50 x 50 x 50 mm cubic samples. The admixture is considered effective if the index exceeds 75% of the reference mix strength at 7 or 28 days, as specified in ASTM C618.

This index is widely used in the areas of quality control and classification of pozzolanic materials. It is used to determine their suitability for use in high-performance concrete mixes and various construction environments.

Figure 3-9 represents an image of tested samples of the strength activity index models. The strength of the study materials was made and gave the results shown in Figure 3-10 at the age of 7 days. The Strength Activity Index with Portland cement is calculated using the ratio of the average compressive strength of the test mixture (A) to that of the control mixture (B), multiplied by 100. The strength activity index of glass powder, marble powder, ceramic powder and carbon black are 106.56 %, 129.17%, 128.66 % and 126.06 respectively.

Figure 3-9. Mortar samples used in testing.

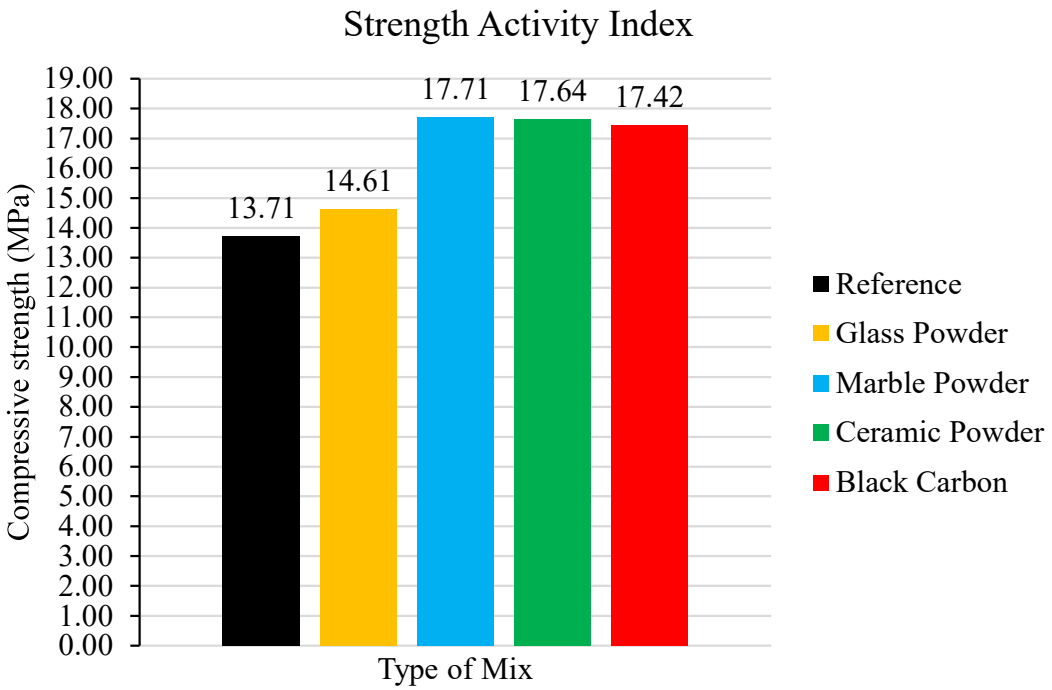

Figure 3-10. Strength activity index.

The results show that all samples achieved values higher than the reference sample, demonstrating the effectiveness of these materials in improving the properties of mixtures.

3.4 Concrete Mix Proportion

Determining the optimal ratio of cement, water, admixtures, and aggregates (both coarse and fine) to achieve the desired performance characteristics is an essential phase in the civil engineering procedure of concrete mix proportioning. The project's specific requirements—namely compressive strength, workability, durability, and climatic conditions—guide this process. Accurate proportioning is essential to ensure the concrete's long-term performance in its intended application, hence preventing issues such as excessive cracking, diminished strength, or inadequate durability. Table 3-11 presents the ratios of the essential components in the concrete mix design

employed in the investigation. The concrete mixture used in this study was designed based on the recommendations provided in ACI 211.4R-08, which offers guidelines for selecting proportions for high-strength concrete mixtures.

Table 3-11. Proportions of the concrete mixes.

Mix proportions based on replacement percent	Cement (**Kg/m3**)	Silica fume (**Kg/m3**)	Sand (**Kg/m3**)	Gravel (**Kg/m3**)	SP (L/100 Kg)	Water/Binder ratio	Additives or Replacement (**Kg/m3**)	Water (**Kg/m3**)
Reference Mix								
0%	450	50	700	950	2.5	0.3	0	150
Carbon black and Graphite Powder (Additives)								
0.5%	448	50	700	950	2.5	0.3	2	149
1%	446	50	700	950	2.5	0.3	5	148
1.5%	443	50	700	950	2.5	0.3	7	147
Marble Powder (Replacement)								
5%	428	50	700	950	2.5	0.3	22	143
10%	405	50	700	950	2.5	0.3	45	136
15%	383	50	700	950	2.5	0.3	68	129
Ceramic Powder and Glass Powder (Replacement)								
5%	428	50	700	950	2.5	0.3	22	150
10%	405	50	700	950	2.5	0.3	45	150
15%	383	50	700	950	2.5	0.3	68	150

3.5 Trial Mixes

Two sets of experimental mixes were prepared. The first set contained the studied materials (ceramic powder, glass powder, marble powder, and carbon black) at ratios of 10%, 20%, 30%, and 40%, with silica fume being

used in the mix. The second set contained the studied materials (ceramic powder, glass powder, marble powder, and carbon black) at ratios of 1%, 3%, 5%, and 7%, with silica fume being used in the mix at the age of 28 days.

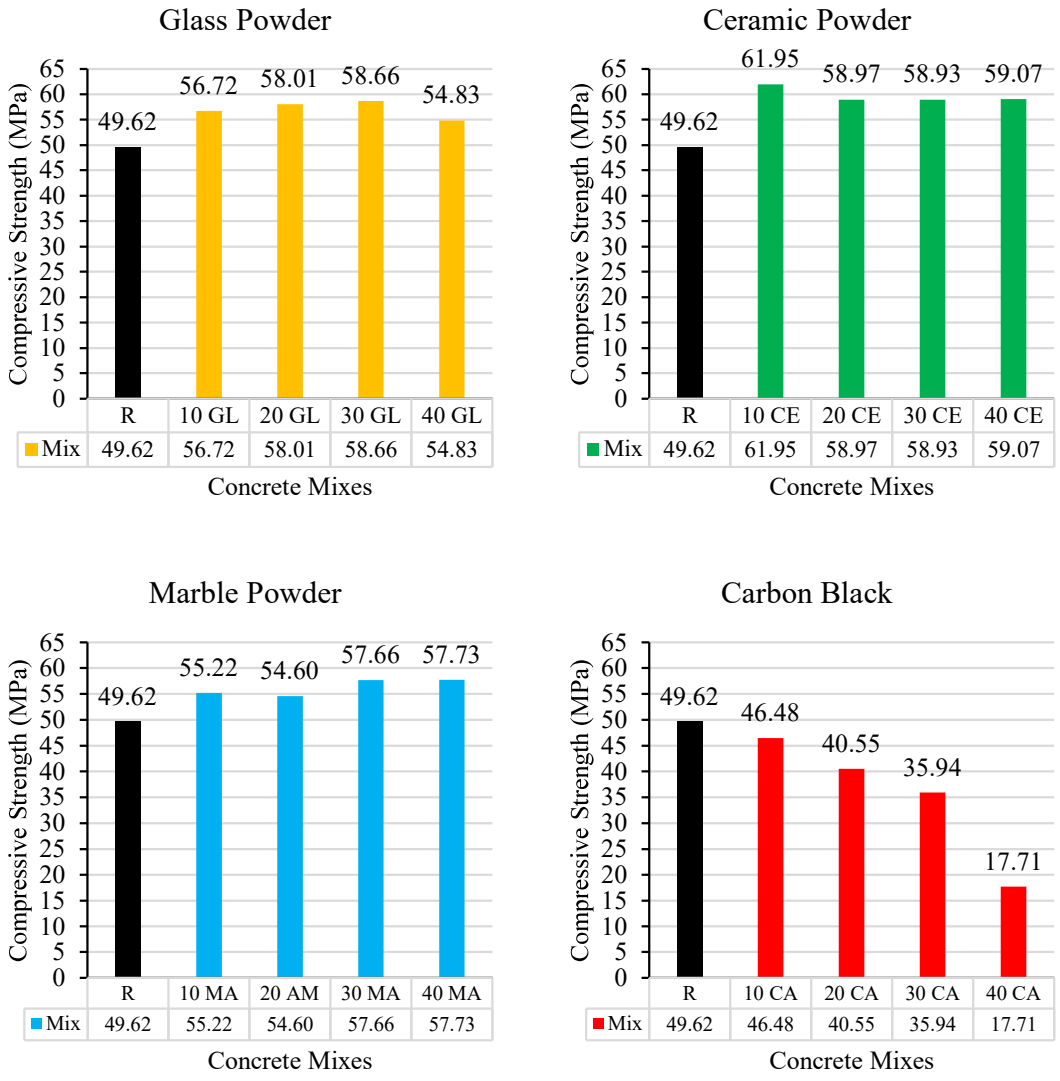

Figure 3-11. Compressive strength results from mixes of materials with different proportions and silica fume.

Several experimental mixtures were conducted to determine the optimum proportions to be used later in the study. Experimental mixtures of ceramic powder, glass powder, marble powder, and carbon black were prepared at ratios of 10%, 20%, 30%, and 40% in the presence of silica fume,

as shown in Figure 3-11 at the age of 28 days. It was concluded that, in general, as the replacement ratio increases, compressive strength decreases significantly.

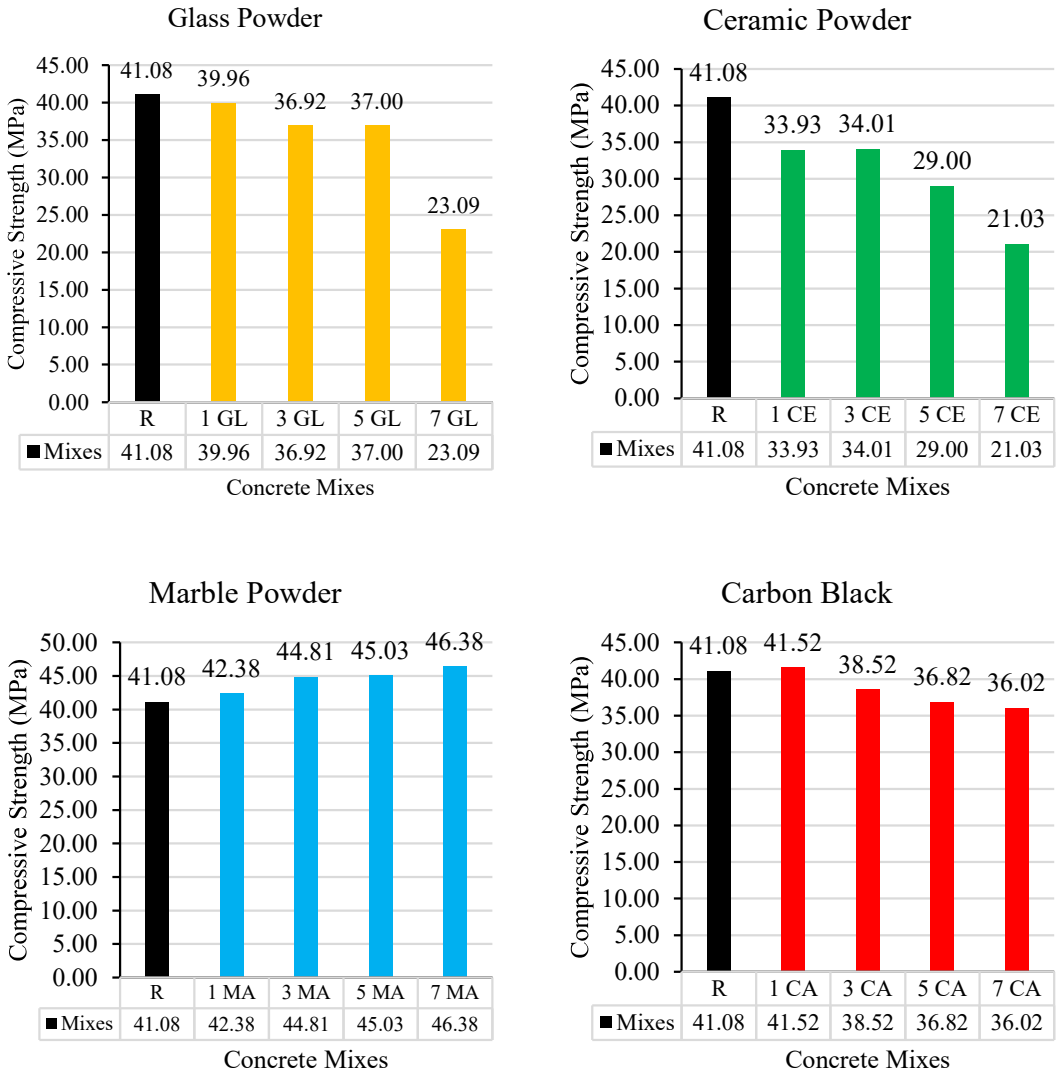

Figure 3-12. Compressive strength results of mixes of materials with different proportions and fly ash.

Experimental mixtures of ceramic powder, glass powder, marble powder, and carbon black were prepared at ratios of 1%, 3%, 5%, and 7% in the presence of fly ash, as shown in Figure 3-12. The results showed that when fly ash is used, the effectiveness of the mixtures is generally reduced.

Based on the above and after reviewing previous research, the percentages shown in Table 3-11 were adopted.

The selection of the replacement ratios for the various powder additives was based on preliminary experimental trials conducted prior to the main study. For graphite and carbon black powders, the additive levels of 0.5%, 1.0%, and 1.5% by weight of cement were adopted, as these percentages were found to be the most effective in enhancing the mechanical performance of the concrete. In contrast, ceramic, marble, and glass powders were used at 5%, 10%, and 15%, since the test results indicated that the most noticeable changes either slight improvement or decline tended to occur around the 10% level.

Additionally, silica fume was selected over fly ash as a supplementary cementitious material due to its superior performance during the preliminary testing stage. These adopted ratios were not only supported by the outcomes of the trial mixes but were also consistent with the findings and recommendations reported in previous research studies by other scholars.

3.6 Casting and Curing of Specimens

The method of preparing the concrete models studied was through the following steps:

1. Prepare the reinforcing steel according to the required measurements that were previously found in the design and then connect them together to form the required reinforcement network.
2. Prepare the plastic molds with the required dimensions (5 × 10 cm cylinders, 10 × 10 × 10 cm cubes, 15 × 15 × 15 cm cubes, 10 × 30 cm small column molds, and 15 × 70 cm large column molds) with

lubrication and cleaning for the purpose of pouring concrete as it shown in Figure 3-13.

3. Place the reinforcing steel in their molds and secure them well by using spacers to adjust the cover evenly on all sides.
4. Prepare the weights of the materials included in the mixture (sand, gravel, and cement etc.) according to the previously specified proportions.
5. Add the weighed materials to a 180-liter mixer and then mix them for 3 to 5 minutes, and finally, empty them into a handcart for the purpose of pouring them into the molds.
6. Pouring concrete into the previously prepared molds with continuous use of an electric vibrator to ensure good compaction and get rid of voids, then polishing the final surface of the molds.
7. After completing the pouring, the concrete molds were covered with a plastic cover to preserve the mixing water, and then all the models were matured by immersion for 28 days.

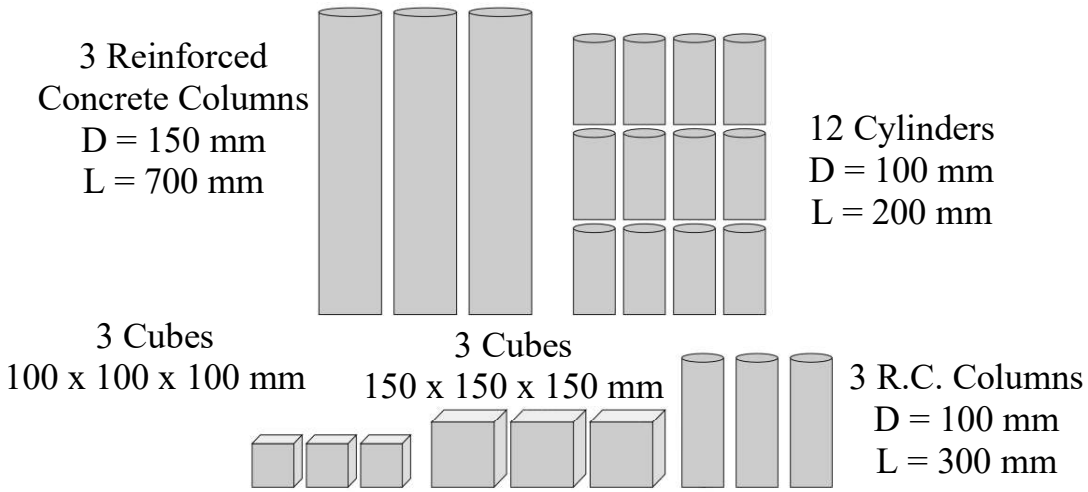

Figure 3-13. Samples were prepared in the study for each concrete mix.

3.7 Concrete Testing

Mechanical tests of concrete are among the most important tools used to evaluate the quality and performance of concrete in engineering applications. These tests include measuring compressive strength, splitting strength, and density. These tests play a crucial role in ensuring that concrete conforms to design standards and engineering specifications.

3.7.1 Compressive Strength

The compressive strength test was performed using concrete cubes with dimensions of 100mm×100mm×100mm, according to Iraqi specification IQS No.52/1984. All cubes were immersed in water for 28 days before testing. The test was performed using a digital hydraulic compression machine of ELE type with a capacity of 2000kN, as shown in Figure 3-14. The compressive strength for each test was calculated based on the average value of three cubes, and all tests were performed at the age of 28 days.

Figure 3-14. Compressive strength test.

3.7.2 Splitting Tensile Strength

The split tensile strength test was performed according to ASTM C496-04 using cylindrical concrete specimens with dimensions of 100 mm × 200 mm. During the test, two thin plywood strips were placed between the specimen on the top and bottom sides of the testing machine to ensure even

load distribution. The test was performed using a 2000 kN ELE digital hydraulic press, as shown in Figure 3-15. The load was applied at an average rate of 1.4 MPa/min until the specimen failed, and the final result was based on the arithmetic mean of the tensile strength of three specimens for each test group.

Figure 3-15. Splitting tensile strength test.

3.7.3 Density

Concrete cubes of dimensions 100mm×100mm×100mm were used to determine the density. The samples were immersed in tap water for 24 hours, and their immersed and saturated masses were measured. After that, the samples were dried in an oven at a temperature of 100–110°C for 24 h, and the dried mass was measured. This test was carried out according to the standard specification ASTM C138-01.

3.7.4 Structural Behavior

To study the behavior of concrete columns exposed to corrosion, concrete columns not exposed to corrosion and those exposed to corrosion were examined under the influence of axial load as shown in Figure 3-16. The concrete column was placed between two thick steel plates at the top and bottom to ensure uniform load distribution and to simulate simple support conditions. The slenderness ratio of the tested column was approximately

18.67, which is relatively less than the limiting value of 22 commonly defined in structural design codes such as ACI for classifying slender columns. The concrete columns not exposed to corrosion were first tested using an electrical loading device to study the structural behavior of sustainable concrete columns. Then, the concrete columns exposed to accelerated corrosion were tested using electric current. One of the most important outputs of this test was the load-deflection curves. These curves were adopted to extract the values of ultimate load, ductility, and toughness to be compared later.

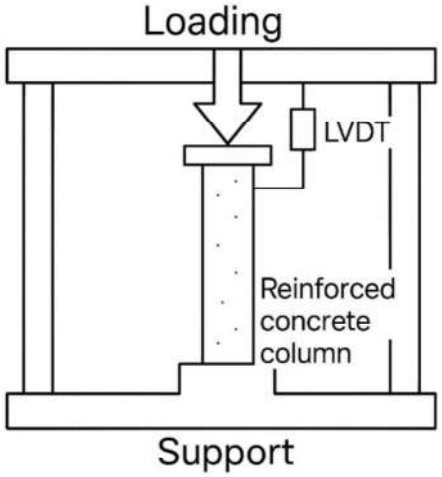

Figure 3-16. Reinforced concrete column test mechanism diagram.

Toughness was calculated by calculating the area under the load-displacement curve resulting from experimental testing of concrete elements. This numerical integration represents the amount of energy absorbed by the structural element up to the moment of failure and is a direct indicator of the element's ability to resist progressive failure. The calculation method was adopted using numerical integration by dividing the curve into small segments and summing the areas between successive load and displacement points. Thus, the strength was estimated in kN/mm. This method is approved in ACI 544.2R for evaluating the performance of reinforced concrete elements.

The ductility of the tested elements was calculated using the ratio of the ultimate displacement at maximum load to the displacement corresponding to a loading point representing 60% of the maximum load. This method is used as a practical alternative to assess the element's ability to withstand deformations after passing the yield stage, particularly in tests that rely on load-displacement curves. This ratio is an accepted indicator of ductile behavior and reflects the extent to which the element retains its load-bearing capacity. This method has been used in a number of studies related to the behavior of reinforced concrete elements(Kim et al., 2022).

3.7.5 Half-Cell Potential Test

This test method addresses the assessment of the electrical corrosion potential of uncoated reinforcing steel in both field and laboratory concrete, aimed at evaluating the corrosion activity of the reinforcing steel. This testing methodology is constrained by electrical circuitry. Concrete surfaces in building interiors and arid conditions lose moisture to the extent that their resistivity increases significantly, necessitating specialized testing techniques. Concrete surfaces that have been coated or treated with sealers may not establish a satisfactory electrical circuit as shown in Figure 3-17.

This testing method is appropriate for both in-service assessment and research and development activities. This testing procedure applies to members irrespective of their dimensions or the thickness of the concrete cover over the reinforcing steel. Concrete cover exceeding 3 inches (75 mm) may lead to an average of neighboring reinforcement corrosion potentials, resulting in diminished capacity to discern variations in relative corrosion activity. This testing approach can be employed at any point throughout the lifespan of a concrete element.

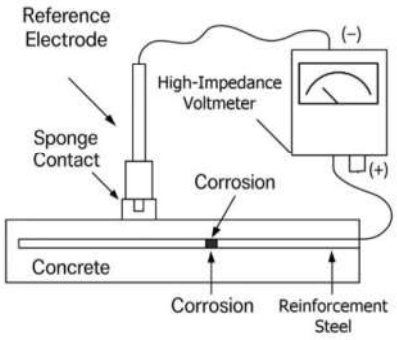

Figure 3-17. Half-cell potential test.

The Standard Test Method for Half-Cell Corrosion Potentials of Uncoated Reinforcing Steel in Concrete (ASTM C876) provides guidelines for interpreting the half-cell potential measurements. The potential values indicate the likelihood of corrosion of reinforcing steel in concrete. Below is the typical table of values used for interpreting the results:

Table 3-12. The potential values of corrosion of reinforcing steel in concrete.

Measured Half-Cell Potential (versus Cu/$CuSO_4$ Electrode)	**Corrosion Likelihood**
Less than -200 mV	90% probability of no corrosion
Between -200 mV and -350 mV	Uncertain likelihood of corrosion
Greater than -350 mV	90% probability of active corrosion

3.7.6 Iron Chloride Penetration Test

This test method covers the determination of the electrical conductance of concrete to provide a rapid indication of its resistance to the penetration of chloride ions according to ASTM C1202 − 17.

This testing method involves measuring the electrical current flowing through 50-mm-thick slices of 100-mm nominal-diameter cores or cylinders over a duration of 6 hours. A direct current potential difference of 60 V is

sustained between the specimen's ends, with one end submerged in a sodium chloride solution and the other in a sodium hydroxide solution. The total charge transferred, measured in Coulombs, has been determined to correlate with the specimen's resistance to chloride ion ingress Figure 3-18.

Qualitative indications of the chloride ion penetrability based on the measured values from this test method are provided in Table 3-13.

Table 3-13. Chloride Ion Penetrability Based on Charge Passed.

Charge Passed (Coulombs)	Chloride Ion Penetrability
>4,000	High
2,000–4,000	Moderate
1,000–2,000	Low
100–1,000	Very Low
<100	Negligible

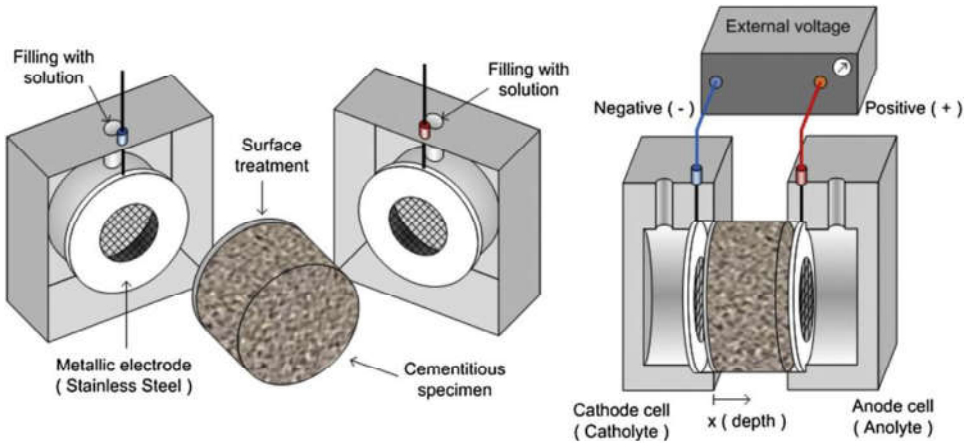

Figure 3-18. Chloride ion penetration test for concrete.

3.7.7 Permeability Under Pressure Test

The water permeability test of concrete under pressure is one of the key experiments used to assess the durability of concrete and its resistance to water penetration. This method involves measuring the depth of water ingress into a concrete specimen after exposing one surface to constant water pressure

for a specified period, in accordance with the British/European standard BS EN 12390-8: Testing hardened concrete – Part 8: Depth of penetration of water under pressure. The test is typically performed on cubic concrete specimens 150*150*150 mm that have been cured for 28 days. Constant water pressure usually 7 bar is applied to one face of the specimen for 72 hours while the remaining sides are sealed to prevent lateral leakage as shown in Figure 3-19. After the test duration, the specimen is split vertically, and the maximum depth of water penetration is measured either visually or by using a colored dye. The result indicates the quality and compactness of the concrete; lower penetration depth reflects higher density and greater resistance to water ingress, which translates to improved durability in wet or aggressive environments. The permeability under pressure for each test was calculated based on the average value of two cubes, and all tests were performed at the age of 28 days. According to common practice, the permeability rating is typically classified as follows:

1. Low permeability: penetration depth ≤ 20 mm
2. Moderate permeability: 20 mm < depth ≤ 50 mm
3. High permeability: penetration depth > 50 mm

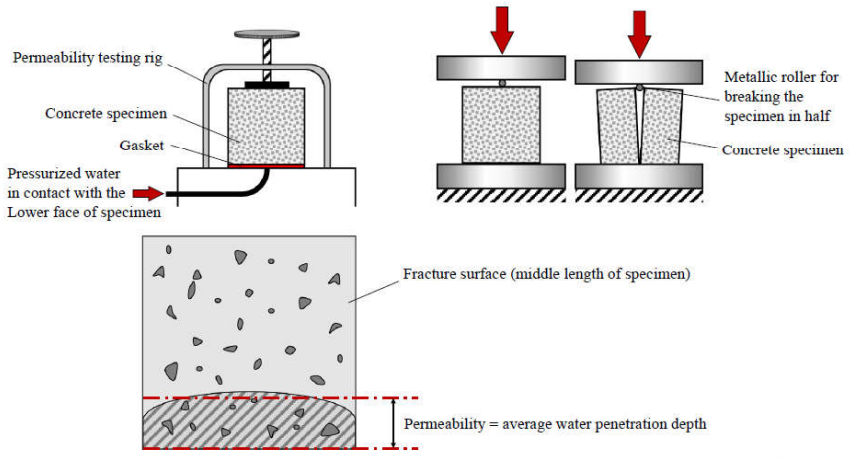

Figure 3-19. Schematic view of permeability under pressure test.

This test is particularly useful in the design of durable concrete mixes for structures exposed to moisture, salts, or chemical attack.

3.8 Reinforced Concrete Columns Construction

The concrete column was designed as per ACI Code 318-19 requirements, as shown in the details below.

3.8.1 Details of Columns

The final design was made using 8 steel bars of 8 mm diameter in the vertical direction with a 4 mm diameter bar in a spiral shape with a spacing between each ring of 4 cm. The diameter of the column was 150 mm, and the total length was 700 mm as shown in Figure 3-20. The casting was done with 15 mm plastic spacers on all sides to ensure the concrete cover, as shown in the attached picture.

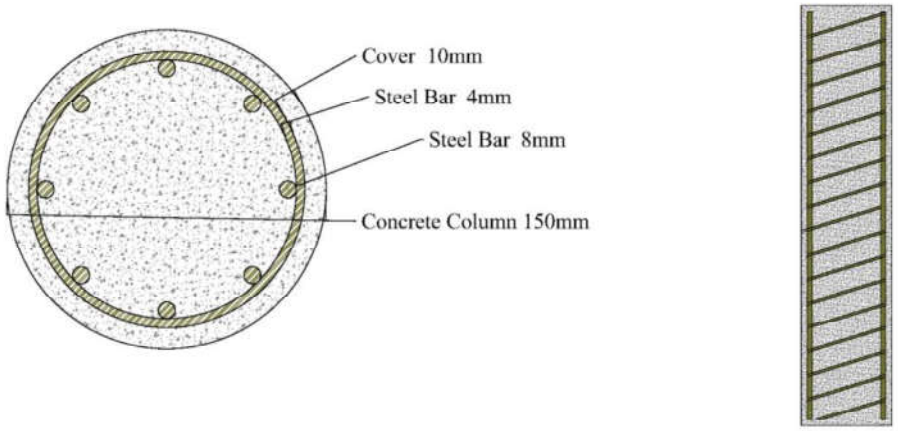

Figure 3-20. Reinforced concrete column diagram used in the study.

3.8.2 Columns Molding

The concrete column was poured according to the dimensions and reinforcement previously specified in the structural design. The molds were oiled, and then the reinforcement steel was placed, surrounded by plastic

spacers to ensure that the cover was evenly distributed from all sides. The concrete was poured in layers with continuous use of an electric vibrator to ensure complete compaction. The concrete was placed in the mold for 24 hours, then it was opened and placed for curing until the required time.

3.9 Accelerated Corrosion Regime

After the columns were treated for 28 days, the columns were placed in a corrosion acceleration system. Corrosion acceleration, which is mainly based on an electrochemical process, is a process that involves three main components: anode, cathode, and electrolyte solution. In this experiment, stainless steel plates were used as the cathode, while a solution containing 3.5% sodium chloride (NaCl) was used as the electrolyte solution as shown in Figure 3-21. To ensure the successive and good wetting and drying process, a 1000-liter plastic water tank was used to place the samples, and then all the samples were connected to tubes connected to the electrolyte solution pumps (NaCl). It is worth noting that when applying a constant direct current (DC) with a current intensity i for a specific period of time t, the mass loss is calculated according to Faraday's law as stated in paragraph 2.10.1. After applying the equation, the following values were reached, which were adopted in the practical program:

Percentage of Corrosion = 1%

I/cm^2 = 200 mA/cm²

Total time = 2.5 days

Number of cycles days = 7 days (each day 8 hrs. wet, 16 hrs. dry)

The selected values were determined based on an extensive set of experimental trials, supported by findings from previous studies. Ultimately, these values were adopted to ensure that the column specimens experienced a

moderate level of corrosion sufficient to reflect the deterioration effects—without leading to excessive swelling or spalling that could cause premature failure. This approach was essential to preserve the structural integrity of the specimens and allow for a meaningful evaluation of the performance improvements achieved by the modified concrete mixtures.

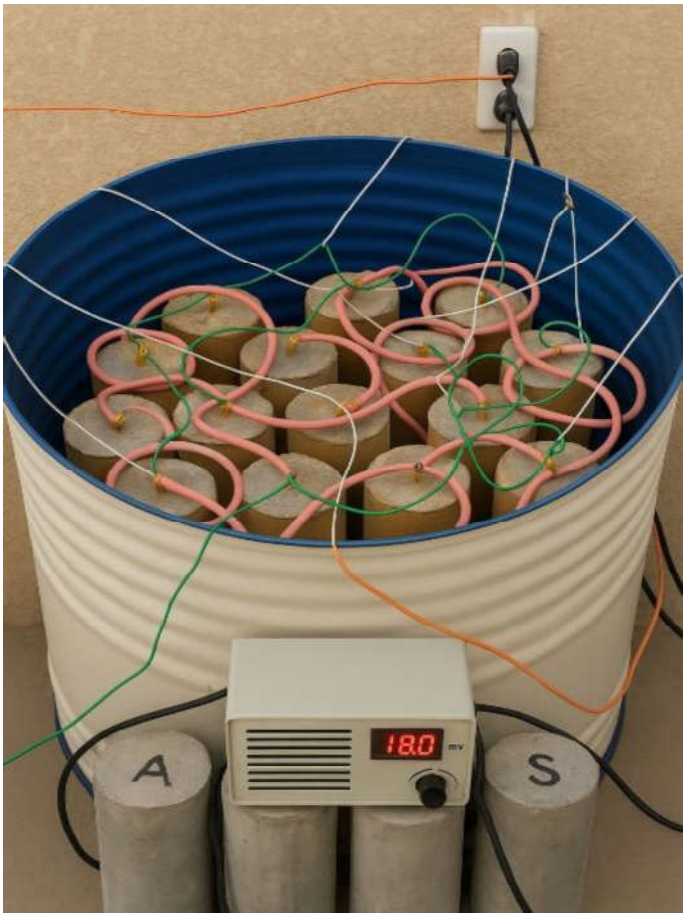

Figure 3-21. The mechanism of accelerating corrosion using electric current for the studied columns.

3.10 Concrete mix coding

A unified coding system was adopted to name the concrete mixes used in this study, based on the type of additive and its percentage of cement replacement sustained materials. Carbon black powder was designated by the

letter (CA), graphite powder by the letter (GA), marble powder by the letter (MA), ceramic powder by the letter (CE), and glass powder by the letter (GL).

The percentage of replacement was attached to each symbol to directly form the mix name. For example, mix (CA0.5) indicates the use of 0.5% carbon black powder, while (GL10) indicates a mix containing 10% glass powder.

Substitution percentages of 0.5%, 1.0%, and 1.5% were used for carbon black and graphite, while percentages of 5%, 10%, and 15% were used for marble, ceramic, and glass.

Table 3-14. Column concrete coding.

Groups	Materials	Percentage	Case	Coding
R	-	0%	Non-Corroded	R
G1	Ceramic	5%	Non-Corroded	5CE
	Ceramic	10%	Non-Corroded	10CE
	Ceramic	15%	Non-Corroded	15CE
G2	Marble	5%	Non-Corroded	5MA
	Marble	10%	Non-Corroded	10MA
	Marble	15%	Non-Corroded	15MA
G3	Glass	5%	Non-Corroded	5GL
	Glass	10%	Non-Corroded	10GL
	Glass	15%	Non-Corroded	15GL
G4	Carbon	0.5%	Non-Corroded	0.5CA
	Carbon	1%	Non-Corroded	1CA
	Carbon	1.5%	Non-Corroded	1.5CA
G5	Graphite	0.5%	Non-Corroded	0.5GR

	Graphite	1%	Non-Corroded	1GR
	Graphite	1.5%	Non-Corroded	1.5GR
CR	-	0%	Corroded	CR
G6	Ceramic	5%	Corroded	C5CE
	Ceramic	10%	Corroded	C10CE
	Ceramic	15%	Corroded	C15CE
G7	Marble	5%	Corroded	C5MA
	Marble	10%	Corroded	C10MA
	Marble	15%	Corroded	C15MA
G8	Glass	5%	Corroded	C5GL
	Glass	10%	Corroded	C10GL
	Glass	15%	Corroded	C15GL
G9	Carbon	0.5%	Corroded	C0.5CA
	Carbon	1%	Corroded	C1CA
	Carbon	1.5%	Corroded	C1.5CA
G10	Graphite	0.5%	Corroded	C0.5GR
	Graphite	1%	Corroded	C1GR
	Graphite	1.5%	Corroded	C1.5GR

For concrete columns, corroded specimens were distinguished from uncorroded specimens by adding the letter "C" at the beginning of the specimen code. For example, the code "C1.5GA" indicates a column containing 1.5% graphite powder that underwent accelerated corrosion, while the code "F1.5" indicates a similar column that was not corroded. This system helped organize test results and accurately compare them across different cases.

Chapter Four: Experimental Results and Discussion

4.1 General

In this chapter, the results obtained through the practical program will be presented, which are represented by different samples of 16 different mixtures. The 16 mixtures consisted of 15 different concrete mixtures containing materials in different proportions, replacing cement, in addition to a reference mixture that did not contain any cement substitute. The substitutes used included carbon, graphite, ceramic, marble, and glass in different proportions of replacement, where all materials were ground before replacement to a size less than 75 microns, as follows:

Mix 1: Reference mix without cement replacement sustained materials.

Mixes 2 to 7: Contain carbon and graphite powder replaced by (0.5%, 1%, 1.5%).

Mixes 8 to 16: contain ceramic, marble and glass powders substitutes (5%, 10%, 15%).

Many samples were cast such as reinforced concrete columns, cubes and concrete cylinders. In this chapter, the results of these samples will be reviewed and analyzed, which are represented by the structural behavior of concrete columns, in addition to the mechanical properties and durability properties of the mixtures. To facilitate the analysis of the results, the following symbols were used to indicate the substituted materials: CA for carbon, GR for graphite, CE for ceramic, MA for marble, and GL for glass.

The study included two groups of columns, each containing 16 columns. The first group was examined directly to demonstrate the effect of using sustainable materials as an alternative to cement. The second group was examined after being subjected to an accelerated corrosion process using an electric current of 200 mA/cm², a salt concentration in the water of 3.5%, and seven cycles of wetting and drying at a ratio of 1/3 for each cycle.

4.2 Mechanical properties

The results shown in Figures 4-1, 4-2, and 4-3 show the mechanical properties (compressive strength, splitting tensile strength, and density) of all the concrete mixtures studied.

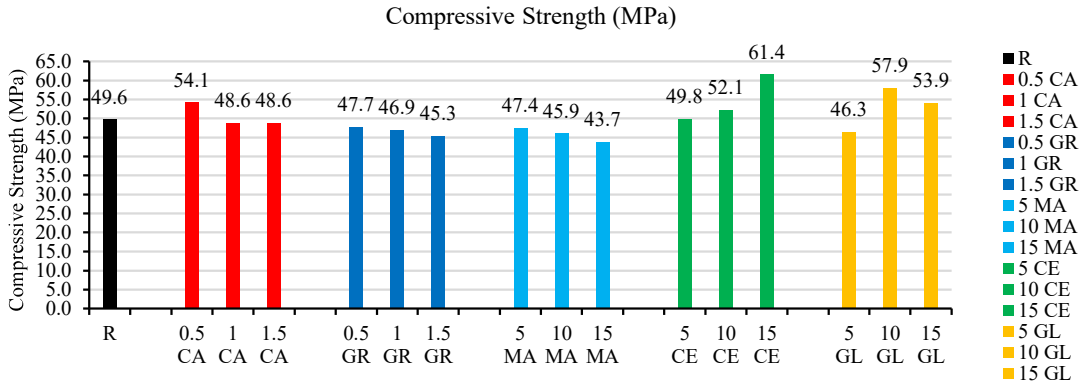

Figure 4-1. Compressive strength for all concrete mixes.

Compressive strength results show a significant increase when using carbon black at a rate of 0.5%. Figure 4-1 shows a 9% increase compared to the reference mix. This demonstrates the effectiveness of carbon black in improving the behavior of concrete mixes at low percentages. When using carbon black at rates of 1% and 1.5%, a slight decrease in strength is evident due to the increased quantity.

When using graphite powder and marble powder, a slight decrease is shown, but this decrease increases with the increase in the percentage of use, as shown in Figure 4-1.

When using ceramic powder, compressive strength increases gradually with increasing application rate. Using 5%, 10%, and 15% ceramic powder resulted in an increase in compressive strength of 0.4%, 5%, and 24%, respectively, compared to the reference mixture, as shown in Figure 4-1.

When using glass powder, the results shown in Figure 4-1 show that using a 5% ratio did not show any effect, while using 10% showed a 16.7% increase, while using a 15% ratio showed an 8.7% increase, a lower value than the previous one.

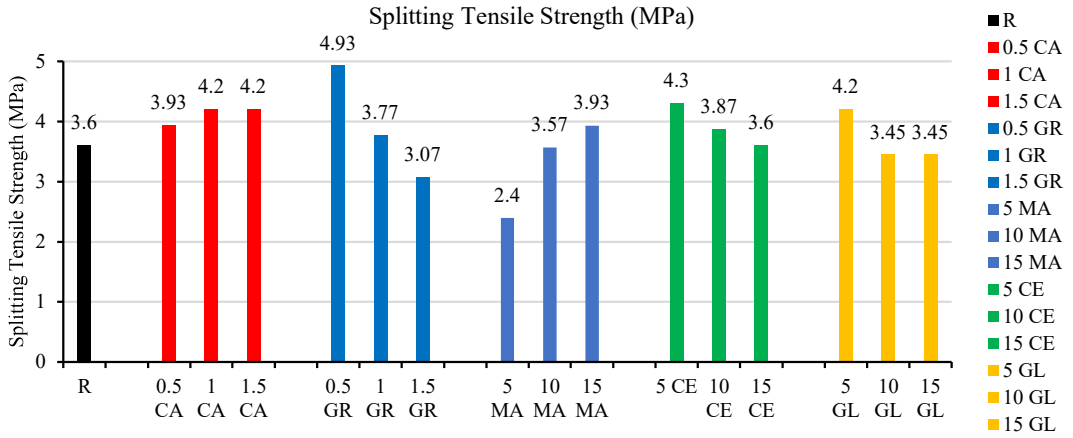

Figure 4-2. Splitting tensile strength for all concrete mixes.

Figure 4-2 shows the splitting tensile strength results for all the mixtures studied. The use of carbon black showed a significant improvement with increasing substitution percentage. Graphite powder showed a decrease with increasing substitution percentage, with behavior similar to that of compressive strength. Conversely, only the use of marble powder showed improvement at 15% substitution. The use of ceramic powder and glass powder showed an initial improvement, followed by a decrease with increasing substitution percentage.

The density shown in Figure 4-3 shows a significant increase when using high-fine materials as a substitute for cement in most mixes. This is due to the effective role of these materials in improving the behavior of concrete mixtures.

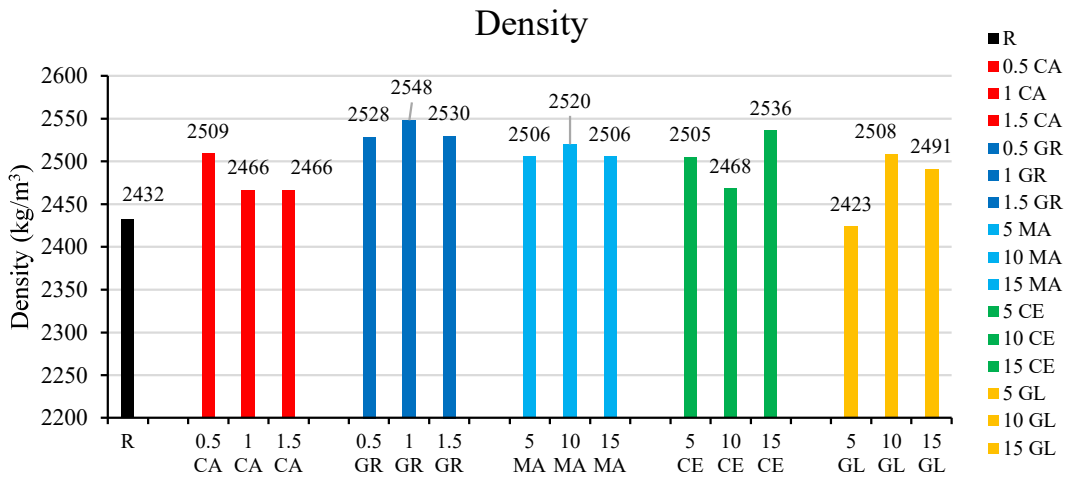

Figure 4-3. Density for all concrete mixes.

4.3 Durability properties

The durability of concrete mixes containing eco-friendly materials as an alternative to cement will be discussed and compared with mixes without additives.

4.3.1 Ion Chloride Penetration

Figure 4-4 shows the results of the chloride ion penetration test for all the concrete mixtures studied.

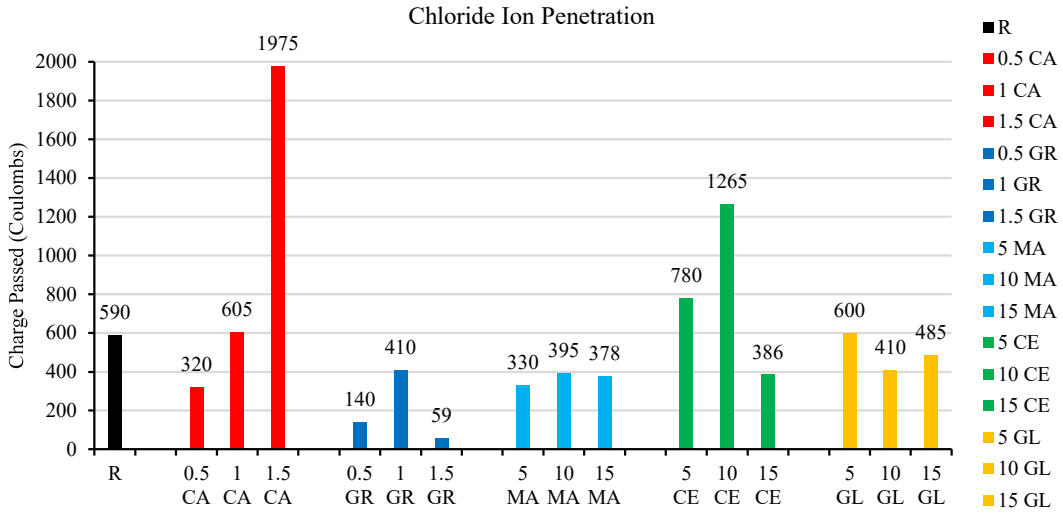

Figure 4-4. Ion chloride penetration for all concrete mixes.

The results show that using 0.5% of carbon black reduces the penetration of chloride ions by 48% compared to the reference mixture value.

The results also show that using graphite at a rate of 0.5%, 1%, and 1.5% reduces the penetration of chloride ions by 76%, 31%, and 90%, respectively, compared to the reference mixture value.

Using marble powder at a rate of 5%, 10%, and 15%, reduces the penetration of chloride ions by 44%, 33%, and 36%, respectively compared to the reference mixture value.

The results also show that using ceramic powder at a rate of 15% reduces the penetration of chloride ions by 35% compared to the reference mixture value.

As for using glass powder at a rate of 10% and 15%, it reduces the penetration of chloride ions by 31% and 18%, respectively, compared to the reference mixture value.

The results of the chloride ion penetration test showed significant variations in the performance of mixes containing different additives. It was observed that the use of graphite powder significantly improved concrete permeability. The mix containing 1.5% graphite recorded the lowest chloride penetration value, at 59. This can be attributed to its structural regularity and lamellar shape, which enables it to efficiently fill the micropores between cement paste particles, as well as its properties in reducing electrochemical conductivity. Conversely, mixes containing carbon black performed well at lower percentages (0.5% and 1%). However, increasing the percentage to 1.5% resulted in a significant deterioration in performance, with chloride penetration reaching 1975. This is due to the possibility of the irregular agglomeration of chloride particles within the mix, which increases permeability rather than decreasing it. Marble powder demonstrated

consistent and acceptable performance at all concentrations (5%, 10%, and 15%), with values ranging from 330 to 395, indicating its effectiveness as a filler that contributes to improving concrete density. Mixtures containing ceramic powder exhibited fluctuating behavior, with the highest chloride penetration value reaching 1265 at 10%, which may indicate poor particle distribution or inhomogeneous interaction with the cement paste, despite a significant improvement at 15%. Glass powder performed well at 10%, with penetration reaching 410. This improvement is attributed to the fine glass containing amorphous silica capable of reacting pozzolanically to a limited degree. Based on the above, materials can be ranked according to their efficiency in reducing chloride ion penetration as follows: graphite powder, marble powder, glass powder, carbon black, and ceramic powder.

4.3.2 Half Cell Potential

Figure 4-5 shows the results of the half-cell potential test for all the concrete mixtures studied.

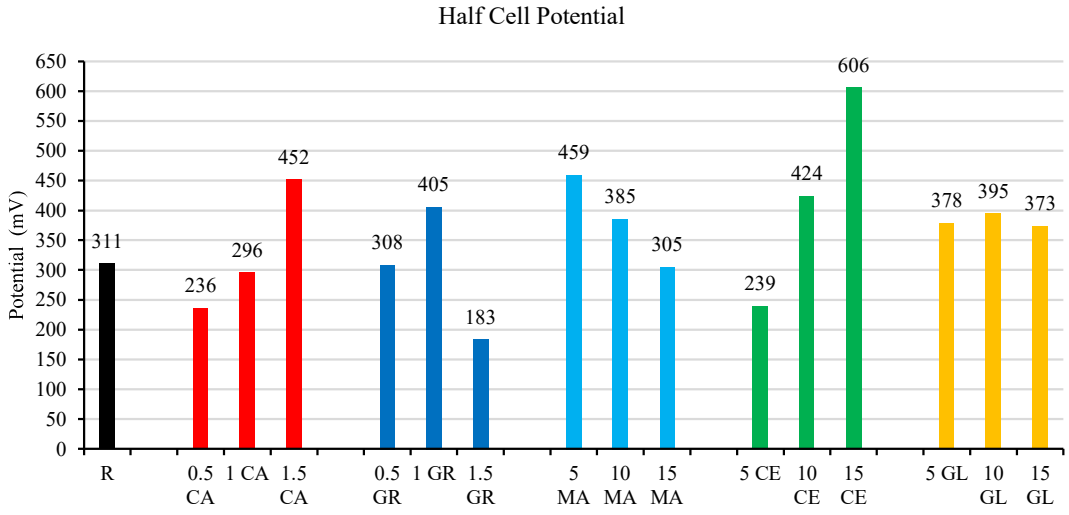

Figure 4-5. Half-cell potential for all concrete mixes.

Half-cell potential test results showed significant variation in the performance of mixes containing different additives in terms of the potential for reinforcing steel corrosion. The mix containing 1.5% graphite powder performed best among all mixes, reaching a potential value of 183 mV, indicating an internal environment with low electrochemical conductivity and reduced potential for corrosion cell formation. This improvement is attributed to graphite's ability to reduce internal moisture and seal micropores.

Carbon black demonstrated good performance at the low percentage (0.5%), reaching a potential value of 236 mV, which is lower than the reference mix, indicating improved corrosion resistance. In contrast, the corrosion potential increased significantly with the use of 1.5% carbon black, reaching a potential value of 452 mV. This is attributed to particle agglomeration and increased local conductivity, which may accelerate the formation of internal corrosion cells.

Mixtures containing ceramic powder also exhibited oscillatory behavior. The 5% ceramic mixture performed well (239 mV), while the potential value increased significantly at 10% and 15% (424 mV and 606 mV, respectively). This indicates that the positive effect of ceramics depends largely on the addition ratio and the nature of the particle distribution.

As for the marble powder, it recorded relatively high values, especially at 5% (459 mV), indicating a high corrosion potential. However, performance improved at 15% (305 mV), reflecting irregular behavior that may be related to the material's weak pozzolanic activity and its reliance solely on the filler effect.

Meanwhile, the glass powder-containing mixtures showed similar performance at all ratios (378–395 mV), indicating a moderate effect in

reducing corrosion potential, possibly due to the partial pozzolanic reaction of the amorphous silica present in the fine glass.

4.3.3 Permeability Under Pressure

Figure 4-6 shows the results of the permeability under pressure test for all the concrete mixtures studied.

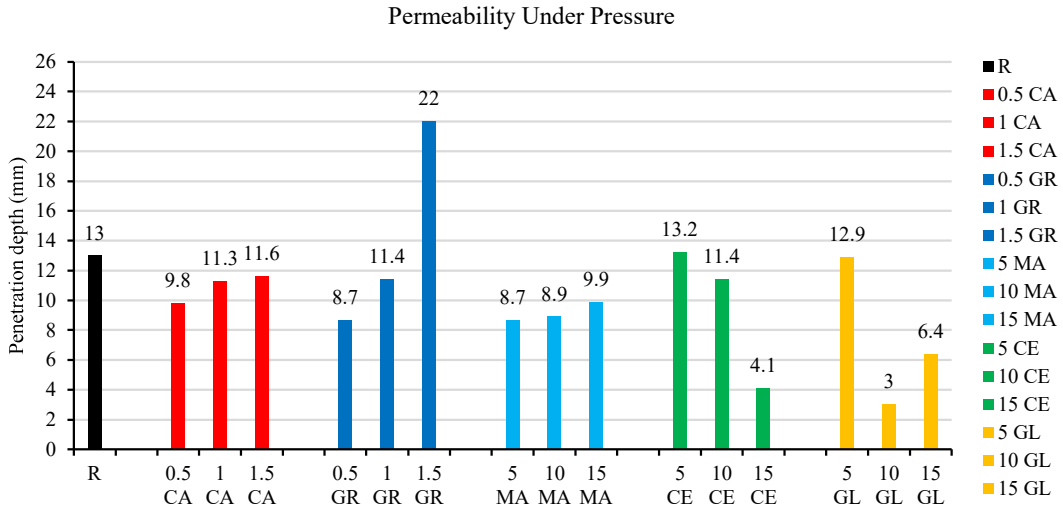

Figure 4-6. Permeability under pressure for all concrete mixes.

The results of the permeability under pressure test showed a significant variation in the behaviour of admixtures in terms of the concrete's resistance to water penetration under pressure. This is a direct indicator of the concrete's density and its ability to resist harmful penetrations.

The 10% glass admixture performed best among all admixtures, with a penetration depth of only 3.0 mm, followed by the 15% ceramic admixture, with a depth of 4.1 mm. This indicates the effectiveness of both materials in enhancing the microstructure of the cement matrix by filling capillary pores and improving density. The superior performance is attributed to the pozzolanic reactivity of the amorphous silica in the glass powder and to the efficient filling and activity effect provided by the ceramic powder.

On the other hand, the alabaster powder admixtures demonstrated stable and acceptable performance at various ratios, with penetration depths ranging from 8.7 to 9.9 mm, indicating the admixture's role as a filler but contributing to improved internal cohesion. As for the carbon black blends, they showed slight improvement at lower ratios (0.5%), while increasing the ratio did not lead to a significant further improvement. At 1.5%, the penetration depth was approximately 11.6 mm, likely due to the agglomeration of fine particles and their poor distribution within the paste.

In contrast, the graphite powder blends showed unexpected behavior. The 0.5% and 1% blends performed well, while the 1.5% blends showed the highest penetration value (22.0 mm). This ratio, however, performed excellently in the chloride penetration and half-cell potential tests.

4.4 General Behavior for Corroded and Non-corroded Concrete Columns

Two groups of reinforced concrete columns were tested; the first group was subjected to natural conditions without exposure to corrosion, while the second group was exposed to a corrosion-inducing environment to evaluate its effect on the structural performance of the columns.

Each group consisted of 16 columns classified into 15 different concrete mixes, in addition to a reference mix that did not contain any cement replacement sustainable materials. The substitutes used included carbon, graphite, ceramic, marble, and glass in different replacement or add ratios.

Concrete columns were tested by applying a concentric axial load to the column and then reading the vertical deflection that occurred as the loading progressed. Figure 4-7 shows images of the tested concrete columns not exposed to corrosion during their structural test.

Non-corroded reference concrete column

Non-corroded concrete column containing ceramic powder (G1)


5MA


10MA

Non-corroded concrete column containing marble powder (G2)

Non-corroded concrete column containing glass powder (G3)


0.5CA


1CA

Non-corroded concrete column containing carbon black (G4)

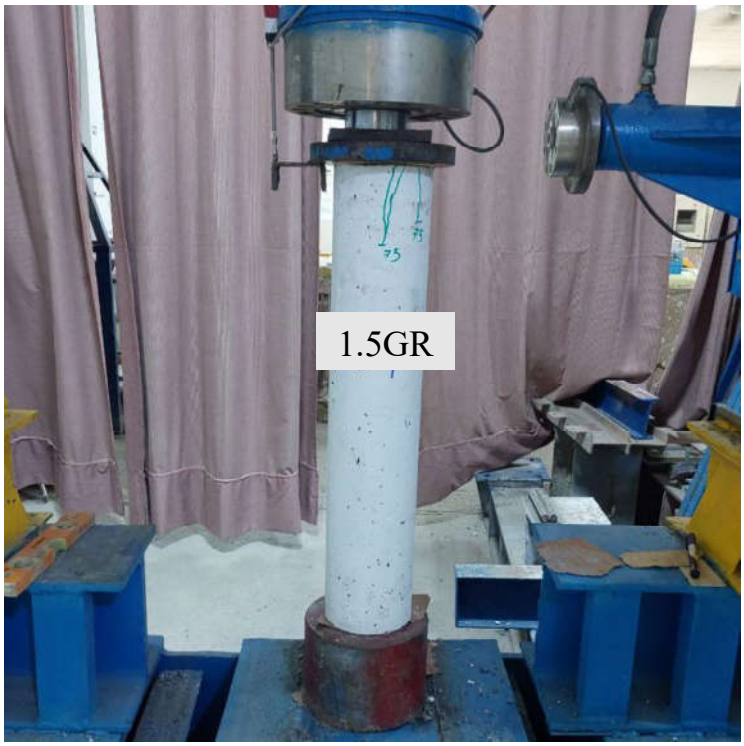

Non-corroded concrete column containing graphite powder (G5)

Figure 4-7. Non-Corroded Concrete Columns Studied During.

The results will be analyzed based on the behavior of the model under loading. The performance of the columns will be compared under different conditions to determine the effectiveness of the substituted materials in improving the resistance of concrete and its effect on its structural properties, especially under the effect of corrosion.

The results of the non-corroded columns shown in Table 4-1. This table show that there is a different improvement depending on the materials used and according to the different proportions.

Figures 4-8, 4-9, and 4-10 show the ultimate load, toughness, and ductility index results, respectively, for all columns not subjected to corrosion.

Table 4-1. Results of non-corroded concrete columns.

Mix	Axial Displacement (mm)	Load (kN)	Toughness (kN.mm)	Ductility Index
R	7.95	616	2446	1.709
0.5 CA	10.37	671	3515	1.572
1 CA	8.62	648	2719	1.699
1.5 CA	7.92	642	2236	1.457
0.5 GR	5.93	688	2252	1.840
1 GR	9.25	646	2362	1.436
1.5 GR	6.37	478	1714	2.130
5 MA	6.76	689	1978	1.440
10 MA	7.76	686	2696	1.686
15 MA	4.24	670	1512	1.708
5 CE	10.40	617	3544	2.058
10 CE	6.23	646	1673	1.323
15 CE	8.66	762	3091	1.134
5 GL	9.27	622	2288	1.403
10 GL	8.72	779	2960	1.470
15 GL	11.65	725	3773	1.638

Figure 4-8 shows the results of the ultimate load for all non-corroded concrete columns. Figure 4-9 show toughness and Figure 4-10 show ductility index for all columns without corrosion. It is clear from the values obtained from the test that the use of carbon and also the use of graphite improves the ultimate load value when used by 0.5%, but this effect decreases with increasing the use percentage. As for the use of marble, it shows a clear improvement, but this effect also decreases with increasing the replacement percentage, but at a lower rate than the previous ones, and it is similar to the behavior of glass, except that the latter shows a slight increase, then a high increase, and then an increase, but less than the previous ones. Finally, ceramics show an improvement with increasing the replacement percentage, as the improvement is gradual with increasing the replacement percentage.

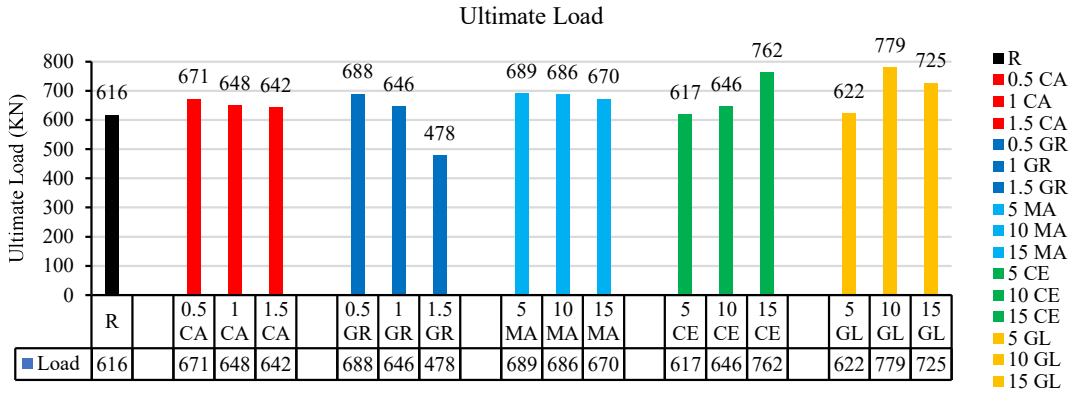

Figure 4-8. Ultimate load for all columns without corrosion.

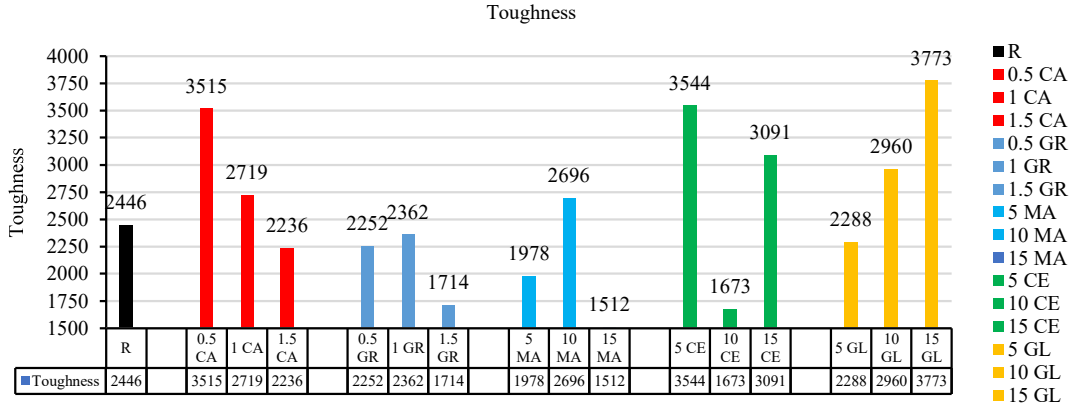

Figure 4-9. Toughness for all columns without corrosion.

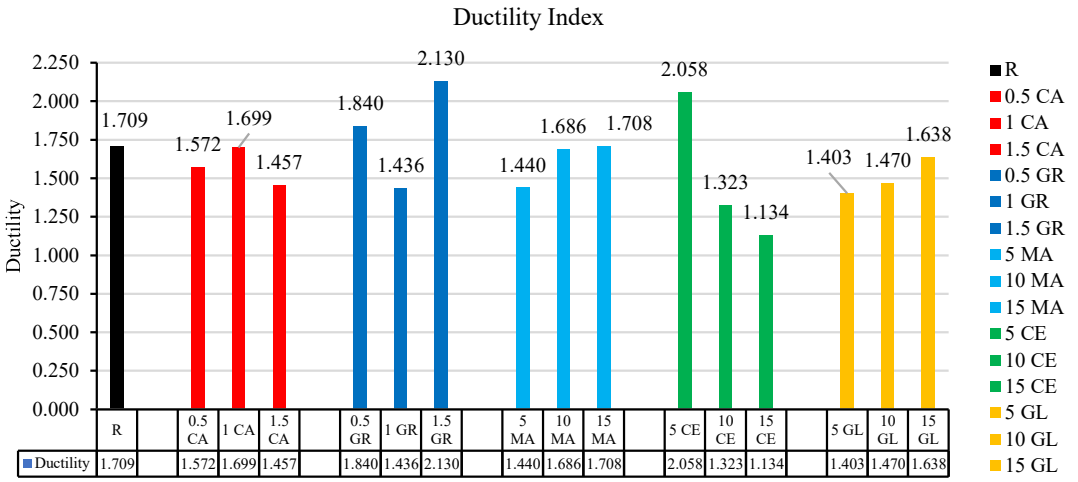

Figure 4-10. Ductility index for all columns without corrosion.

Figure 4-11 shows images of the tested concrete columns exposed to corrosion during their structural test.

Corroded reference concrete column


5M
C5CE


C10CE

Corroded concrete column containing ceramic powder (G6)

Corroded concrete column containing marble powder (G7)


C5GL


C10GL

Corroded concrete column containing glass powder (G8)

Corroded concrete column containing carbon black (G9)


C0.5GR


C1GR

Corroded concrete column containing graphite powder (G10)

Figure 4-11. Pictures of concrete columns studied during testing subjected to corrosion.

Table 4-2. Results of concrete columns exposed to corrosion.

Mix	Axial Displacement (mm)	Load (kN)	Toughness (kN.mm)	Ductility Index
C R	7.39	495	1.547	1679
C 0.5 CA	7.26	646	1.578	2179
C 1 CA	11.42	584	2.240	3986
C 1.5 CA	6.88	575	1.459	1422
C 0.5 GR	9.13	663	1.463	2480
C 1 GR	6.88	630	1.530	1560
C 1.5 GR	8.86	470	1.391	1290
C 5 MA	3.34	402	1.560	622
C 10 MA	8.61	601	2.146	3042
C 15 MA	5.87	642	1.565	1698
C 5 CE	8.70	600	1.350	1894
C 10 CE	8.84	627	1.513	2529
C 15 CE	9.44	620	1.608	2698
C 5 GL	8.73	697	1.403	1770
C 10 GL	7.19	600	1.554	1994
C 15 GL	9.69	604	1.707	2931

Figures 4-12, 4-13 and 4-14 show the ultimate load, toughness, and ductility index results, respectively, for all columns subjected to corrosion.

The results shown in Figure 4-12 show that the corrosion effect was significantly less in columns containing cement replacement sustained materials compared to the reference mixture. The effect of these materials shown in the previous paragraph became clear when these columns were exposed to corrosion. When using carbon and graphite, it is clear that the corrosion effect is less than the reference mixture, but this effect decreases with increasing the replacement ratio. As for using marble, it reduces the effect with increasing the replacement ratio. Also, using ceramics and glass reduces the corrosion effect, as this effect decreases with increasing the replacement ratio.

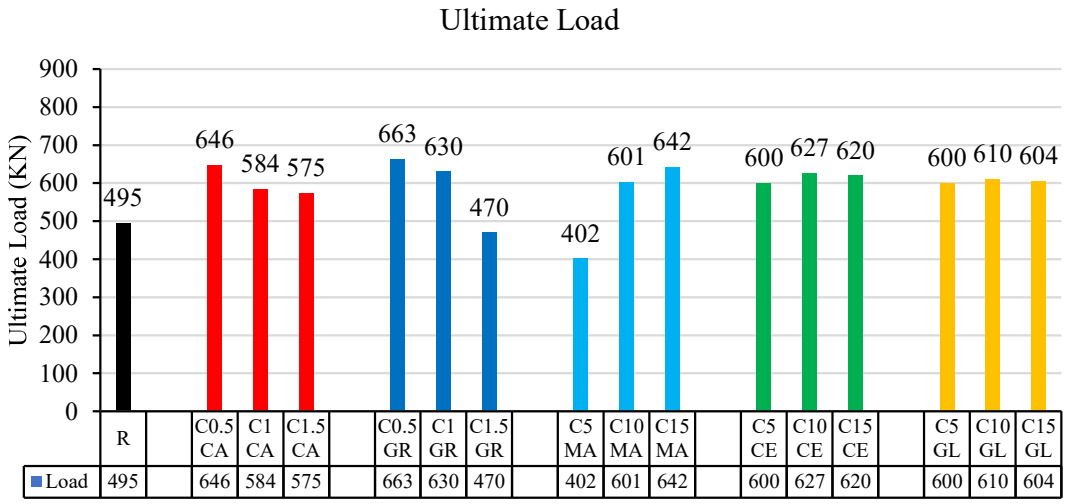

Figure 4-12. Ultimate load for all columns with corrosion.

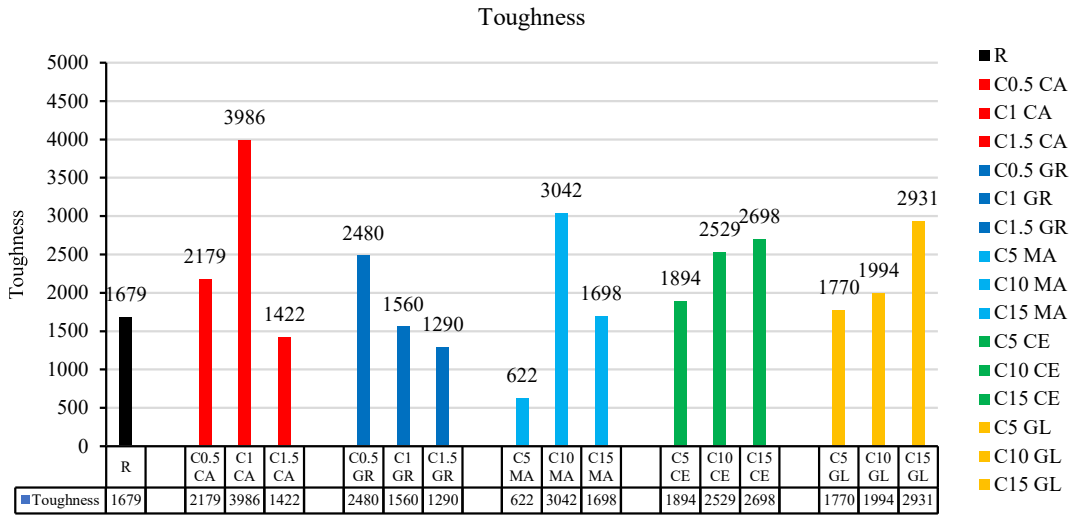

Figure 4-13. Toughness for all columns with corrosion.

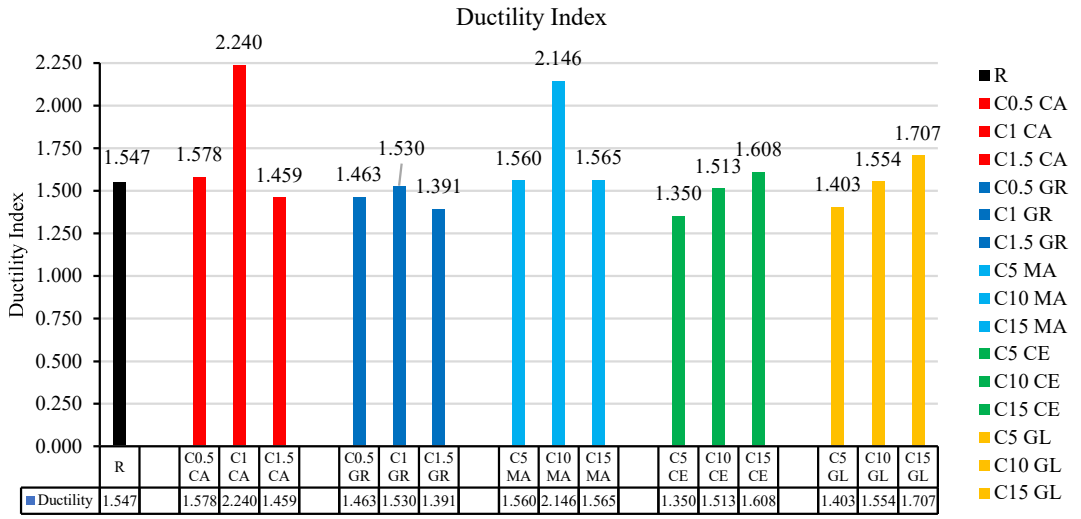

Figure 4-14. Ductility index for all columns with corrosion.

4.5 Non-corroded concrete columns

In this paragraph, the results of concrete columns not exposed to the process of accelerated corrosion, obtained through laboratory tests, will be analyzed.

4.5.1 Effect of using ceramic powder on concrete

The results showed a significant improvement in the ultimate load of the studied concrete columns when using ceramic powder. As the percentage of cement replacement sustained materials increased, this effect appeared clearly, as shown in Figures 4-15 and 4-16.

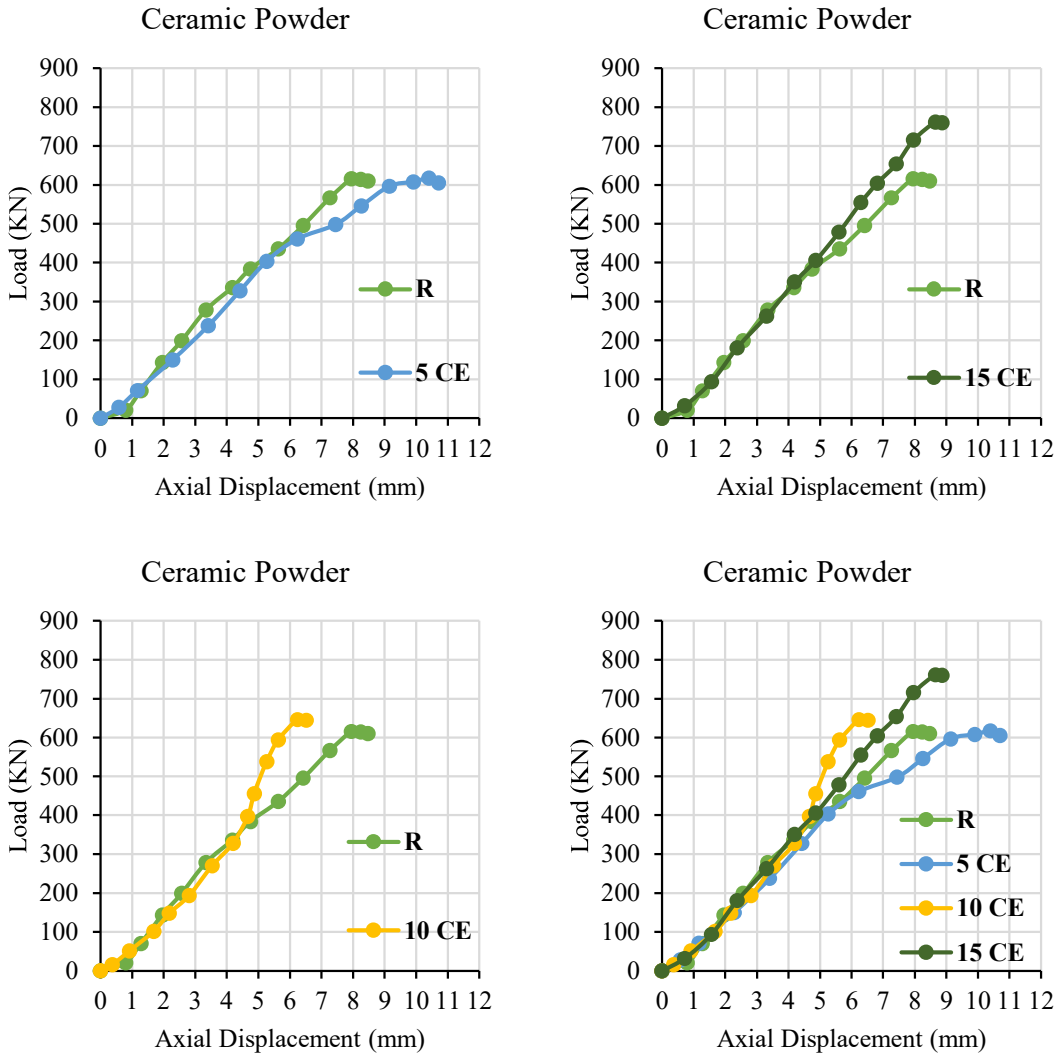

Figure 4-15. Load deflection curves for non-corroded columns containing ceramic powder (G1).

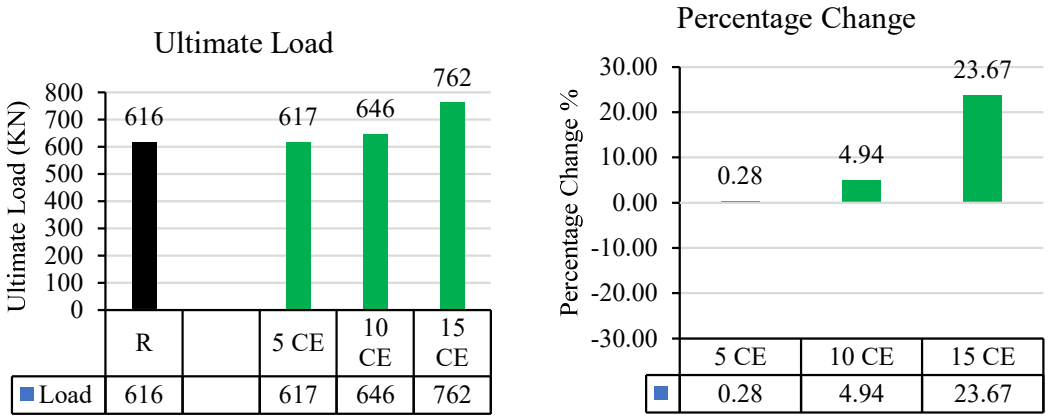

Figure 4-16. Ultimate load for columns containing ceramic powder.

When replacing part of the cement with ceramic by 5%, the ultimate load slight improvement of 0.28% was shown, but this improvement increased when replacing by 10% to be 4.94%, and then the percentage of replacement by 15% had the highest increase of 23.67%.

Previous literature supports these results, as the behavior of the material is similar to what has been achieved, as shown by the results of a study conducted by (Heidari et al., 2013). The compressive strength of the samples containing ceramic powder developed more at each replacement ratio compared to the control concrete sample. The difference in strength development between the samples can be attributed to the pozzolanic reaction.

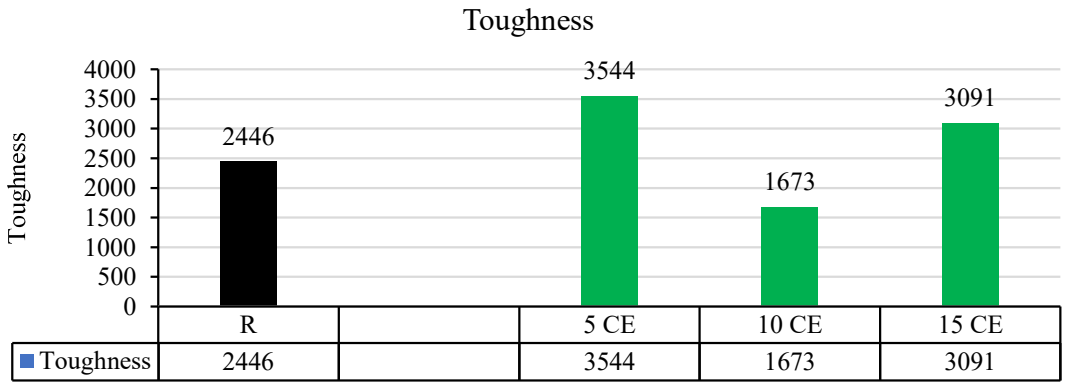

Figure 4-17. Toughness for columns containing ceramic powder.

In conjunction with the results for the ultimate load of the columns, the toughness results shown in Figure 4-17 show a good improvement when using a percentage of 5% and 15% ceramics, as it increased by 45% and 26%, with a noticeable decrease when using a rate of 10% by 32%. The general behavior shows a reduction with increasing replacement percentage.

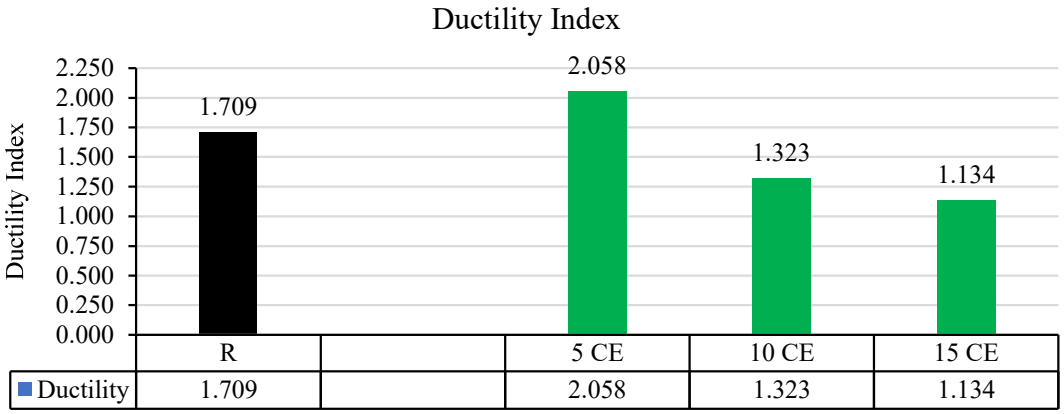

Figure 4-18. Ductility index for columns containing ceramic powder.

In addition to the above, Figure 4-18 shows the ductility index results of reinforced concrete columns containing different percentages of ceramics. The results showed that using a small percentage of ceramics improves ductility index while increasing it reduces the amount of ductility index. Replacing 5% of ceramics improves plasticity by 20%, but using 10% and 15% reduces ductility index by 22% and 33%, respectively.

As previous studies have shown that the ceramic tile waste powder may react with calcium hydroxide to produce more C-S-H gel, it has no cementitious effect like cement, and secondary hydration depends on the hydration of cement (Donatello et al., 2010). Therefore, higher ceramic powder content may mean that less cement can participate in the hydration reaction with water and less C-S-H gel was produced, which resulted in the

higher porosity and lower compressive strength of concrete, especially at an early age (Kannan et al., 2017).

4.5.2 Effect of using marble powder on concrete

The results of using marble as a partial substitute for cement, the values of which are shown in Figures 13 and 14, showed a clear improvement in the ultimate load of the concrete column when using marble.

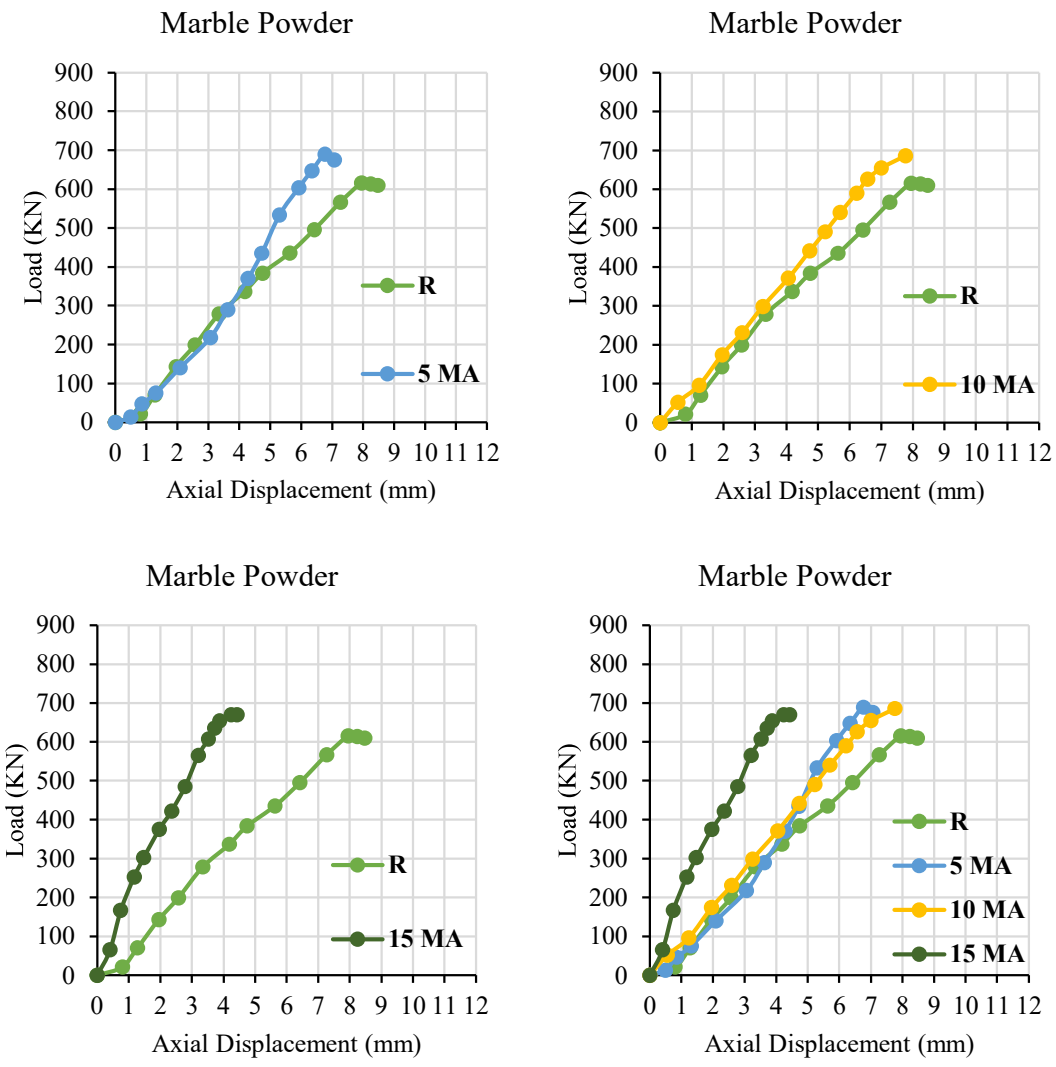

Figure 4-19. Load deflection curves for non-corroded columns containing marble powder (G2).

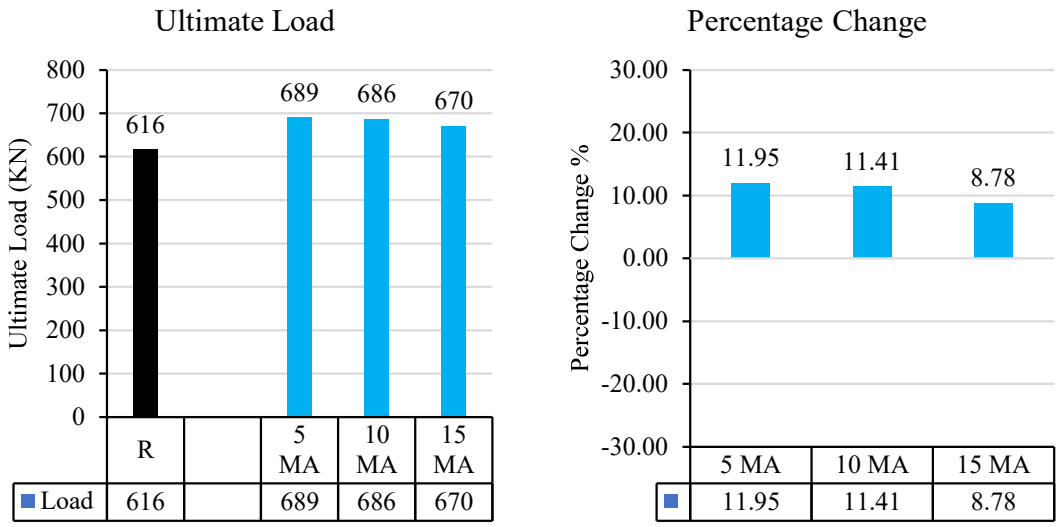

Figure 4-20. Ultimate load for columns containing marble powder.

Figure 4-20 shows that the percentage of increase in the ultimate load for column 5 A is 11.85%, while column 10 A shows an increase of 11.36%, and column 15 A has a rise of 8.76%.

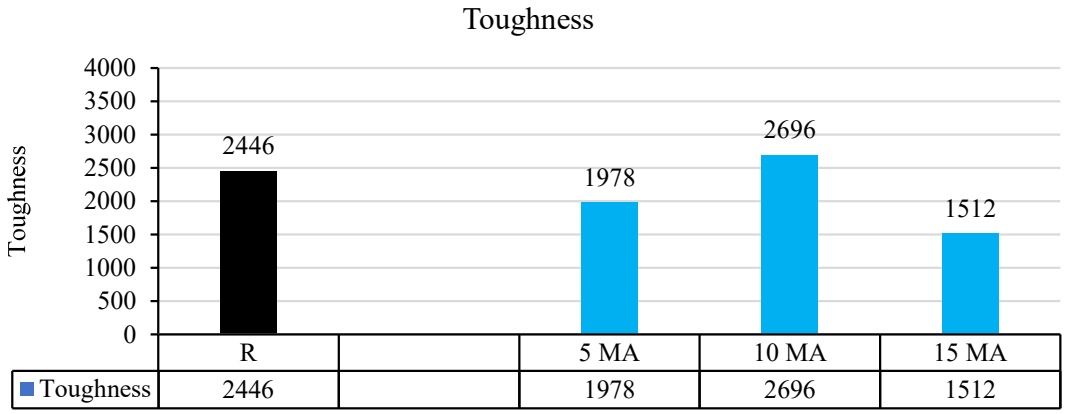

Figure 4-21. Toughness for columns containing marble powder.

The results shown in Figure 4-21 show that adding 10% marble leads to a good improvement in toughness. Adding 10% marble led to a 10% improvement, while using 5% and 15% led to a decrease in the toughness value by 19% and 38%, respectively.

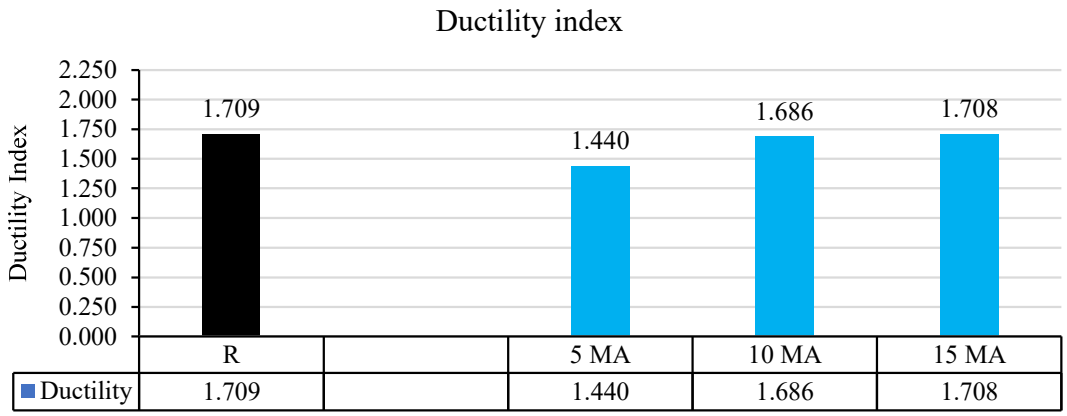

Figure 4-22. Ductility index for columns containing marble powder.

The ductility index results shown in Figure 4-22 show that adding marble in different proportions led to a significant decrease. Using 5%, 10%, and 15% led to a decrease of 16%, 1.3%, and 0.06%, respectively, in the ductility index values.

Previous literature shows that the increase can be explained by the pore-filling effect of fine limestone powder, which provides suitable nuclei for hydration and stimulates the hydration process as a result. The use of WMP in concrete has shown an effect as a filler, where this addition is inert and is treated as a very fine aggregate that fills the voids in the concrete. The use of WMP reduced the porosity in the concrete matrix physically, and had important binding properties developed due to the chemical hydration of calcite and C_3A (Ergün, 2011).

Previous studies have also shown that when marble dust was used as a substitute for cement, the results showed that increasing the amount of marble dust led to a decrease in compressive strength. This decrease was due to the dilution of C_2S and C_3S components, which are the main elements of cement and responsible for providing strength when marble dust was added (Demirel, 2010).

4.5.3 Effect of using glass powder on concrete

The results shown in Figure 4-23 and Figure 4-24 showed that there was an improvement in the ultimate load of the columns containing glass waste powder.

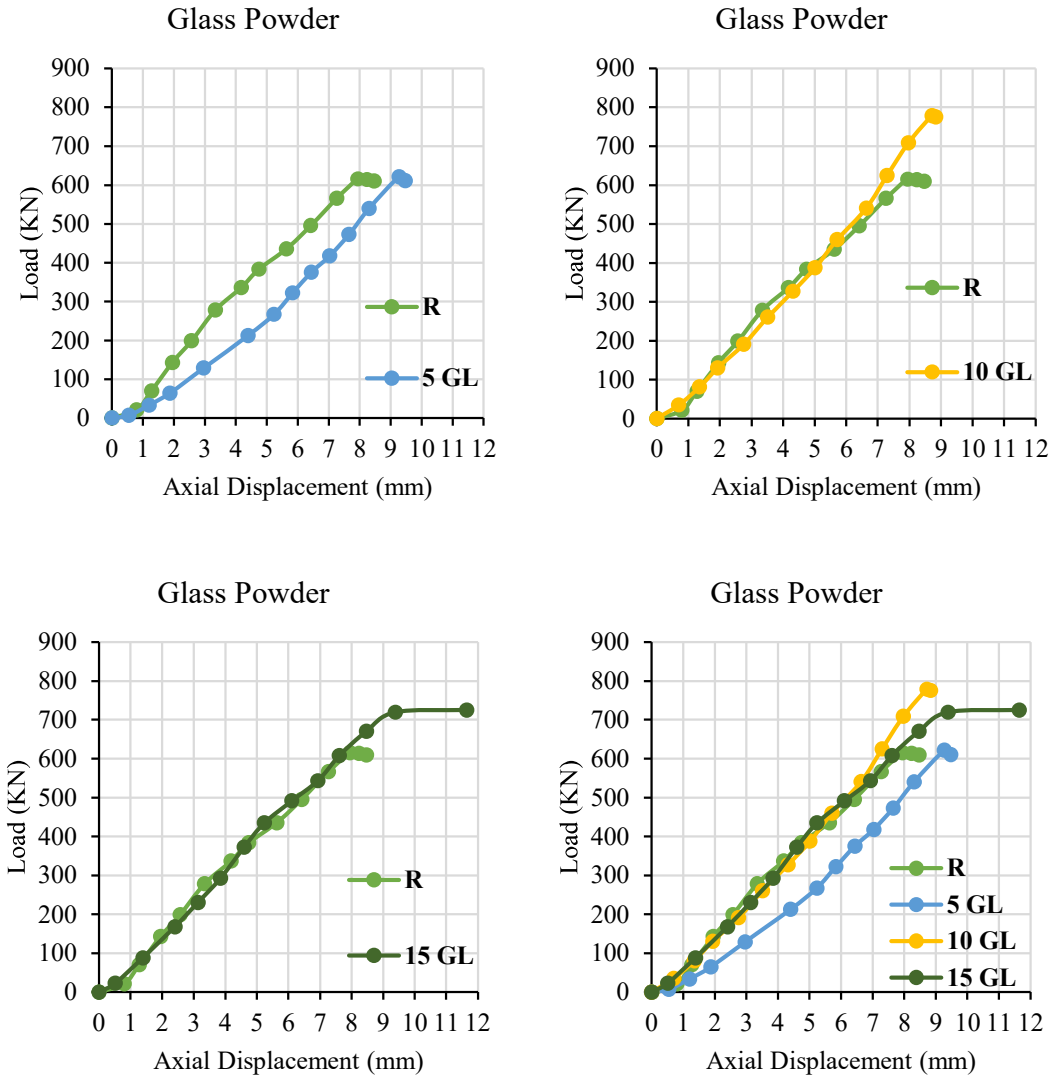

Figure 4-23. Load deflection curves for non-corroded columns containing glass powder (G3).

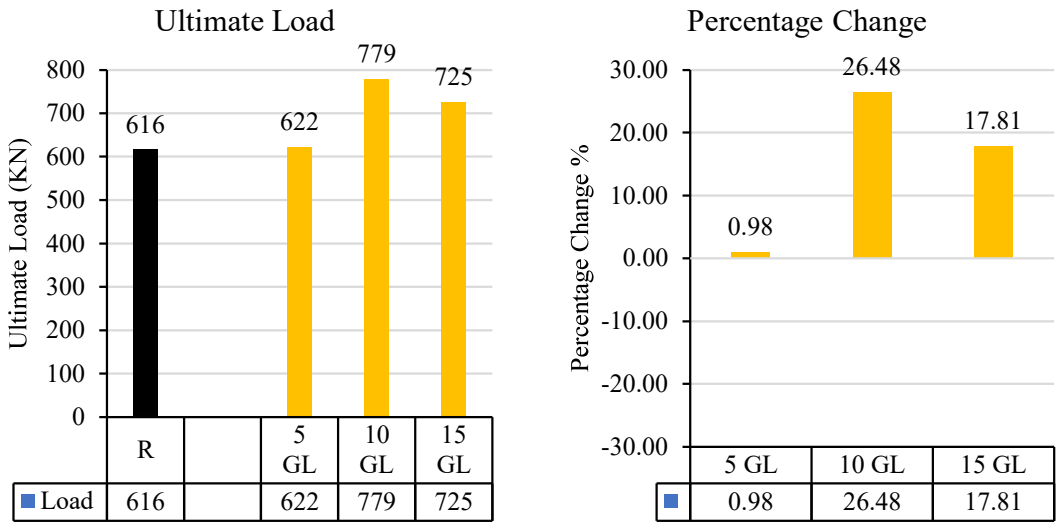

Figure 4-24. Ultimate load for columns containing glass powder.

The test results showed that the column containing 5% glass powder increased by 1%, the column containing 10% glass powder increased by 26.46%, and the column containing 15% glass powder increased by 17.69%.

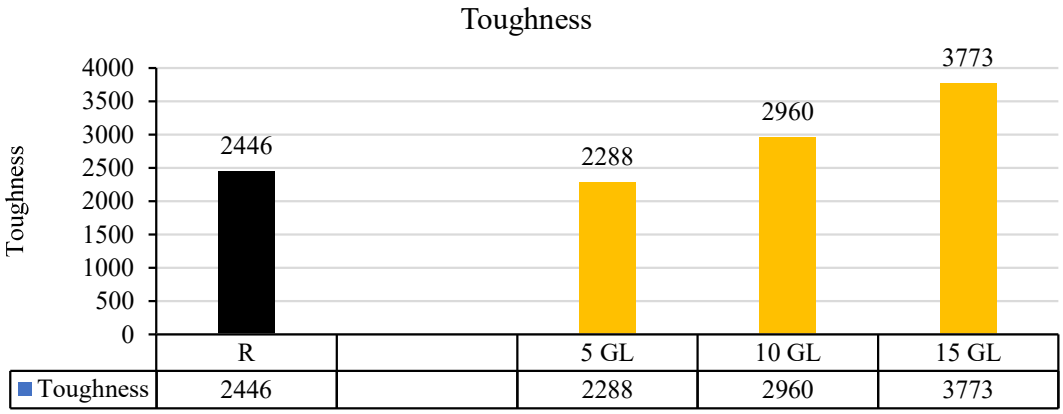

Figure 4-25. Toughness for columns containing glass powder.

The toughness results shown in Figure 4-25 show that adding marble in different proportions led to an increase except for the 5% proportion, where using proportions of 10% and 15% led to an increase in toughness values by

21% and 54%, respectively, with a decrease when using the 5% proportion by 6.5%.

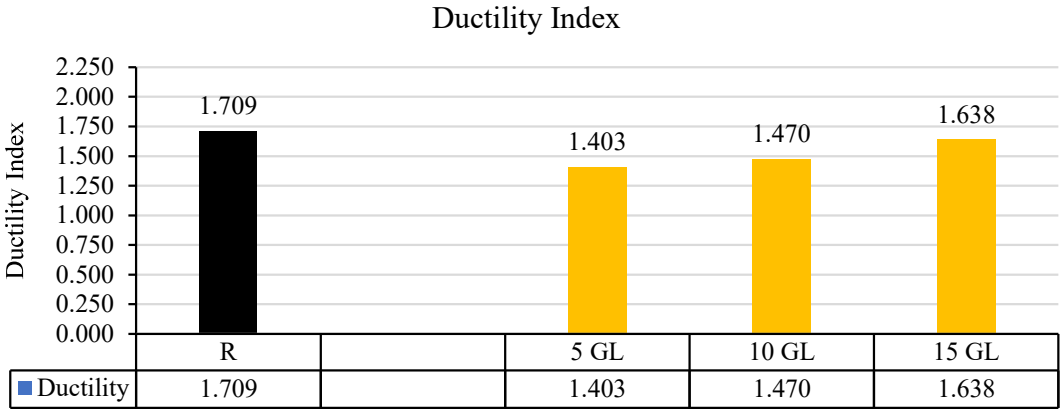

Figure 4-26. Ductility index for columns containing glass powder.

As for ductility index, Figure 4-26 shows that adding glass to the concrete mixture reduces ductility index. When using a ratio of 5%, 10%, and 15%, it reduces ductility index by 18%, 14%, and 4%, respectively.

Previous literature explains this behavior, as it shows that the compressive strength is higher for specimens containing very fine glass (<100 µm), and the strength shows a tendency to decline as particle size increases (Shi et al., 2005). The results showed that cement replacement sustained materials between 10% and 20% yielded the highest strength (Federico et al., 2009). When waste glass powder is used, the calcium ions will favor the pozzolanic reaction in combination with a relatively high rate of C-S-H formation, and over time, any alkali-silica reaction product will take on the texture of C-S-H. The pozzolanic reaction of glass powder will produce a type of calcium silicate hydrate. This product may be a lithium silicate or perhaps a pozzolanic formation of C-S-H, which has the potential to contribute to additional strength(Madandoust et al., 2013).

4.5.4 Effect of using carbon black on concrete

The results showed that there is a slight improvement in the ultimate load of concrete columns that were tested using carbon, as shown in Figure 4-27 and Figure 4-28.

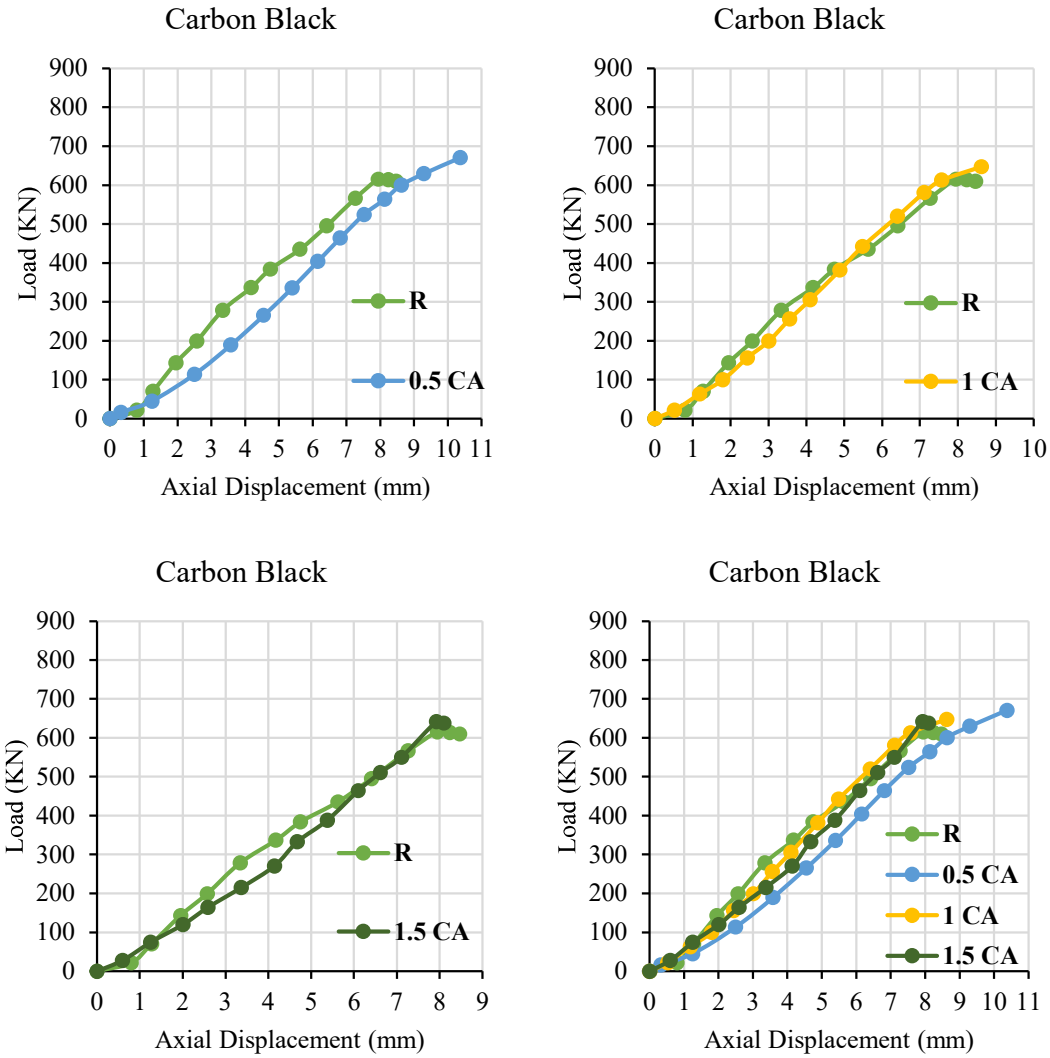

Figure 4-27. Load deflection curves for non-corroded columns containing carbon black powder (G4).

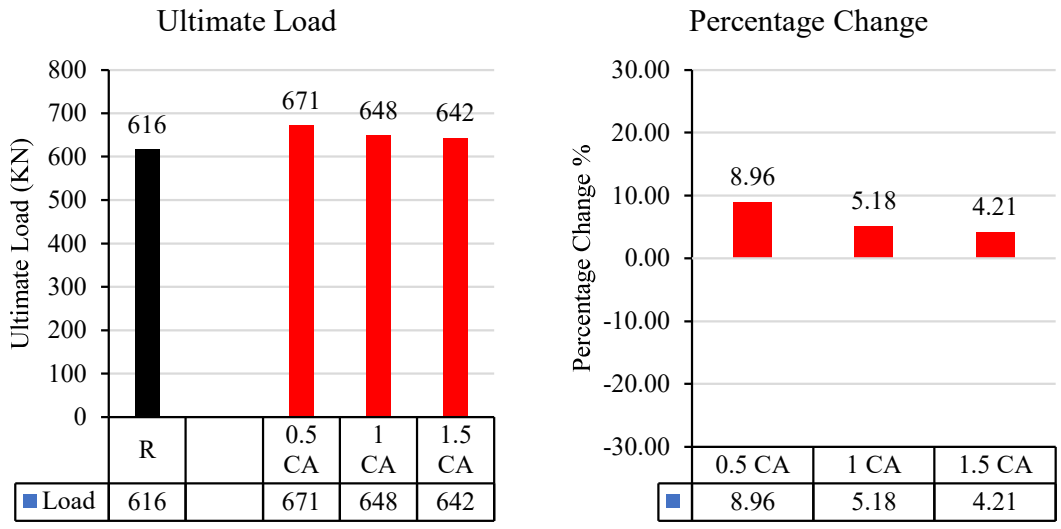

Figure 4-28. Ultimate load for columns containing carbon black powder.

The use of carbon in the concrete column at a rate of 0.5% had the highest improvement of 8.93%, which is the highest result among the other columns. As for the column that contains 1% carbon, it had an improvement of 5.19%, and the column that contains 1.5% carbon had an improvement of 4.22%.

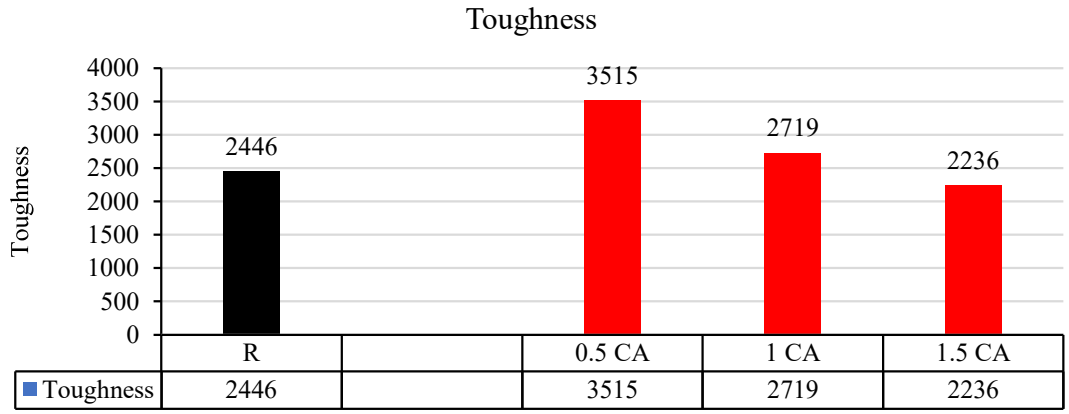

Figure 4-29. Toughness for columns containing carbon black powder.

The use of carbon black in small proportions as a substitute for cement showed a good improvement in the toughness results, as shown in Figure 4-

29, but this improvement begins to gradually decrease with increasing the replacement ratio. The results show that using a ratio of 0.5% and 1% increases the amount of toughness by 44% and 11%, respectively, while replacing 1.5% of cement reduces toughness by 9%.

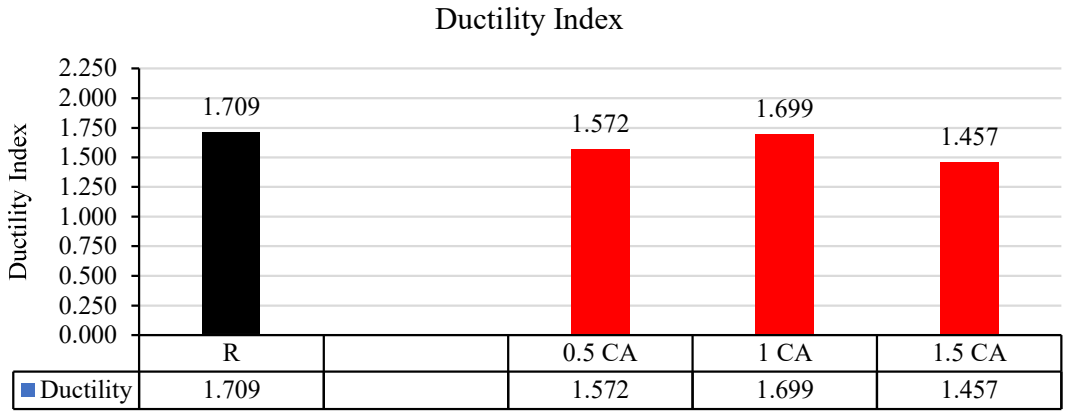

Figure 4-30. Ductility index for columns containing carbon black powder.

Ductility index only showed a decrease as illustrated in Figure 4-30 when using carbon black. When using 0.5%, 1%, and 1.5%, the ductility index values were 8%, 0.6%, and 15%, respectively, compared to the reference mixture. The results show that ductility index decreases with increasing replacement ratio.

Previous studies show that the use of carbon black as a partial cement substitute in concrete significantly affects its properties. When added in low proportions, carbon black can enhance compressive strength due to its ability to fill the micropores between cement particles, which improves density and reduces the permeability of concrete. It also acts as a water-repellent for cement particles, which speeds up the reaction process in the concrete mix. In addition, carbon black acts as an effective material in reducing carbon dioxide emissions by reducing the cement content in the concrete mix, making it a sustainable option. However, excessive proportions of carbon black may lead

to negative effects, such as reduced tensile and flexural strength and increased brittleness, due to the agglomeration of fine particles (Fayaz et al., 2018).

4.5.5 Effect of using graphite powder on concrete

The use of graphite in reinforced concrete columns shows a significant improvement in ultimate load, as shown in Figure 4-31 and Figure 4-32.

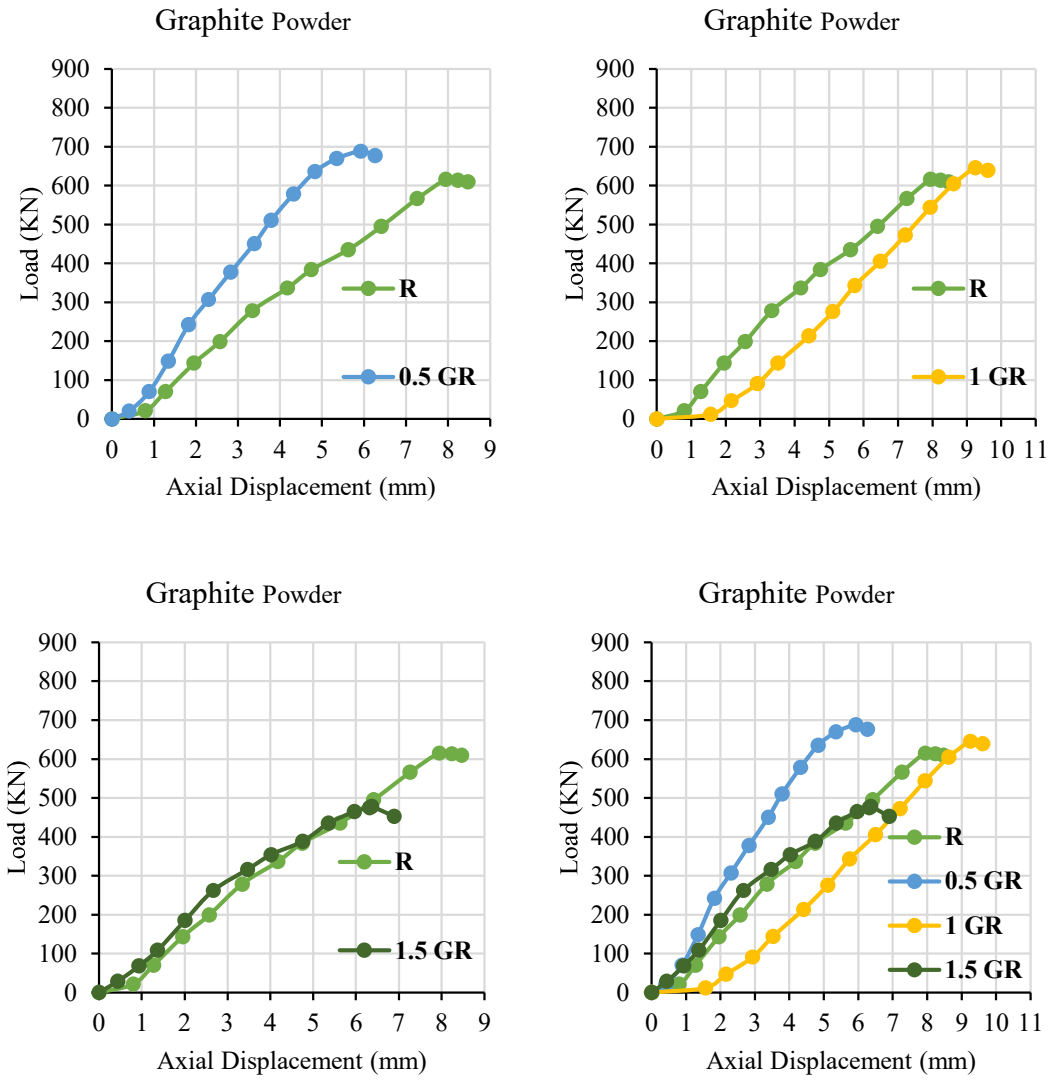

Figure 4-31. Load deflection curves for non-corroded columns containing graphite powder (G5).

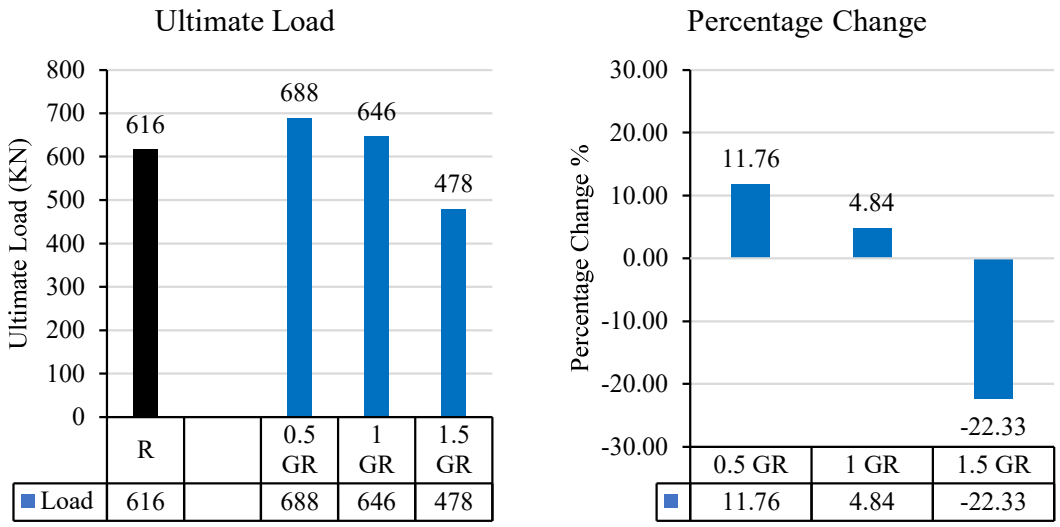

Figure 4-32. Ultimate load for columns containing graphite powder.

The ultimate load of the column containing 0.5% graphite shows an improvement of 11.69%. The use of 1% graphite shows a 4.87% improvement in the ultimate load of the column. As for the column with a concrete mix containing 1.5% graphite, it showed a decrease of 22.4%.

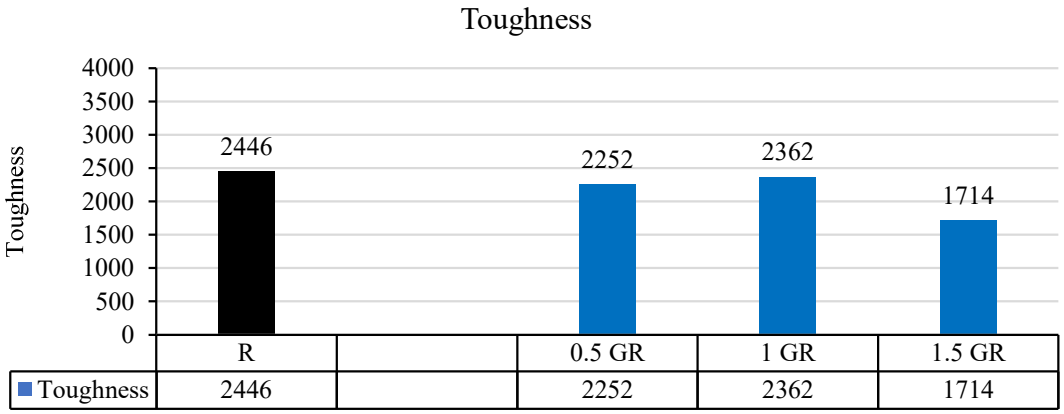

Figure 4-33. Toughness for columns containing graphite powder.

The results shown in Figure 4-33 show that using graphite as a substitute for cement in small proportions leads to a slight decrease in

toughness, especially in small proportions. The results showed that using 0.5%, 1%, and 1.5% led to a decrease of 8%, 3.5%, and 30%, respectively, in toughness values compared to the reference mixture.

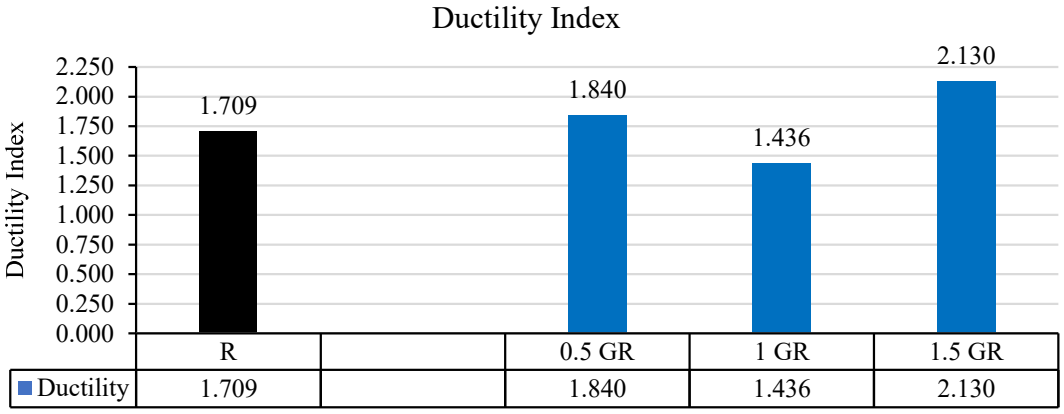

Figure 4-34. Ductility index for columns containing graphite powder.

Figure 4-34 shows the results obtained for ductility index. In general, ductility index improves when using graphite. At 0.5% and 5.1%, there is an improvement in ductility index by 7.7% and 25%, respectively, except for the 1% ratio, where there was a decrease of 16% compared to the reference mixture.

Previous studies show that compared with concrete without graphite waste, adding a certain amount of graphite waste can increase the cohesion of cementitious materials. However, adding a large amount of graphite waste will increase the crack density between cementitious materials, which will increase the possibility of penetrating cracks or large-scale pores(Liu et al., 2022). Graphite content exceeding 1% has been shown to be detrimental to the electrical and physical properties of concrete (Al-Bayati et al., 2020).

4.6 Corroded Concrete Columns

In this paragraph, the results of concrete columns exposed to the process of accelerated corrosion obtained through laboratory tests will be analyzed.

4.6.1 Effect of using ceramic powder on concrete

The results shown in Figures (35 and 36) show the results of reinforced concrete columns after being exposed to the process of accelerated corrosion by electric current, in which 5%, 10%, and 15% of the cement were replaced with ceramic powder.

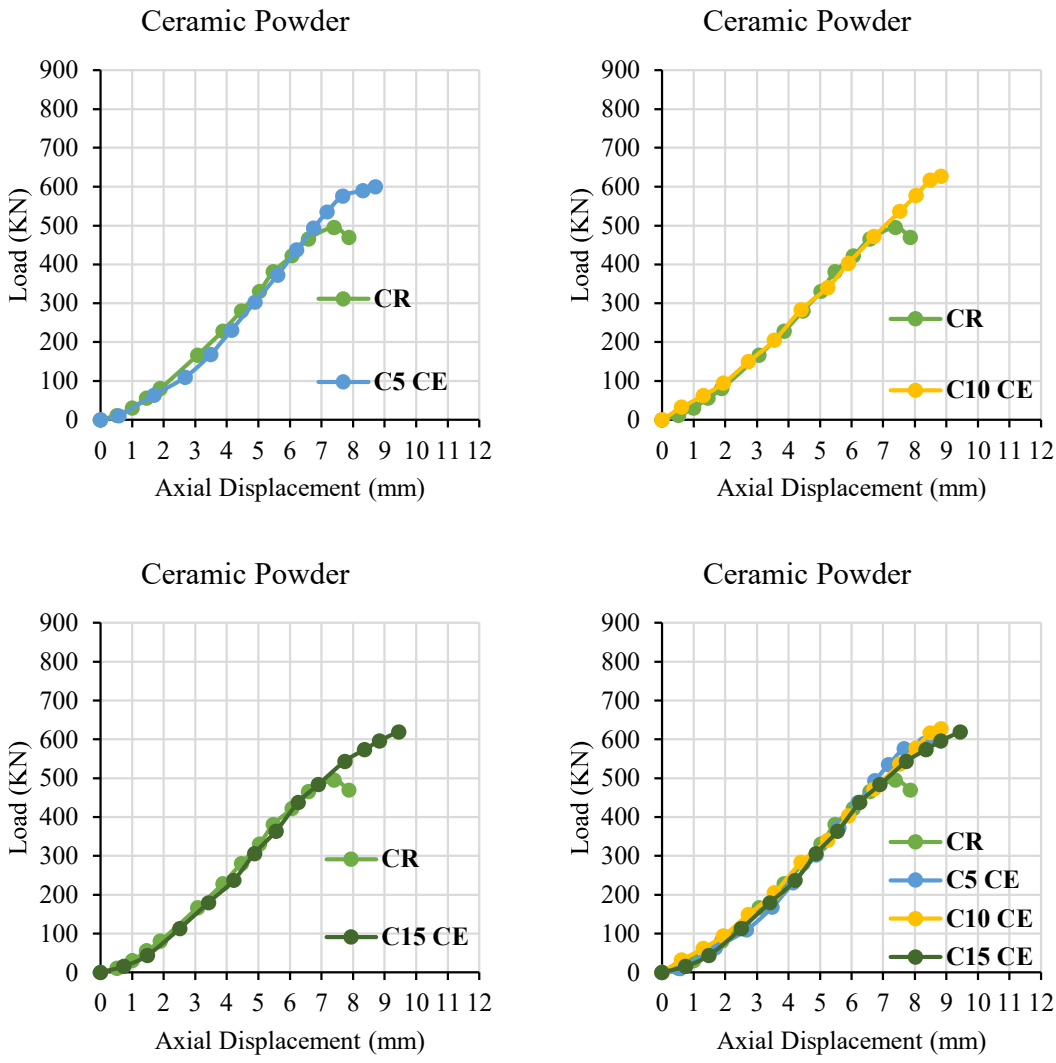

Figure 4-35. Load deflection curves for corroded columns containing ceramic powder (G6).

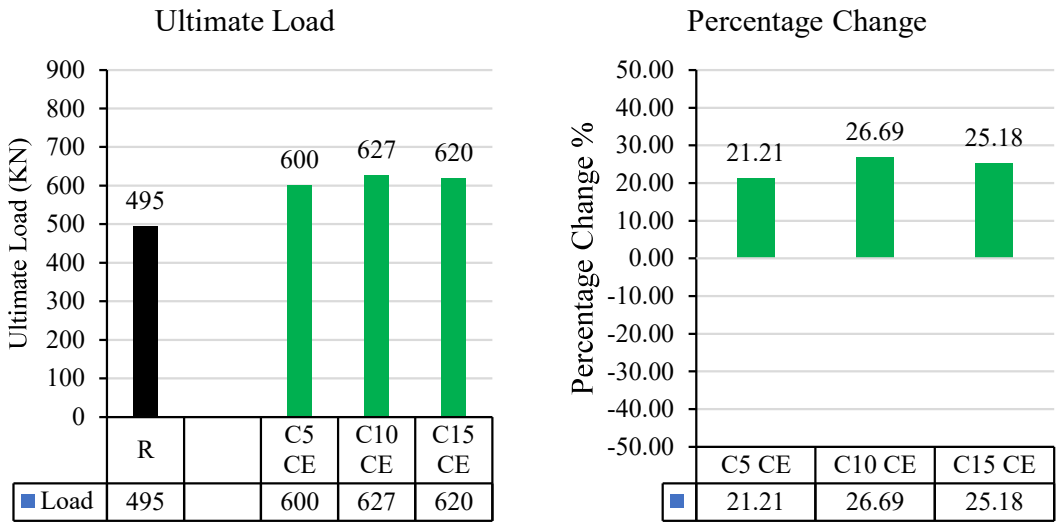

Figure 4-36. Ultimate load for columns containing ceramic powder.

The concrete columns containing ceramic powder after exposure to the process of accelerating corrosion by electric current showed a slight increase in the ultimate load compared to the concrete column of the reference mixture, as shown in Figure 4-36. The results showed that the concrete columns containing 5%, 10%, and 15% ceramic powder were higher by 21%, 27%, and 25% compared to the column with the reference mixture.

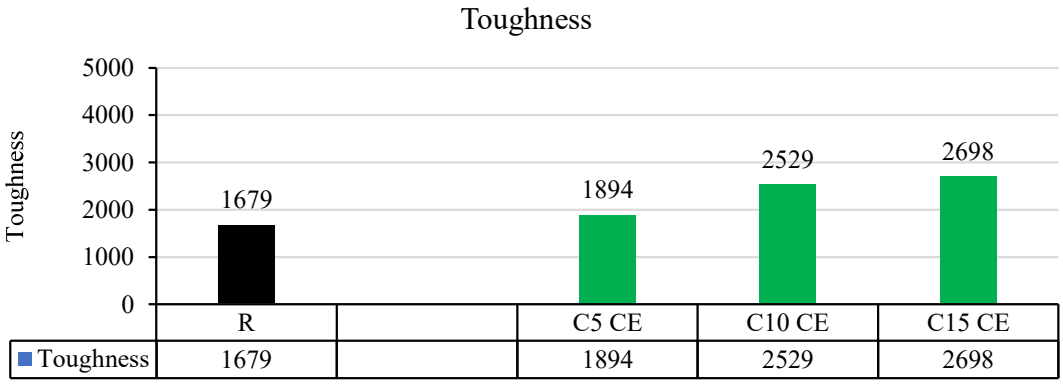

Figure 4-37. Toughness for columns containing ceramic powder.

The toughness results shown in Figure 4-37 showed that the reference mixture was lower than the other mixtures containing ceramic powder. The

results showed that the mixtures containing 5%, 10%, and 15% ceramic powder had higher toughness by 13%, 51%, and 61% than the reference mixture.

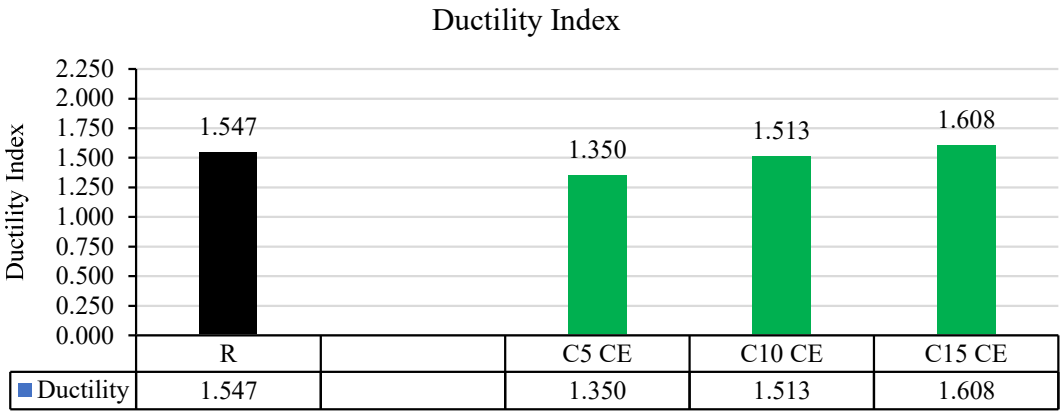

Figure 4-38. Ductility index for columns containing ceramic powder.

The ductility index results in Figure 4-38 show that the effect of concrete columns containing ceramic powder exposed to accelerated cycles on electric current corrosion is less than the concrete column of the reference mixture. The ductility index of the mixtures containing 5% and 10% is lower by 13% and 2%, respectively, while 15% is higher by 4% compared to the column with the reference mixture.

4.6.2 Effect of using marble powder on concrete

The results shown in Figure 4-39 and Figure 4-40 show the results of reinforced concrete columns after being exposed to the process of accelerated corrosion by electric current, in which 5%, 10%, and 15% of the cement were replaced with marble powder.

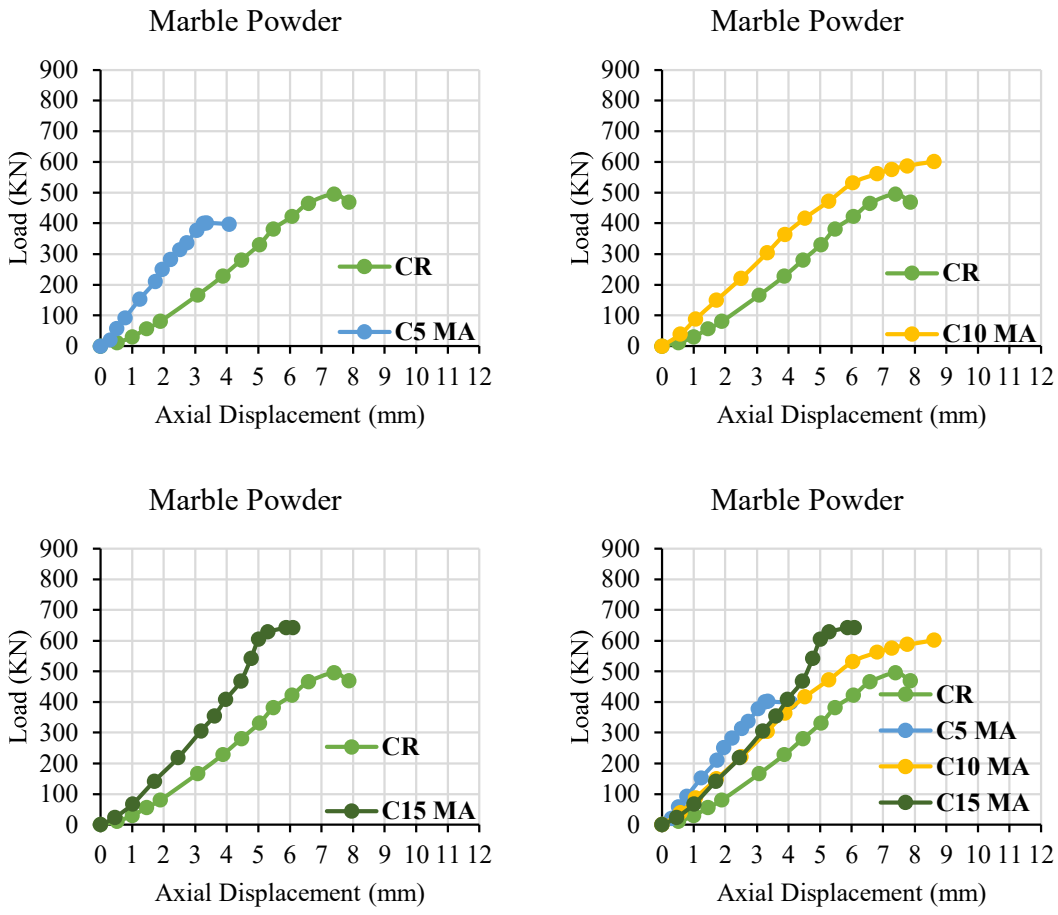

Figure 4-39. Load deflection curves for corroded columns containing marble powder (G7).

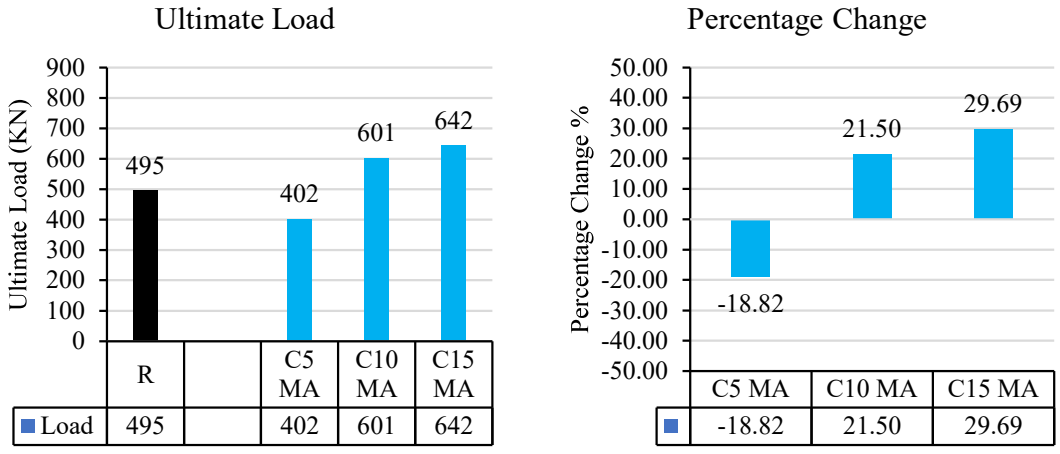

Figure 4-40. Ultimate load for columns containing marble powder.

Figure 4-40 shows the results of the ultimate load of reinforced concrete columns containing marble when subjected to the process of accelerating corrosion by electric current. The results showed that the column containing 5% marble decreased by 19%, while the columns containing 10% and 15% were higher by 21% and 30% respectively compared to the column with the reference mixture.

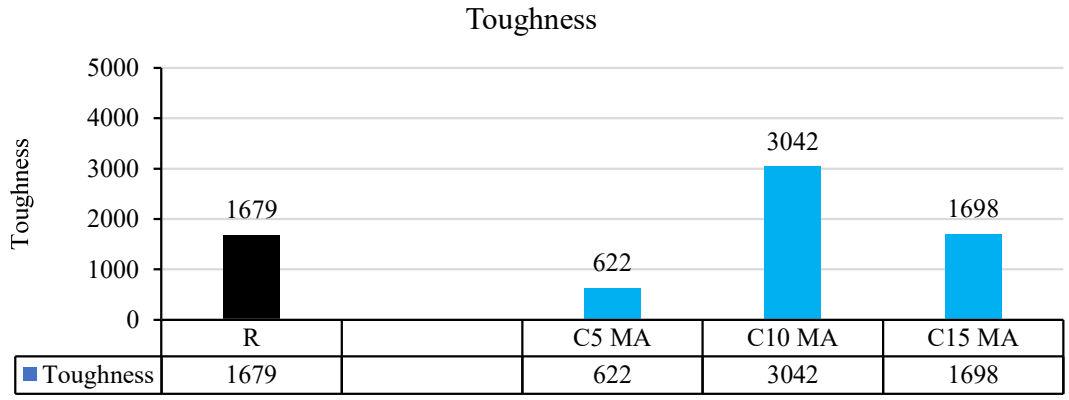

Figure 4-41. Toughness for columns containing marble powder.

Figure 4-41 shows the toughness results of concrete mixtures containing marble. The results showed that the mixtures containing 5% decreased by 63%, while the mixtures containing 10% and 15% increased by 81% and 1% respectively.

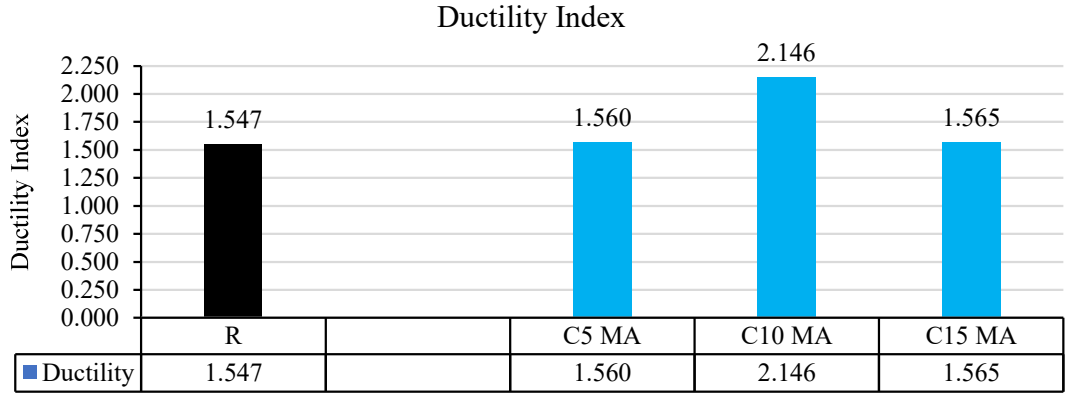

Figure 4-42. Ductility index for columns containing marble powder.

Regarding Figure 4-42, it shows the ductility index results of concrete mixtures containing marble. The results showed that the mixtures containing 5%, 10% and 15% were higher by 1%, 39%, and 1% respectively.

4.6.3 Effect of using glass powder on concrete

The results shown in Figure 4-43 and Figure 4-44 show the results of reinforced concrete columns after being exposed to the process of accelerated corrosion by electric current, in which 5%, 10%, and 15% of the cement were replaced with glass powder.

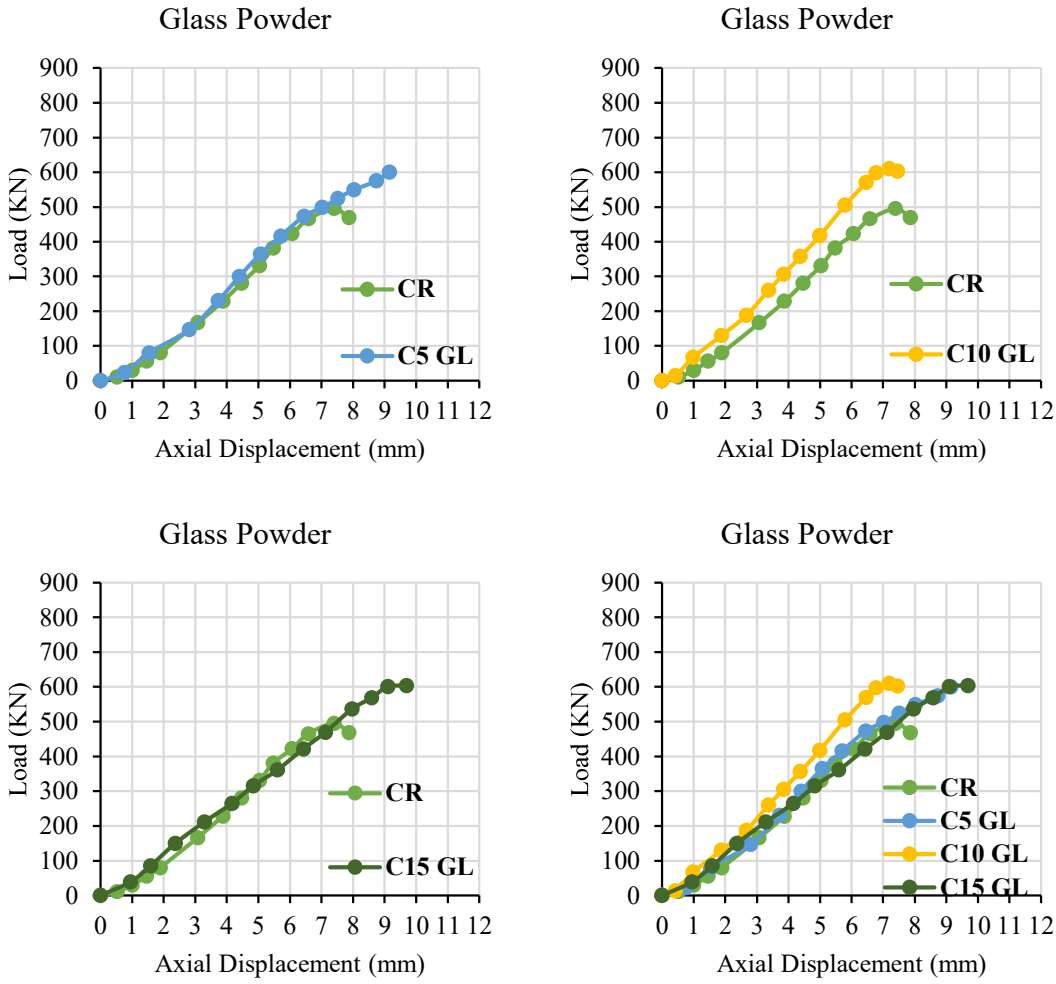

Figure 4-43. Load deflection curves for corroded columns containing glass powder (G8).

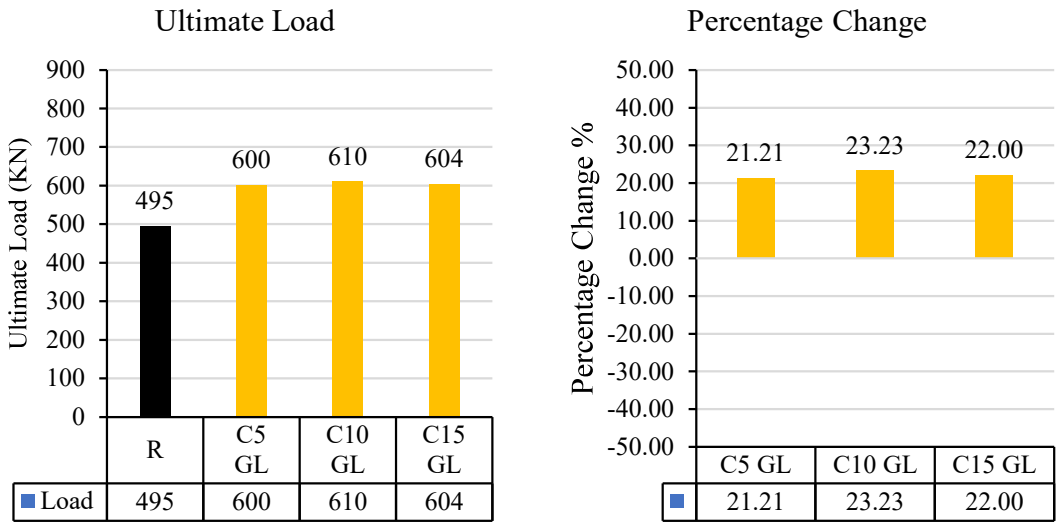

Figure 4-44. Ultimate load for columns containing glass powder.

The ultimate load results shown in Figure 4-44 show that concrete columns containing glass powder are less affected than the column with the reference mixture. The results show that the mixtures containing 5%, 10% and 15% glass are higher than the column with the reference mixture by 21.21%, 23.23% and 22% respectively.

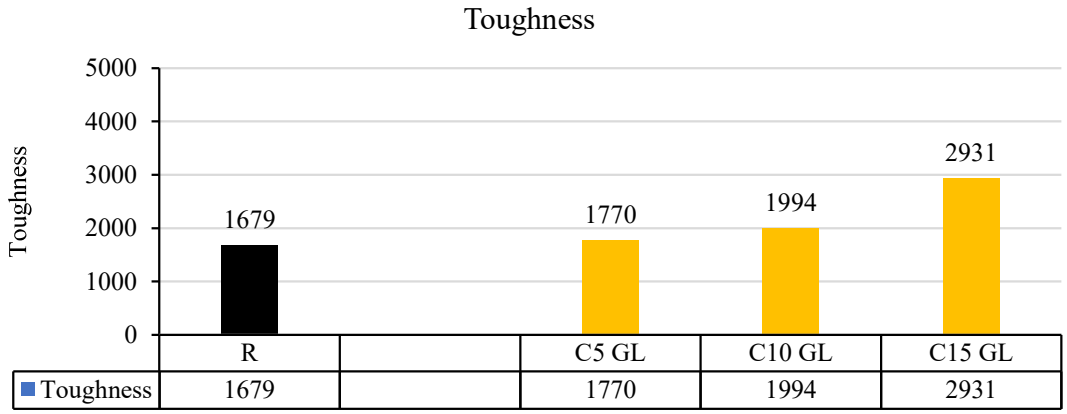

Figure 4-45. Toughness for columns containing glass powder.

The toughness results shown in Figure 4-45 show that the columns containing glass powder are less affected than the columns with the reference

mixture. The results show that the toughness in the columns containing 5%, 10%, and 15% is higher by 5%, 19%, and 75%, respectively.

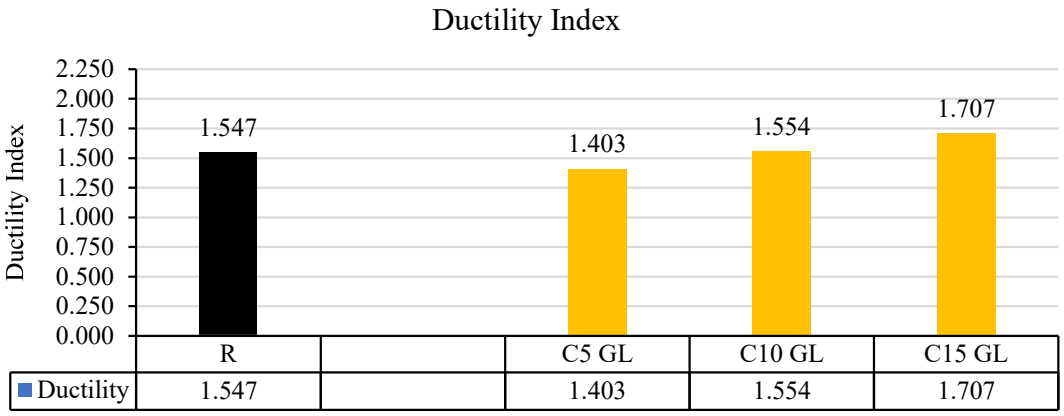

Figure 4-46. Ductility index for columns containing glass powder.

As for the results shown in Figure 4-46, the ductility index of the column with the reference mixture was higher than the ductility index values of the concrete columns containing glass powder. As shown in the Figure above, the reinforced concrete columns containing 5% and 10% glass powder were lower by 9% and 1%, respectively. In comparison, the column with the concrete mixture containing 15% glass powder was higher by 10% compared to the column with the reference mixture.

4.6.4 Effect of using carbon black on concrete

The results shown in Figures (51 and 52) show the results of reinforced concrete columns after being exposed to the process of accelerated corrosion by electric current, in which 0.5%, 1%, and 1.5% of the cement were replaced with carbon black.

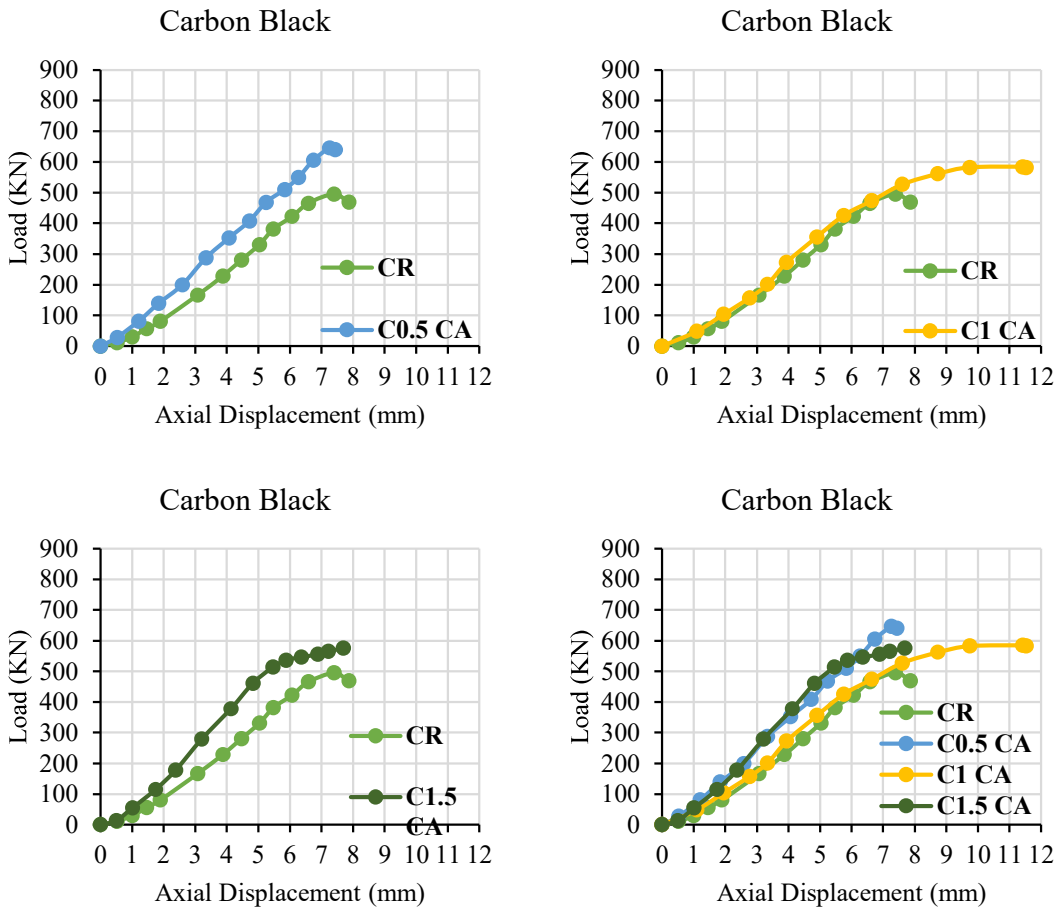

Figure 4-47. Load deflection curves for corroded columns containing carbon black powder (G9).

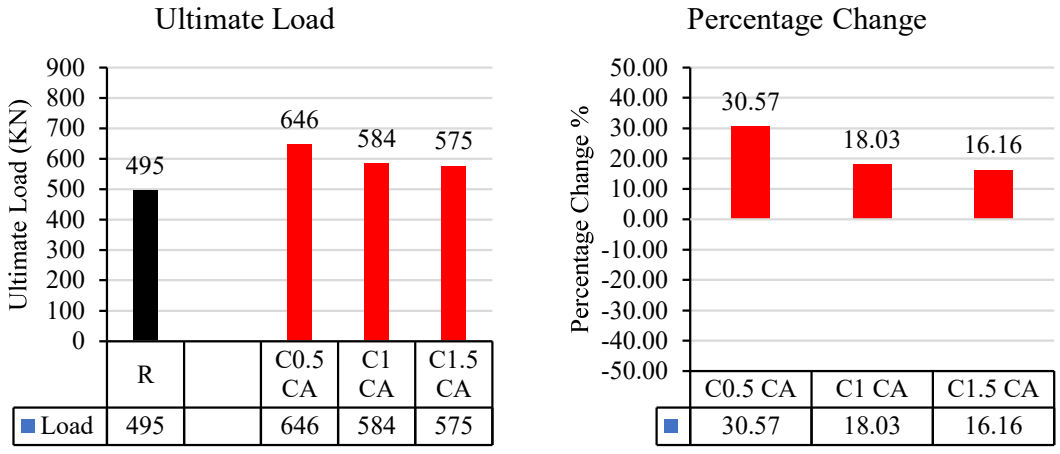

Figure 4-48. Ultimate load for columns containing carbon black powder.

Figure 4-48 shows the results of the ultimate load for concrete columns containing carbon, which shows that they are less affected by the process of accelerating corrosion by electric current. The results show that concrete columns containing carbon black at a rate of 0.5%, 1%, and 1.5% are higher by 31%, 18% and 16% respectively.

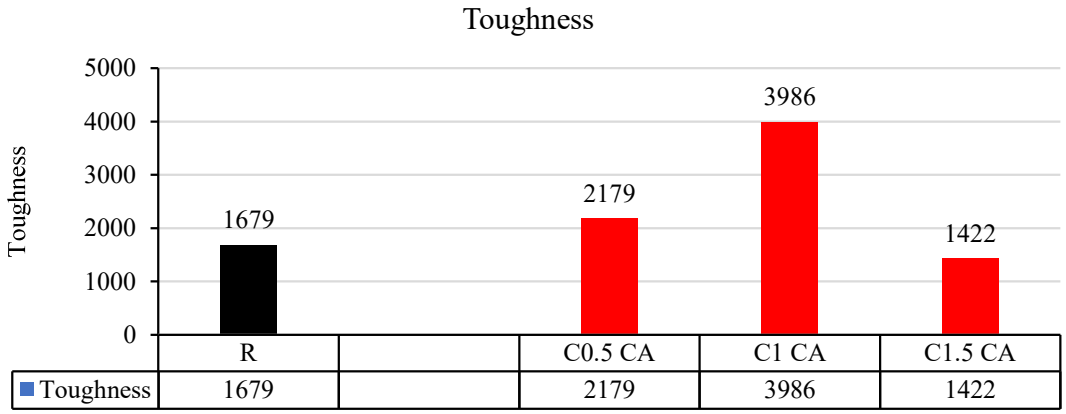

Figure 4-49. Toughness for columns containing carbon black powder.

As for the toughness, its results were fluctuating, as shown in Figure 4-49. It appears that the mixtures containing carbon black at a rate of 0.5% and 1% are higher by 30% and 137%, while the mixture containing 1.5% is lower by 15% compared to the column with the reference mixture.

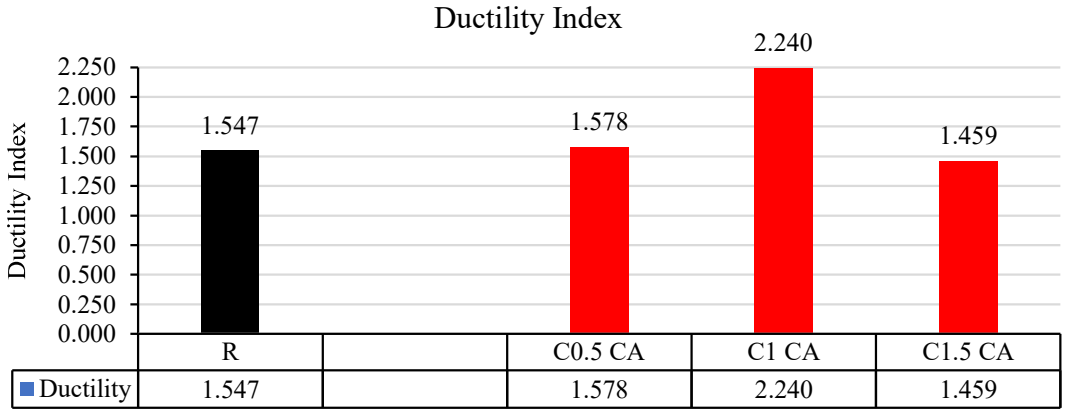

Figure 4-50. Ductility index for columns containing carbon black powder.

As for ductility index, it showed a behavior similar to that of toughness, as shown in Figure 4-50. The results shown in Figure 4-50 show that the mixtures with ratios of 0.5% and 1% are higher by 2% and 45%, respectively, while the column containing 1.5% is lower by 6% compared to the column with the reference mixture.

4.6.5 Effect of using graphite powder on concrete

The results shown in Figure 4-51 and Figure 4-52 show the results of reinforced concrete columns after being exposed to the process of accelerated corrosion by electric current, in which 0.5%, 1%, and 1.5% of the cement were replaced with graphite.

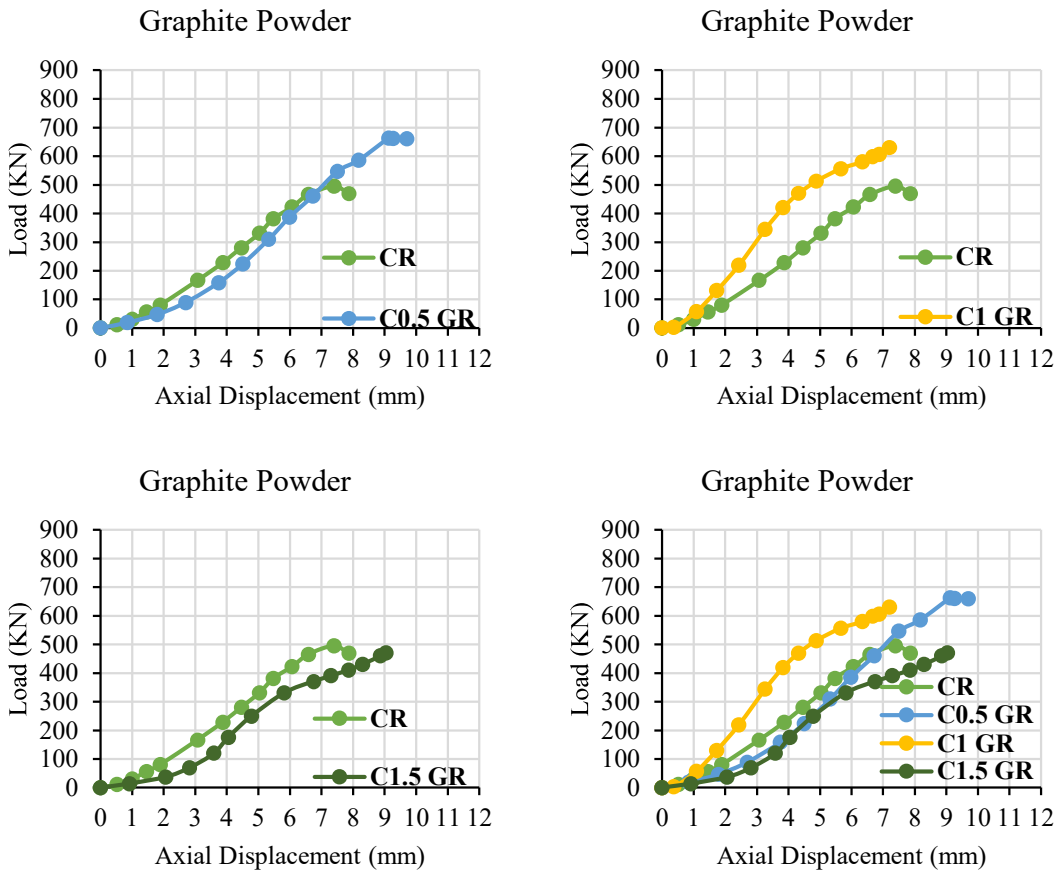

Figure 4-51. Load deflection curves for corroded columns containing graphite powder (G10).

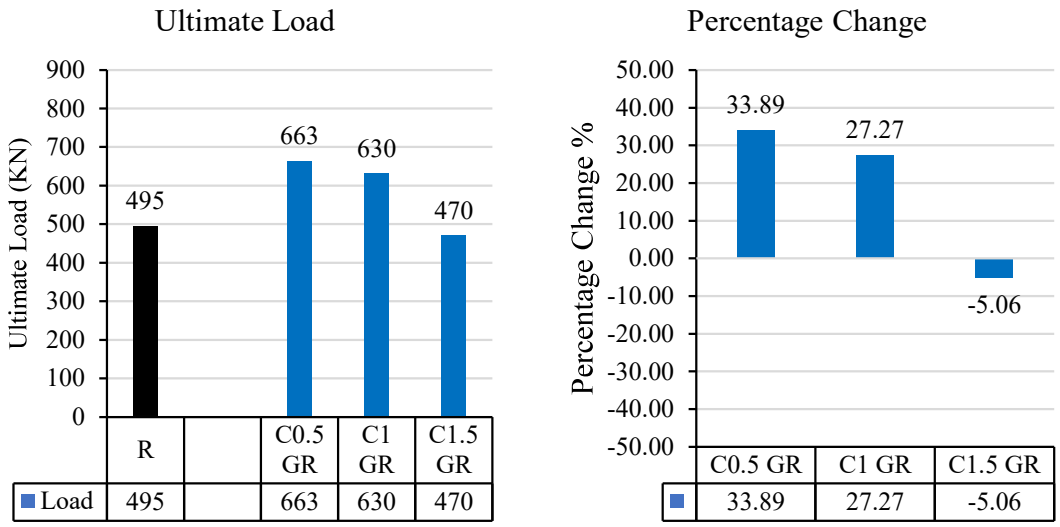

Figure 4-52. Ultimate load for columns containing graphite powder.

The ultimate load results shown in Figure 4-52 show that the columns with lower ratios are less affected by the process of accelerating corrosion by electric current than the column with the reference mixture. The columns with 0.5% and 1% ratios are 34% and 27% higher, respectively, while the column with 1.5% ratio is 5% lower compared to the column with the reference mixture.

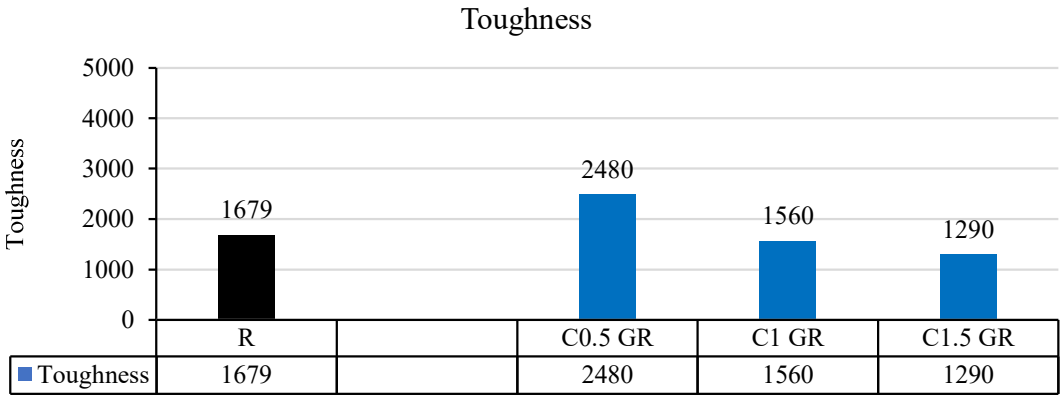

Figure 4-53. Toughness for columns containing graphite powder.

As for the toughness, the results shown in Figure 4-53 show that the lowest value is higher than the reference value, unlike the other values. The 0.5%

ratio is 48% higher, while the 1% and 1.5% ratios showed a decrease of 7% and 23%, respectively, compared to the column with the reference mixture.

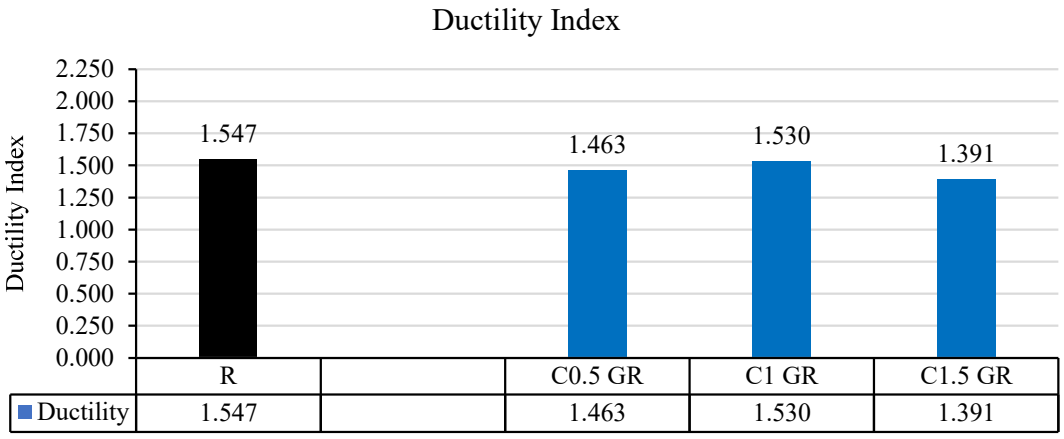

Figure 4-54. Ductility index for columns containing graphite powder.

Figure 4-54 shows the results of the ductility index, which show that there was a decrease in all columns. The results show that the columns containing graphite at a rate of 0.5%, 1%, and 1.5% had their ductility index values decreased by 5%, 1%, and 10%, respectively, compared to the column with the reference mixture.

4.7 Comparison between corroded and non-corroded concrete columns

In this paragraph, a comparison will be made between the results obtained for concrete columns that were subjected to the process of accelerating corrosion using electric current and concrete columns that were not subjected to the process of accelerating corrosion using electric current.

4.7.1 Effect of using ceramic powder on concrete

The Figures below show a comparison between the results of columns containing 5%, 10%, and 15% ceramic powder in the normal condition and the condition that was exposed to the electric current acceleration corrosion process.

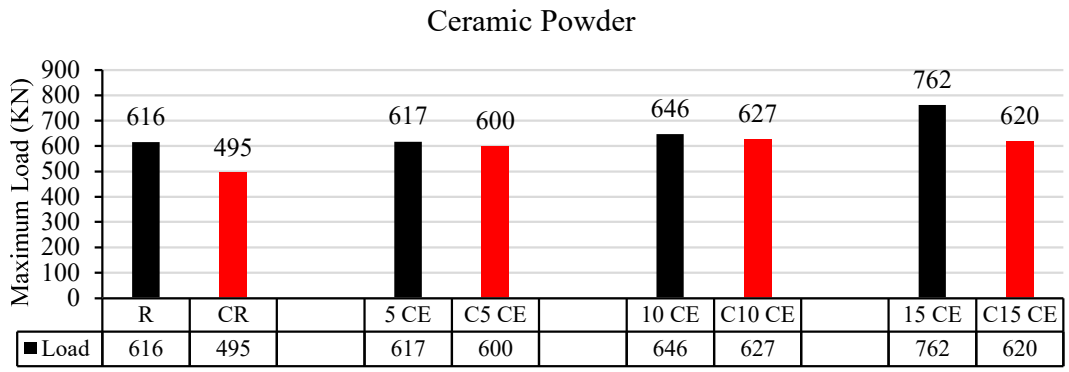

Figure 4-55. Ultimate load results of columns exposed and non-exposed to corrosion containing ceramic powder.

The results shown in Figure 4-55 show the ultimate load results for concrete columns. The results show that the mixtures containing ceramic powder at a rate of 0%, 5%, 10%, and 15% before corrosion decreased by 19.6%, 2.7%, 3.4%, and 18.6%, respectively, compared to the columns that were exposed to the process of accelerating corrosion by electric current. It is noted that the mixture that does not contain ceramic powder is the mixture with the least decrease compared to the other mixtures.

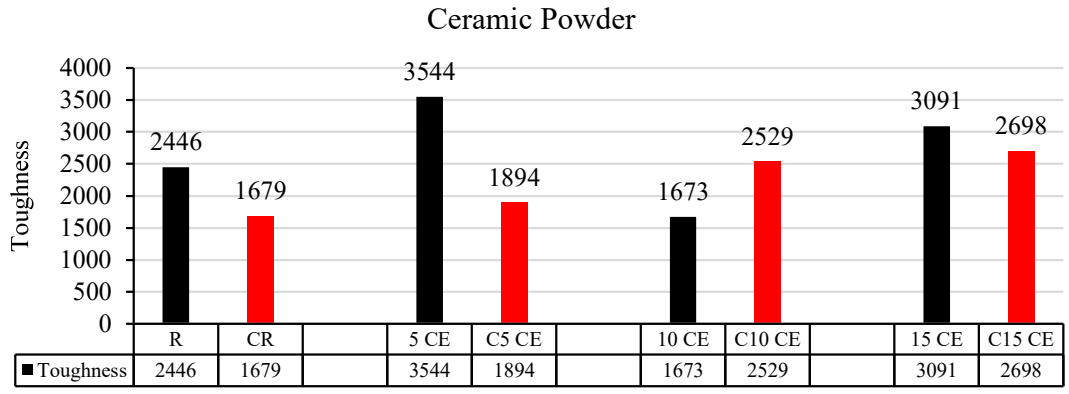

Figure 4-56. Toughness results of columns exposed and non-exposed to corrosion containing ceramic powder.

As for toughness, the results of which are shown in Figure 4-56, the mixtures containing ceramic powder are less affected than the mixture that does not contain ceramic powder, except for the mixture with a ratio of 5%.

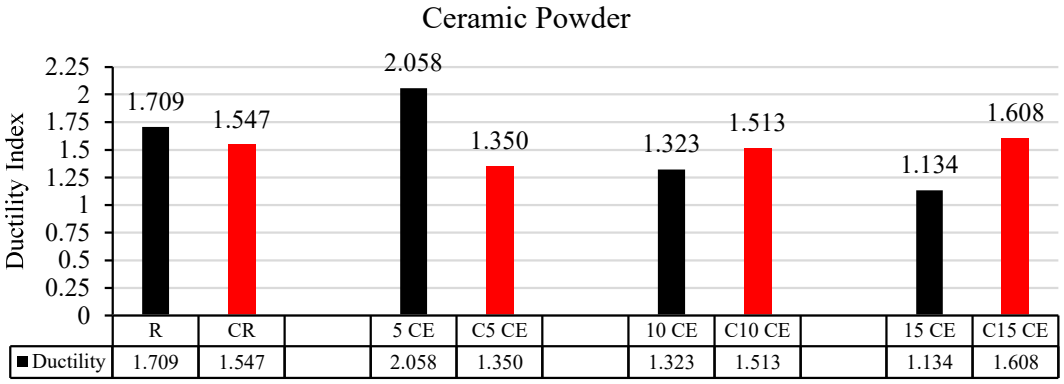

Figure 4-57. Ductility index results of columns exposed and non-exposed to corrosion containing ceramic powder.

Ductility index shows a similar behavior to that of toughness, the results of which are shown in Figure 4-57. Mixtures containing ceramic powder are less affected than mixes not containing ceramic powder, except for the mix with a ratio of 5%.

4.7.2 Effect of using marble powder on concrete

The Figures below show a comparison between the results of columns containing 5%, 10%, and 15% marble powder in the normal condition and the condition that was exposed to the electric current acceleration corrosion process.

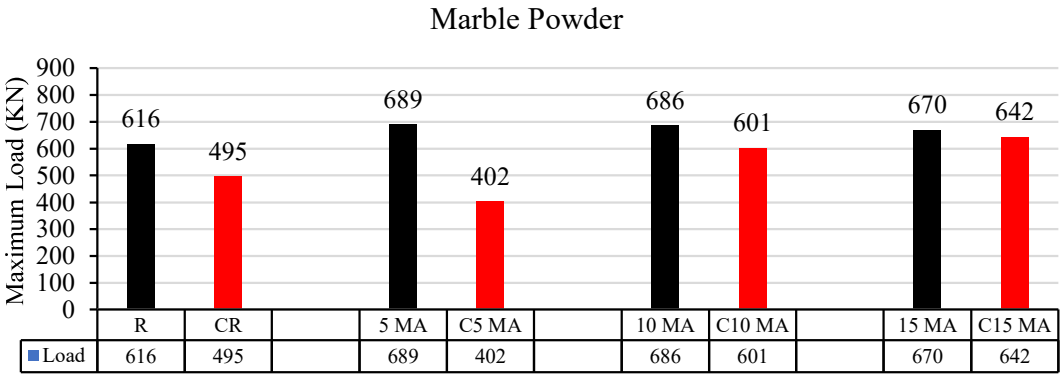

Figure 4-58. Ultimate load results of columns exposed and non-exposed to corrosion containing marble powder.

Figure 4-58 shows the results of the ultimate load for concrete mixes containing marble powder. Comparing concrete columns subjected to corrosion age and normal concrete columns, it is clear that the mixes with ratios of 0%, 5%, 10%, and 15% decreased by 19.6%, 41.6%, 12.4% and 4%. It is clear that the use of marble powder reduced the effect of the corrosion process.

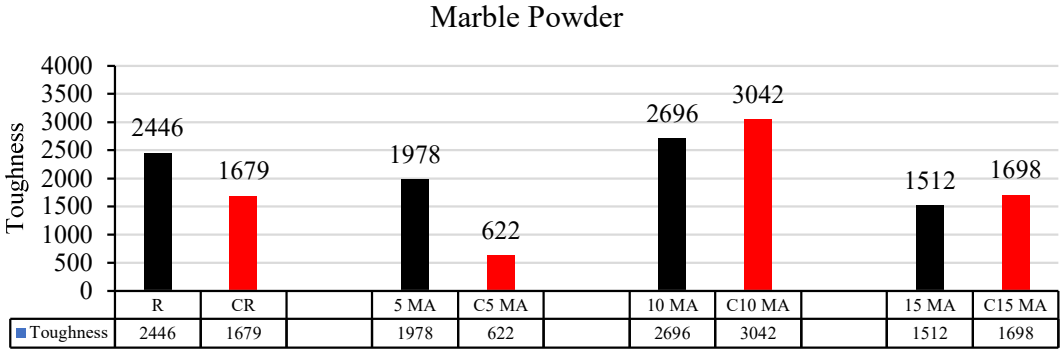

Figure 4-59. Toughness results of columns exposed and non-exposed to corrosion containing marble powder.

Figure 4-59 shows a comparison of the toughness results between concrete columns exposed to corrosion and concrete columns not exposed to corrosion. It is clear that increasing the percentage of marble powder addition reduced the effect of corrosion in general, except for the mixture containing 5% marble powder.

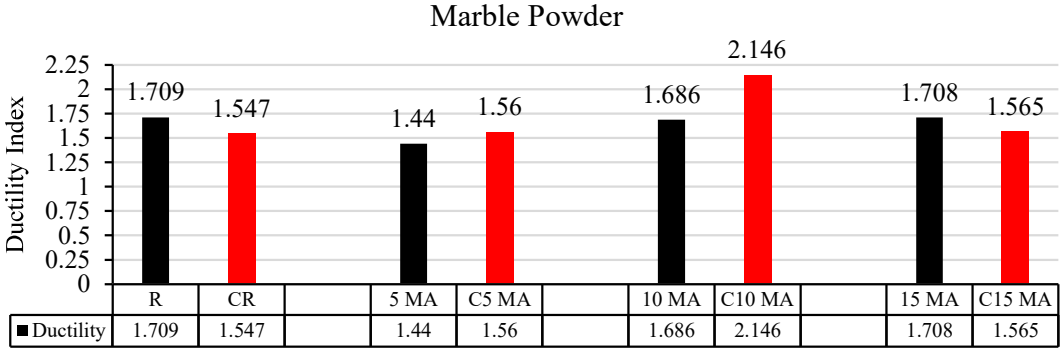

Figure 4-60. Ductility index results of columns exposed and non-exposed to corrosion containing marble powder.

Also, adding marble powder reduced the impact of concrete columns and maintained their ductility index, as shown in the results presented in Figure 4-60.

4.7.3 Effect of using glass powder on concrete

The Figures below show a comparison between the results of columns containing 5%, 10%, and 15% glass powder in the normal condition and the condition that was exposed to the electric current acceleration corrosion process.

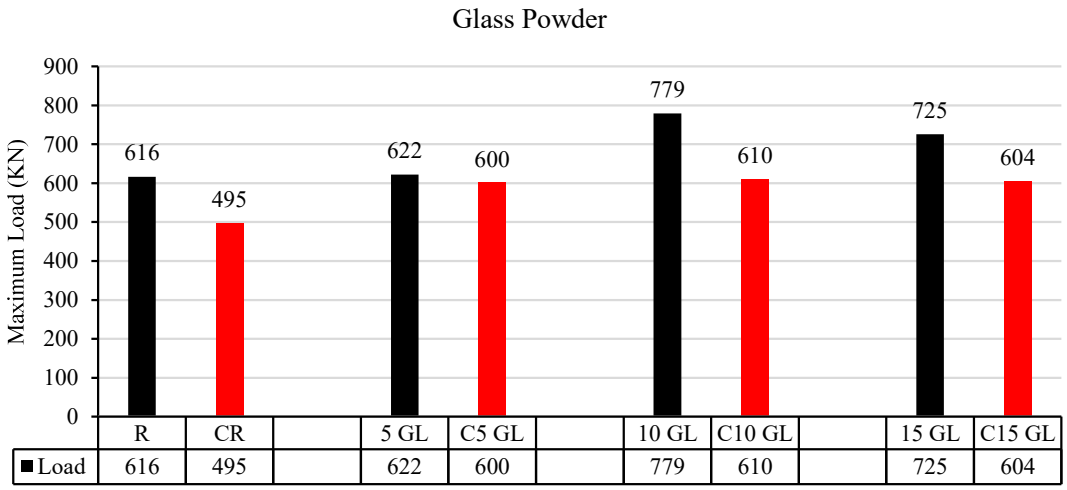

Figure 4-61. Ultimate load results of columns exposed and non-exposed to corrosion containing glass powder.

Figure 4-61 shows the ultimate load results of concrete mixtures containing glass powder. Comparing concrete columns subjected to corrosion with normal concrete columns, it is clear that the mixtures with ratios of 0%, 5%, 10%, and 15% decreased by 19.6%, 3.5%, 21.7%, and 16.7%, respectively. It is clear that the use of glass powder reduced the effect of the corrosion process.

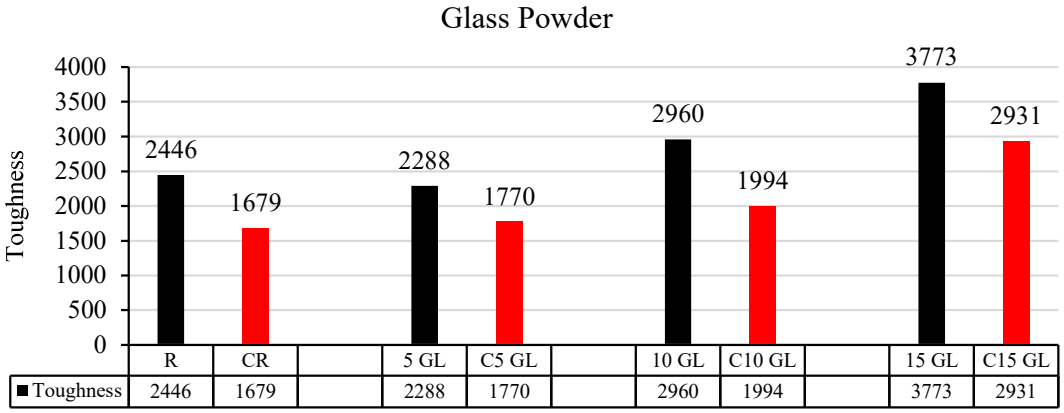

Figure 4-62. Toughness results of columns exposed and non-exposed to corrosion containing glass powder.

Figure 4-62 shows a comparison of the toughness results between concrete columns exposed to corrosion and concrete columns not exposed to corrosion. It is clear that increasing the percentage of glass powder addition reduced the effect of corrosion in general.

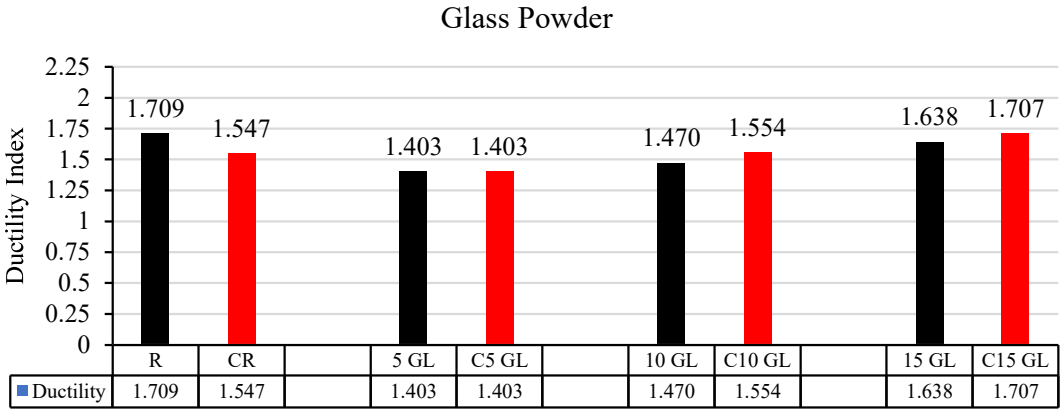

Figure 4-63. Ductility index results of columns exposed and non-exposed to corrosion containing glass powder.

Also, adding glass powder reduced the impact of concrete columns and maintained their ductility index, as shown in the results presented in Figure 4-63.

4.7.4 Effect of using carbon black on concrete

The Figures below show a comparison between the results of columns containing 0.5%, 1%, and 1.5% carbon black powder in the normal condition and the condition that was exposed to the electric current acceleration corrosion process.

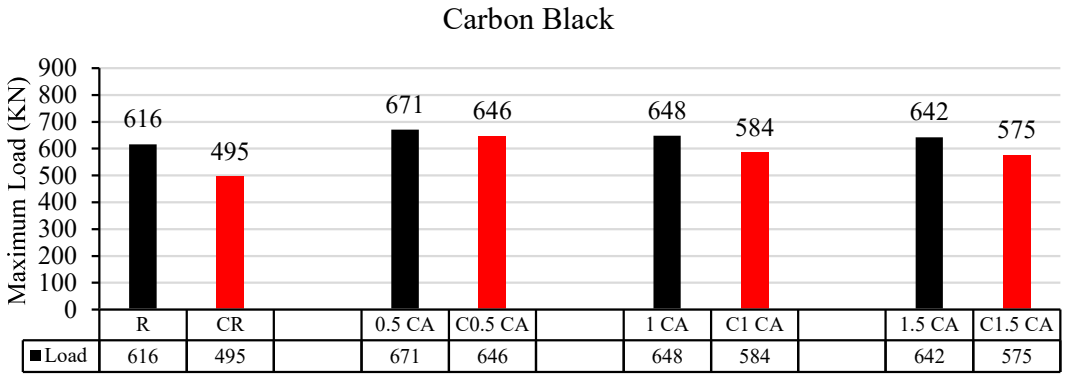

Figure 4-64. Ultimate load results of columns exposed and non-exposed to corrosion containing carbon black powder.

Figure 4-64 shows the results of the ultimate load for concrete mixes containing carbon black powder. Comparing concrete columns subjected to corrosion age and normal concrete columns, it is clear that the mixes with ratios of 0%, 0.5%, 1%, and 1.5% decreased by 19.6%, 3.7%, 9.9%, and 10.4%. It is clear that the use of carbon black powder reduced the effect of the corrosion process.

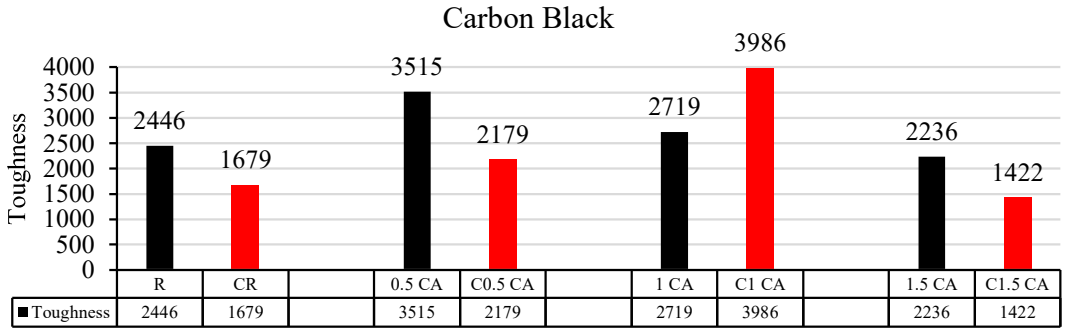

Figure 4-65. Toughness results of columns exposed and non-exposed to corrosion containing carbon black powder.

Figure 4-65 shows the results of the toughness of concrete columns containing black carbon powder. It shows that the use of carbon has preserved the toughness from being significantly affected, especially in the mixture containing 1% black carbon powder.

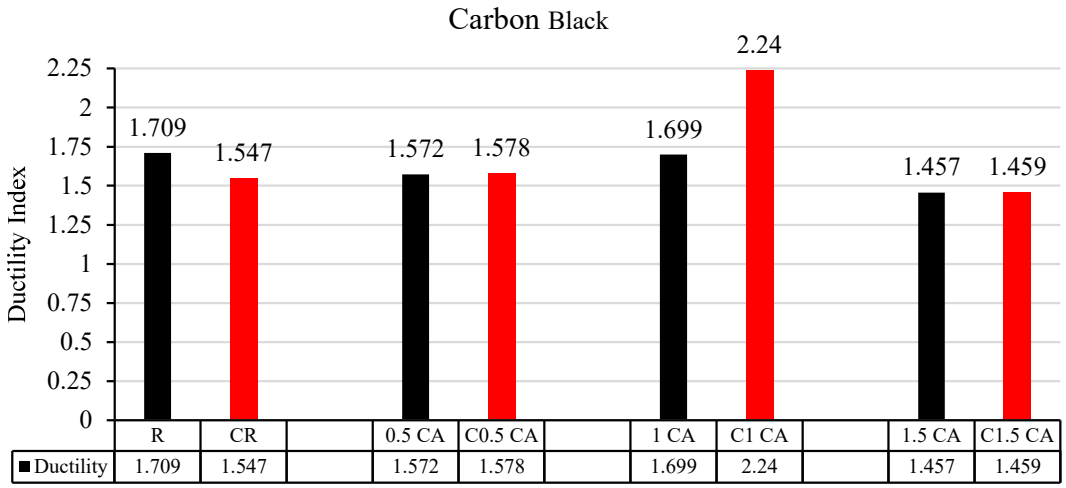

Figure 4-66. Ductility index results of columns exposed and non-exposed to corrosion containing carbon black powder.

Also, adding carbon black powder reduced the impact of concrete columns and maintained their ductility index, as shown in the results presented in Figure 4-66.

4.7.5 Effect of using graphite powder on concrete

The Figures below show a comparison between the results of columns containing 0.5%, 1%, and 1.5% graphite powder in the normal condition and the condition that was exposed to the electric current acceleration corrosion process.

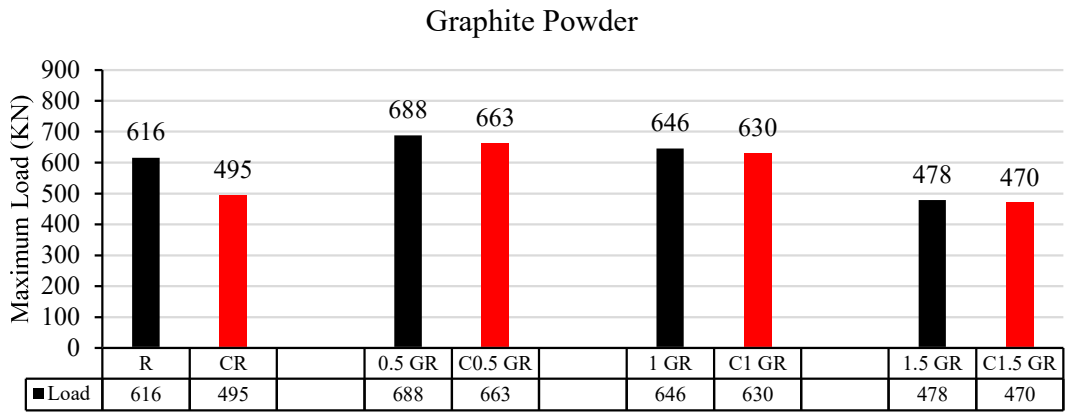

Figure 4-67. Ultimate load results of columns exposed and non-exposed to corrosion containing graphite powder.

Figure 4-67 shows the ultimate load results for concrete mixes containing graphite powder. Comparing concrete columns subjected to corrosion age and normal concrete columns, the mixes with ratios of 0%, 0.5%, 1%, and 1.5% decreased by 19.6%, 3.6%, 2.5%, and 2.1%, respectively. The use of graphite powder reduced the effect of the corrosion process.

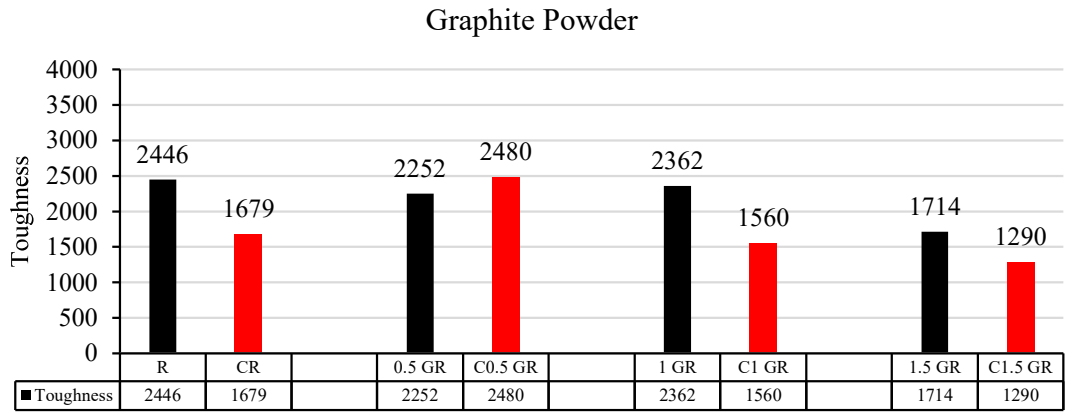

Figure 4-68. Toughness results of columns exposed and non-exposed to corrosion containing graphite powder.

Figure 4-68 shows the toughness results of concrete columns containing graphite powder. It shows that the use of carbon has preserved the

toughness from being significantly affected, especially in the mixture containing 0.5% graphite powder.

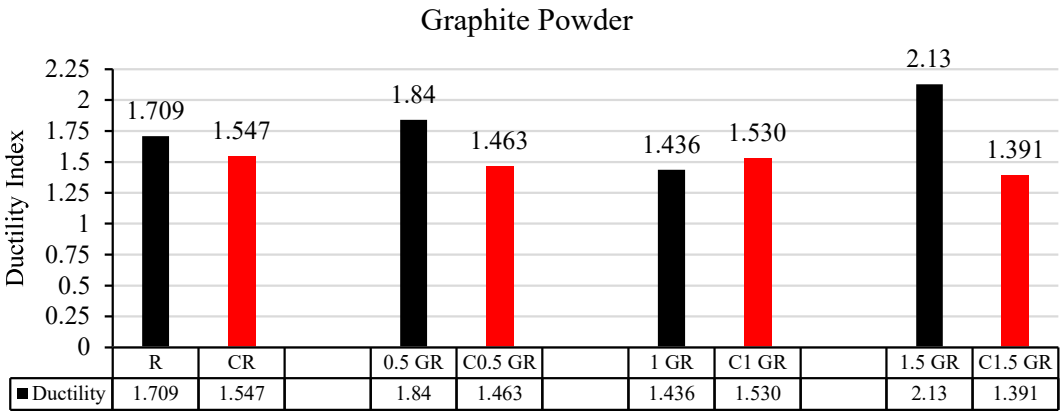

Figure 4-69. Ductility index results of columns exposed and non-exposed to corrosion containing graphite powder.

The addition of graphite powder also reduced the impact of concrete columns and maintained their ductility index slightly, especially in the mixture containing 1% graphite, as shown in the results in Figure 4-69.

Chapter Five: Finite Element Analysis

5.1 General

This chapter aims to develop a model based on experimental results using nonlinear finite elements to verify the suitability of material properties, element shapes, and convergence requirements. It also aims to study the response of short circular section columns made of non-corroded and corroded concrete. In addition, new parameters are analyzed in terms of their structural behavior based on a model achieved using the nonlinear finite element method (ABAQUS 2019).

5.2 Description of Finite Element Modeling

This section reviews the assembly process of the tested columns, along with the loading methodology and boundary conditions adopted.

5.2.1 Modeling of the Used Material

The identical geometry, material properties, loading conditions, and boundary constraints employed in the experimental work were replicated in finite-element modeling to simulate the tested columns. The modeling of the control column comprises four components: concrete, primary reinforcement, spiral, and steel plates, as depicted in Figure (5-1). The components are created individually for subsequent assembly into the control model. During the contraction phase, all components, including the primary reinforcement and the stirrups embedded inside the concrete, were interconnected by the embedded region constraint. Conversely, the tie limitations were employed to secure the steel plate to the concrete.

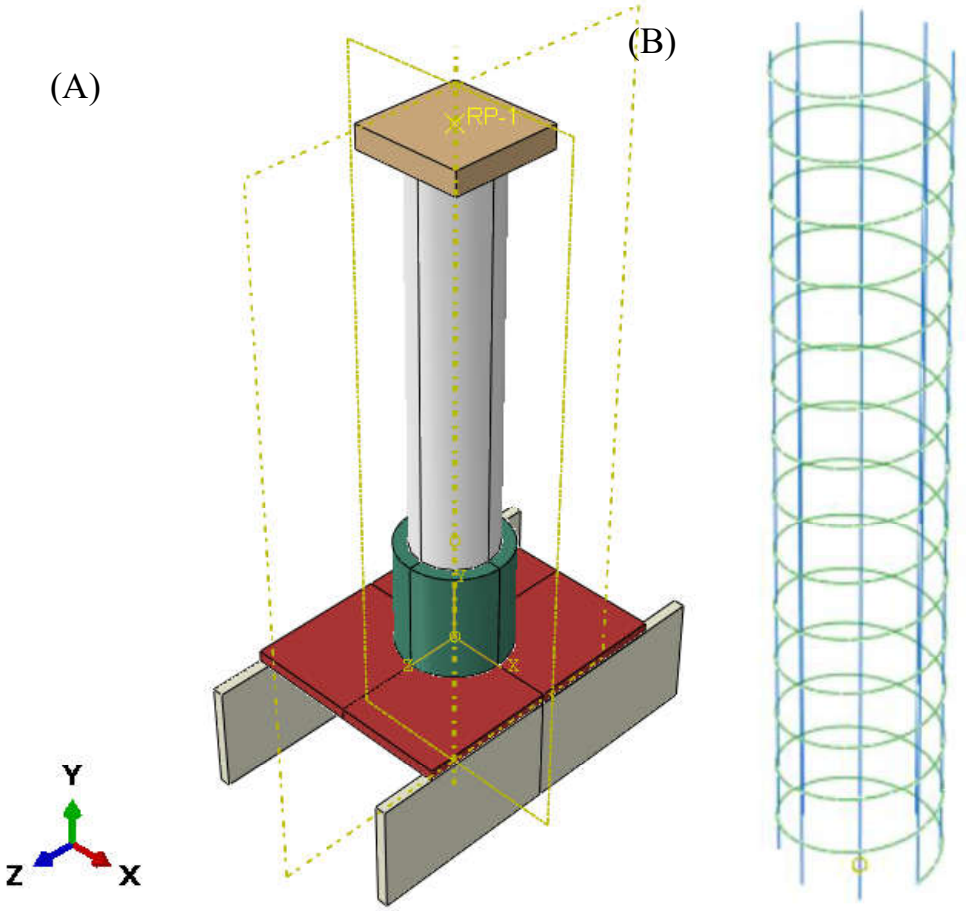

Figure 5-1. The assembled parts (A) steel reinforcement (B) the concrete model.

5.2.1.1 Concrete

All specimens were fabricated with uniform dimensions of a circle cross-section (150 mm diameter) and an overall length of 700 mm. In 3D finite element analysis, concrete is modeled as a linear solid brick element. Table 5-1 presents the fundamental features assumed in the modeling of concrete.

Table 5-1. General properties used in the model for the damaged concrete.

Dilation angle (Degree)	30
Eccentricity (mm)	0
Fb0/fc0	1.16
k	0.667
Viscosity parameter	0
Poisson Ratio	0.2

5.2.1.2 Steel reinforcement

The vertical reinforcement of the column was represented by an 8 mm diameter rebar with the number 8 as used in the experimental model. The stirrup reinforcement was represented by a 4 mm diameter rebar in a spiral shape with a 4 cm spacing, as used in the experimental model. The elastic modulus and Poisson ratio of the used rebar were assumed 200 GPa and 0.3, respectively.

5.2.1.3 Steel plates

A piece of iron measuring 200 x 200 x 40 mm was used at the top of the column, with an iron cylinder with a diameter of 200 mm and a height of 200 mm at the bottom of the column. The steel cylinder is supported from below by a 20 mm thick iron plate. This iron plate was supported by two other 20 mm thick iron plates, each to represent the practical test accurately. Everything described in the program was identical to what was present in the practical test. The elastic modulus and Poisson ratio of the used rebar were assumed 200 GPa and 0.3, respectively.

5.2.2 Mesh Sensitivity Analysis in ABAQUS

In the finite element analysis conducted using ABAQUS, a mesh size sensitivity study was performed to evaluate the influence of element size on

the accuracy and stability of the results. Several mesh sizes were tested, and after analyzing the convergence behaviour and the variation in key output parameters, a uniform mesh size of 10 mm was selected for all parts of the model. This mesh size provided a good balance between computational efficiency and result accuracy, ensuring reliable simulation of the structural behaviour.

5.2.3 Loading stage and boundary condition

Loads were applied to the steel plates of each specimen like the experimental work. Loads were applied to a 200×200×40 mm steel plate under a uniformly distributed load of 20 N. Simultaneously, the steel plates were evaluated statically for the steel plates beneath the columns for all specimens, as shown in Figure 5-2.

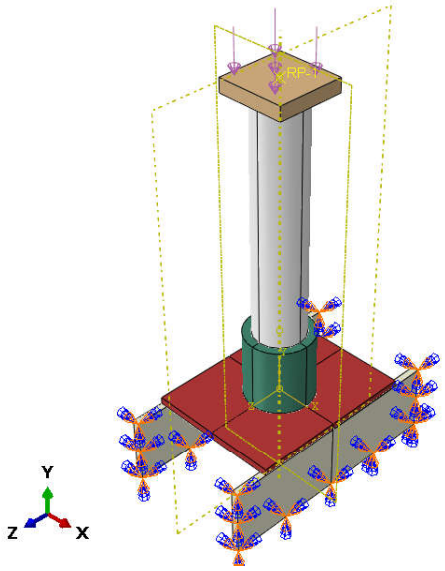

Figure 5-2. Loading and boundary conditions for the models.

5.3 Comparative study between FEM and experimental results

This section presents a comparative analysis of the experimental results and finite element outcomes for the ultimate capacity and vertical load displacement of all examined columns.

5.3.1 Load-displacement behavior

Figures (5-3) to (5-7) depict a comparison between the experimental and FEM load versus vertical deflection curves. Vertical deflections were recorded at the upper edge of the steel plate for all examined columns in a manner analogous to the experimental tests. The comparison demonstrated the validity of the ABAQUS numerical analysis about the experimental data presented in Chapter Four.

Figures (5-3) to (5-7) show the results of concrete columns before being exposed to the effect of corrosion.

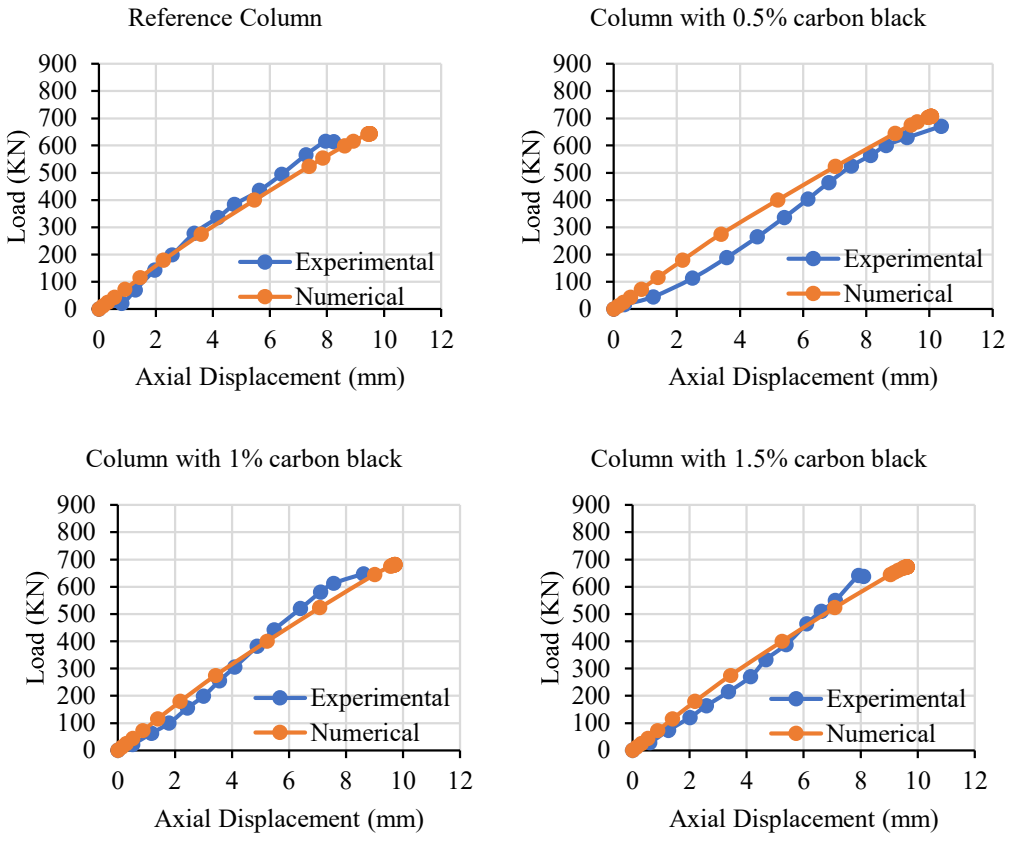

Figure 5-3. Experimental and numerical results for columns containing carbon black in different proportions.

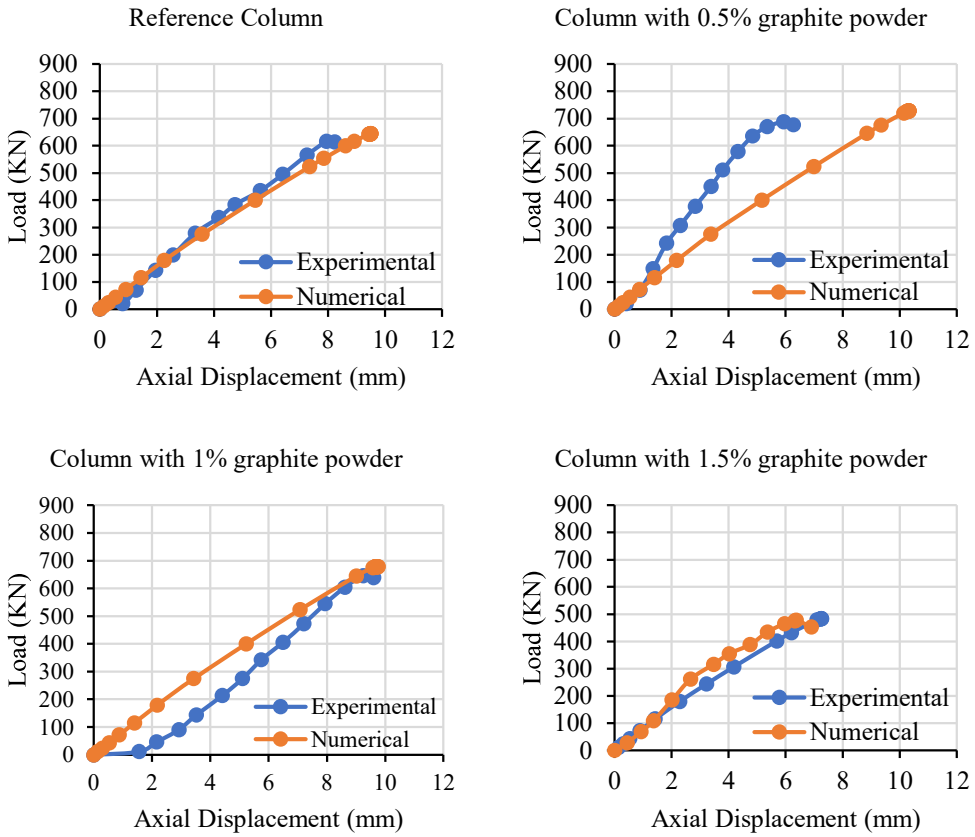

Figure 5-4. Experimental and numerical results for columns containing graphite powder in different proportions.

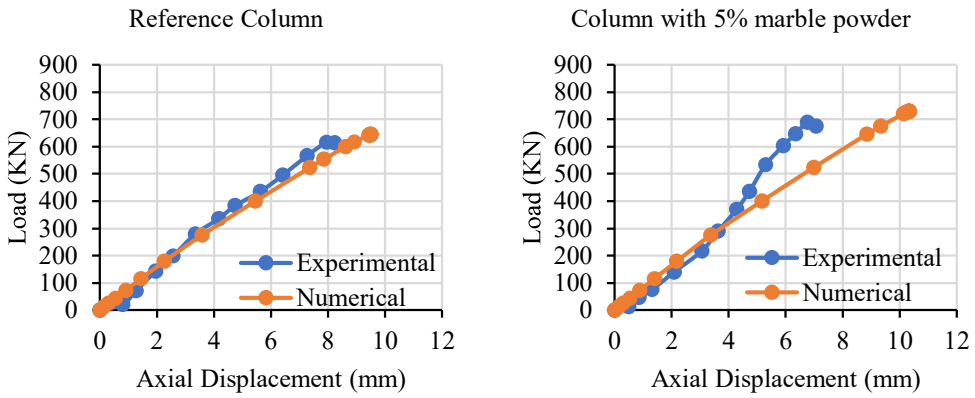

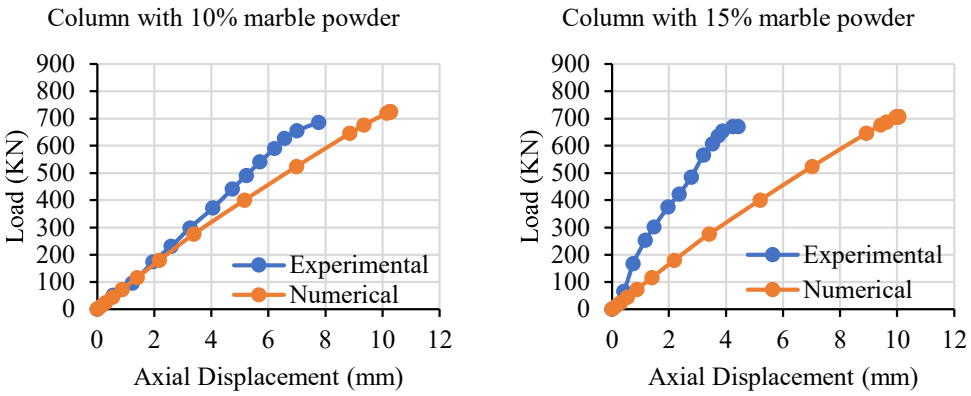

Figure 5-5. Experimental and numerical results for columns containing marble powder in different proportions.

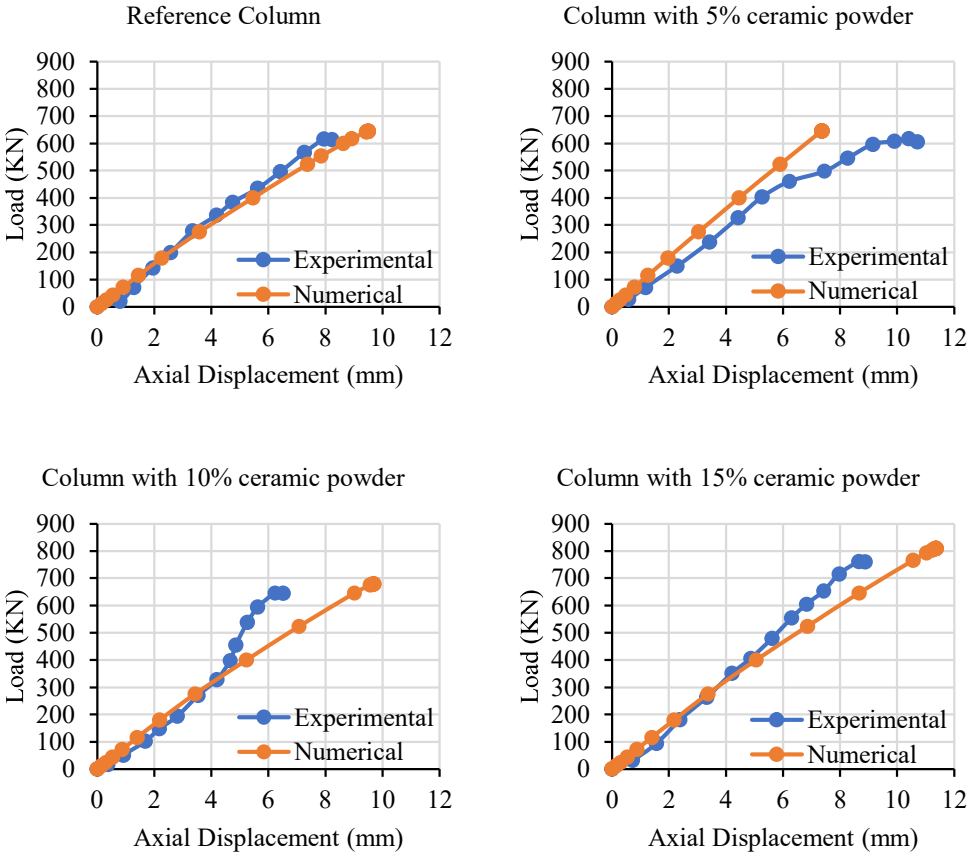

Figure 5-6. Experimental and numerical results for columns containing ceramic powder in different proportions.

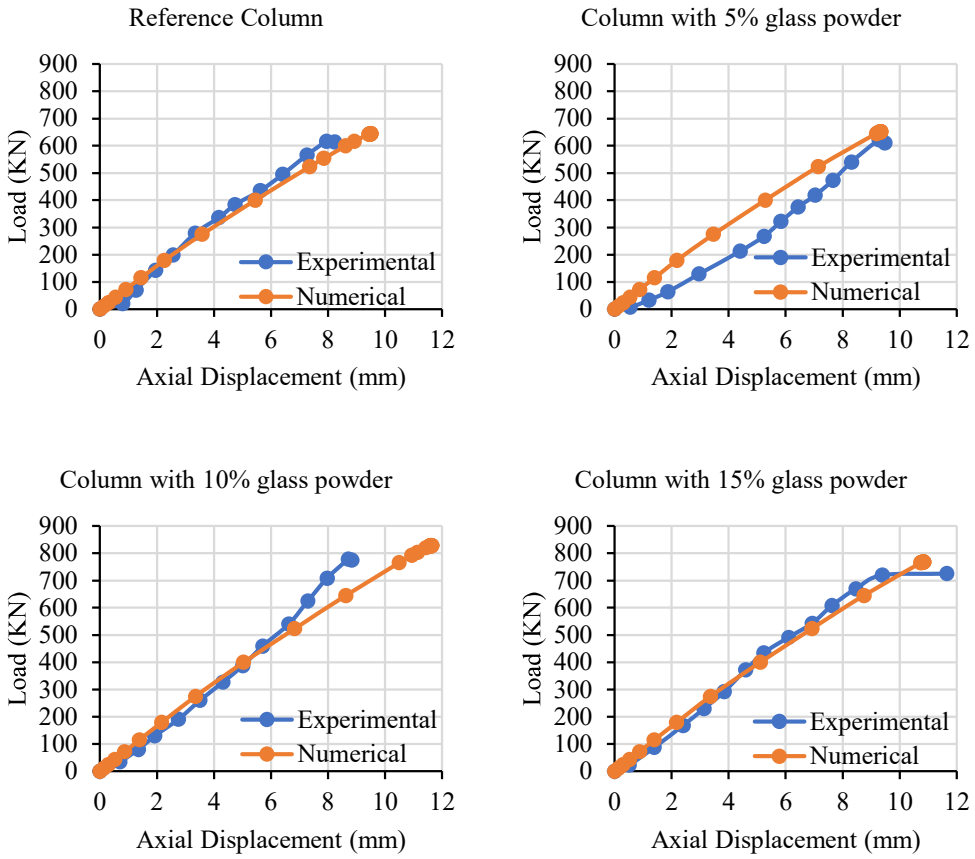

Figure 5-7. Experimental and numerical results for columns containing glass powder in different proportions.

Figures (5-8) to (5-12) show the results of concrete columns before they were exposed to the effect of corrosion.

Table 5-2 shows the percentage difference between the ultimate load value of the model obtained from the Abacus and the ultimate load value obtained from the experimental test of non-corroded concrete columns. The results show that the difference is small, with the highest difference not exceeding 6.5%. Therefore, the values are considered acceptable for the study purposes.

Table 5-2. Percentage difference between the ultimate load obtained from ABAQUS and experimental results for columns not subjected to corrosion.

Column	Percentage	Column	Percentage	Column	Percentage	Column	Percentage
R	4.61%	**0.5GR**	5.72%	**10MA**	5.71%	**15CE**	6.20%
0.5CA	5.45%	**1GR**	5.02%	**15MA**	5.46%	**5GL**	4.70%
1CA	5.17%	**1.5GR**	1.10%	**5CE**	4.53%	**10GL**	6.45%
1.5CA	5.02%	**5MA**	5.71%	**10CE**	5.12%	**15GL**	5.92%

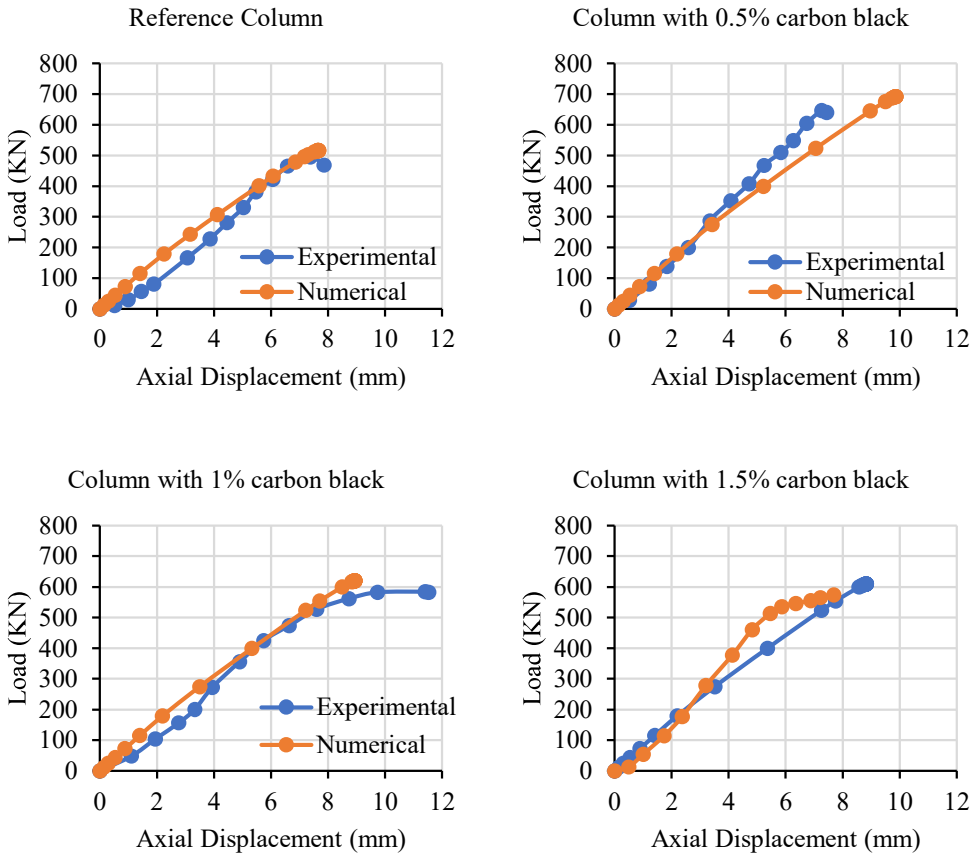

Figure 5-8. Experimental and numerical results for columns containing carbon black in different proportions and subjected to corrosion.

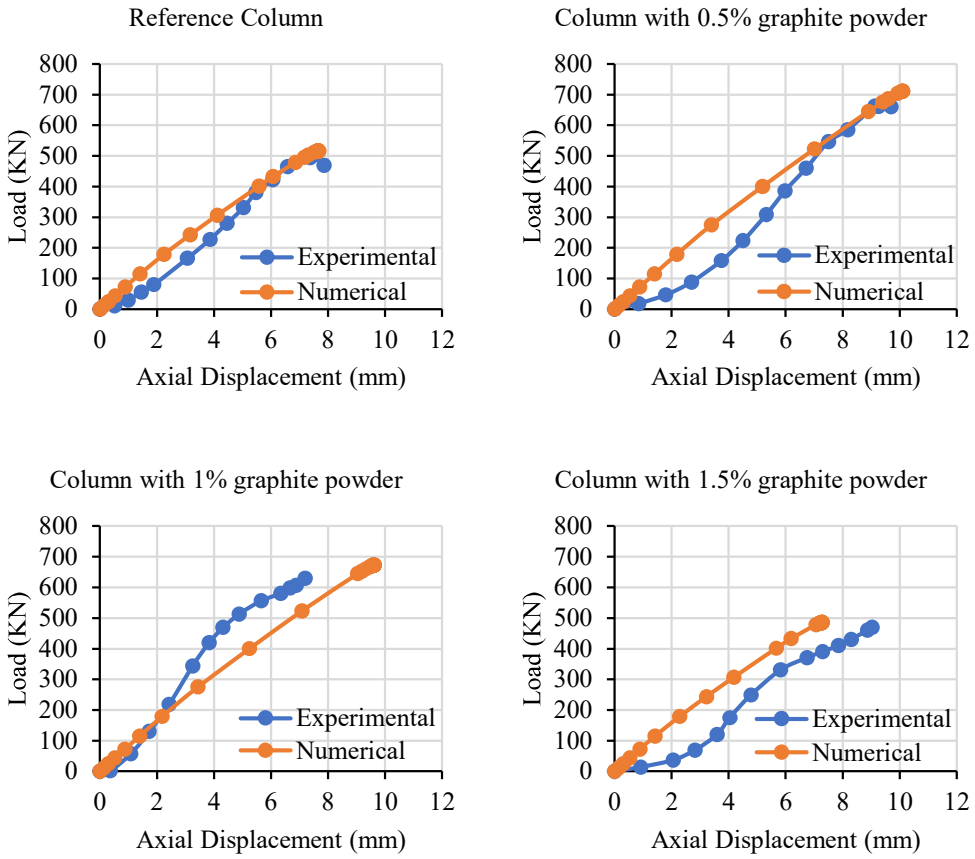

Figure 5-9. Experimental and numerical results for columns containing graphite powder in different proportions and subjected to corrosion.

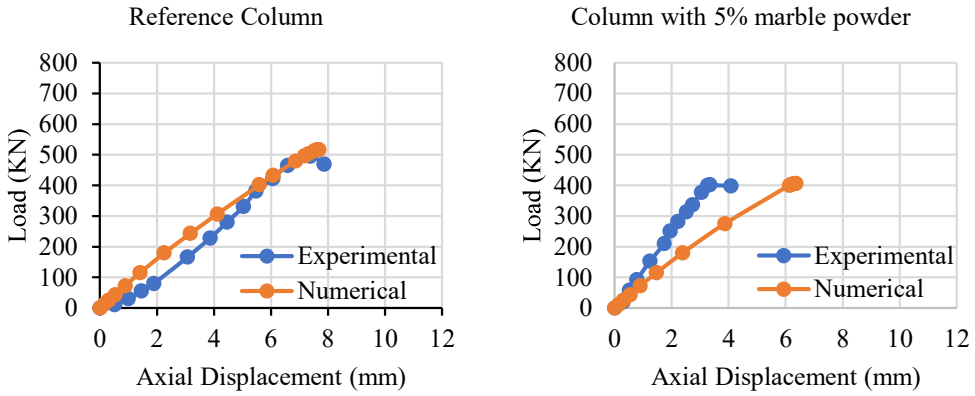

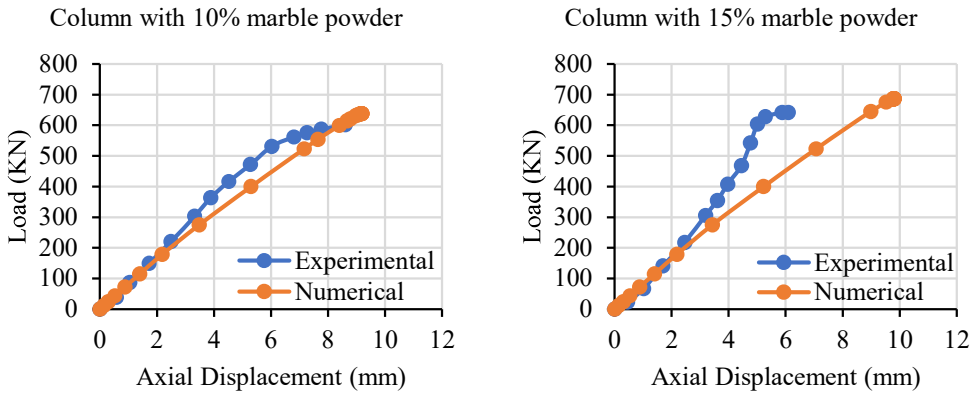

Figure 5-10. Experimental and numerical results for columns containing marble powder in different proportions and subjected to corrosion.

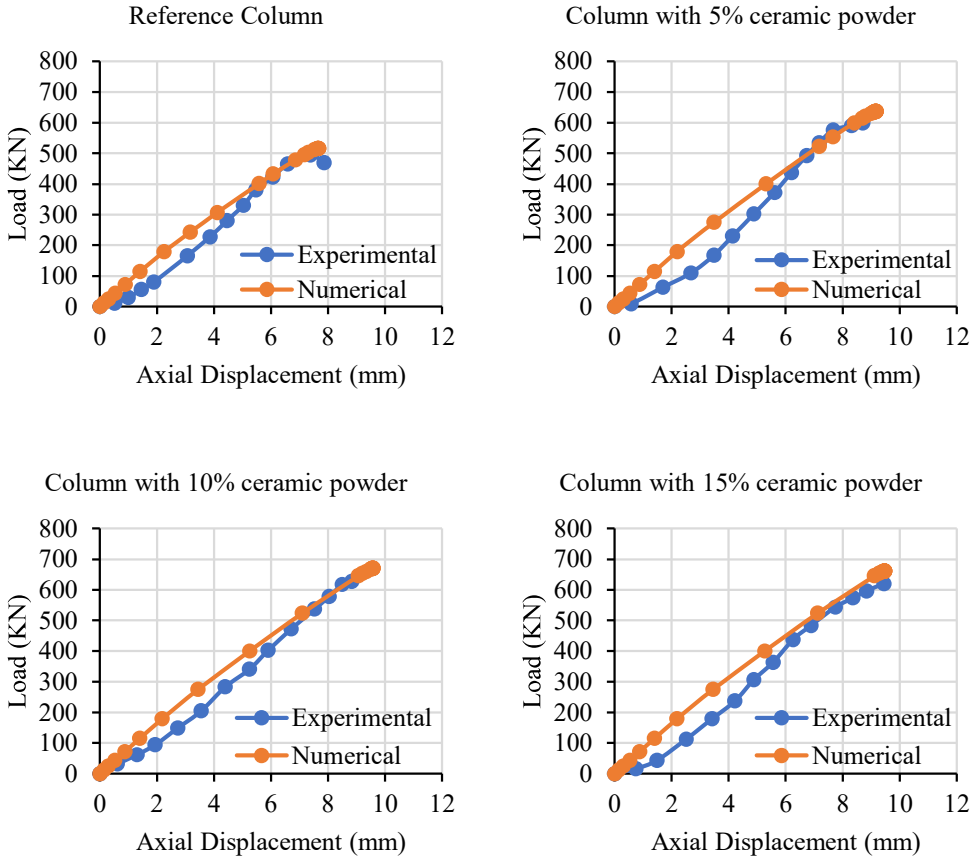

Figure 5-11. Experimental and numerical results for columns containing ceramic powder in different proportions and subjected to corrosion.

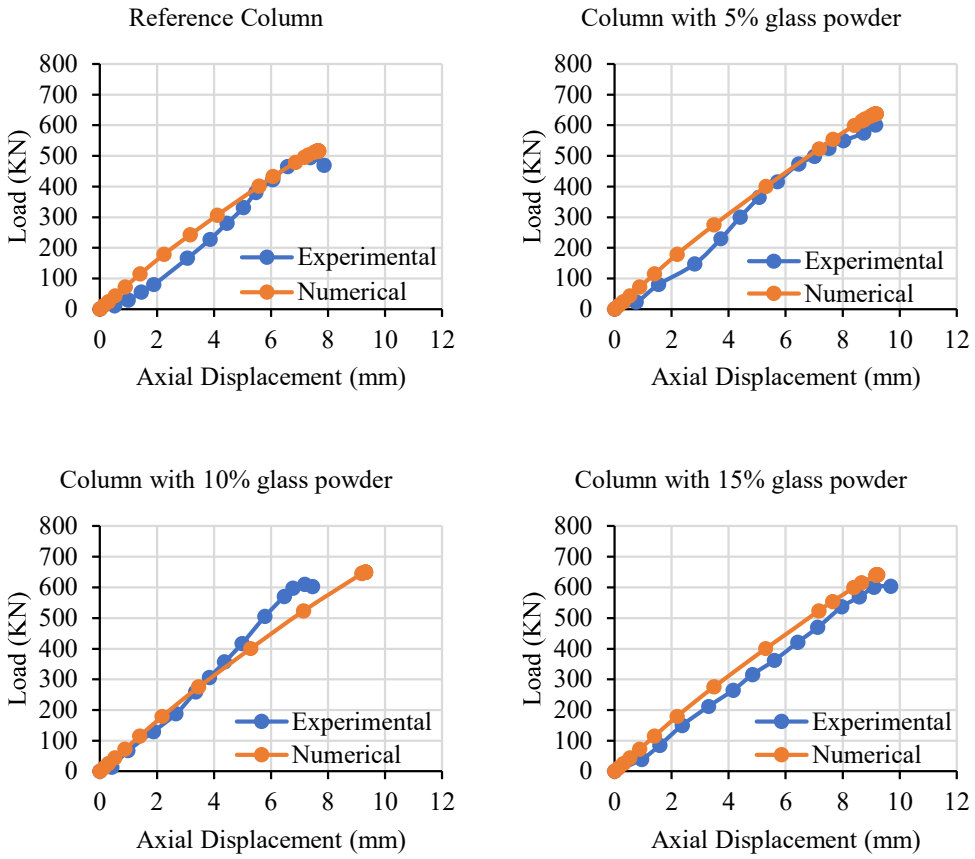

Figure 5-12. Experimental and numerical results for columns containing glass powder in different proportions and subjected to corrosion.

Table 5-3 shows the percentage difference between the ultimate load value of the model obtained from the Abacus and the ultimate load value obtained from the experimental test of corroded concrete columns. The results show that the difference is small, with the highest difference not exceeding 7.25%. Therefore, the values are considered acceptable for the study purposes.

Table 5-3. Percentage difference between the ultimate load obtained from ABAQUS and experimental results for columns subjected to corrosion.

Column	Percentage	Column	Percentage	Column	Percentage	Column	Percentage
CR	4.35%	**C0.5GR**	7.25%	**C10MA**	6.14%	**C15CE**	6.69%
C0.5CA	7.07%	**C1GR**	6.84%	**C15MA**	6.98%	**C5GL**	6.16%
C1CA	6.15%	**C1.5GR**	3.30%	**C5CE**	6.16%	**C10GL**	6.55%
C1.5CA	6.06%	**C5MA**	1.13%	**C10CE**	6.77%	**C15GL**	6.15%

5.4 A study on the impact of using ties instead of spiral bindings

The effect of using ties instead of spiral reinforcement was studied by modeling them in the Abaqus program, as illustrated in Figure 5-13.

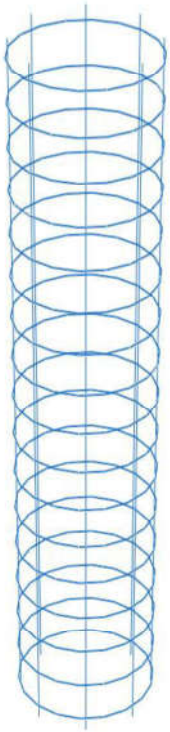

Figure 5-13. Reinforcement of the concrete column using ties in ABAQUS

A number of columns were studied using ties instead of spiral, with the same specific properties studied previously. After completing the analysis, the results concluded that using ties instead of spiral showed a significant decrease, as shown in Table 5-4.

Table 5-4. Results of the ultimate load for concrete columns with spiral reinforcement and ties, with the percentage decrease between the two values.

Column Symbol	Ultimate load of the spiral column	Ultimate load of the ties column	Percentage of Decrease
R	672	639	4.91 %
0.5CA	707	704	0.43 %
0.5GR	727	725	0.28 %
5MA	728	727	0.14 %
15CE	845	814	3.67 %
10GL	834	829	0.6 %

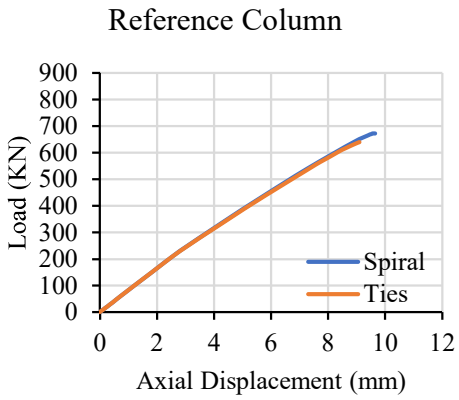

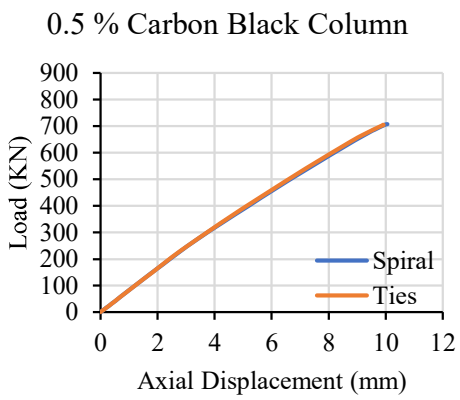

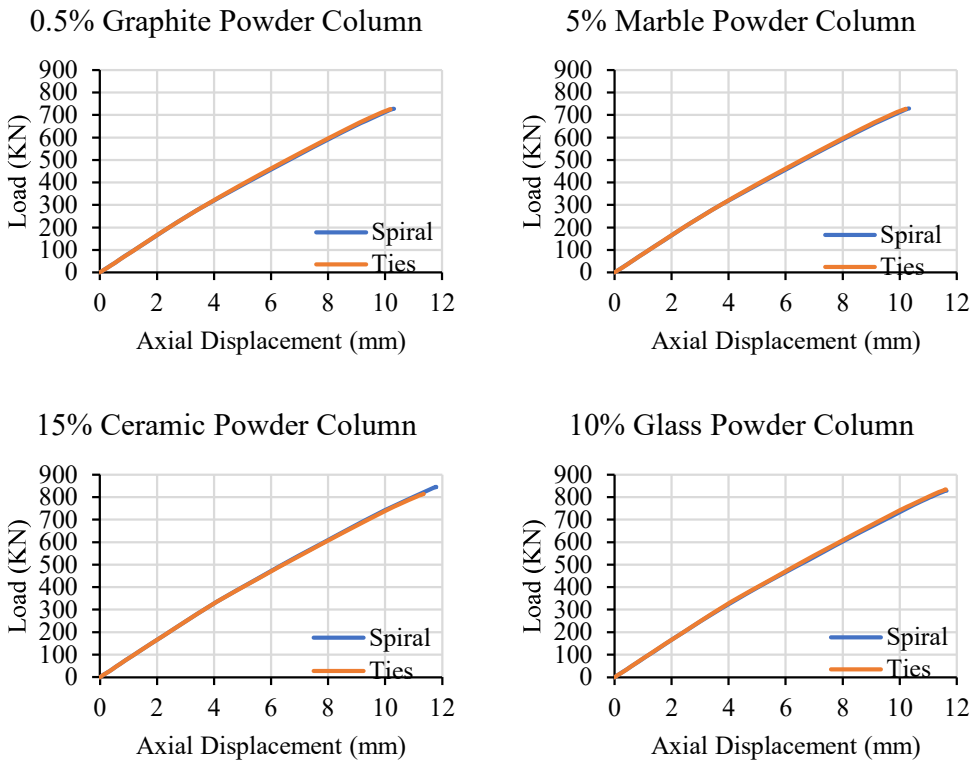

Figure 5-14. Load-deflection curve for concrete columns modeled using the Abacus program showing the difference between using ties instead of spiral.

The results shown in Table 5-4 show that all columns showed a decrease when using tie reinforcement instead of spiral reinforcement. "The reduction in the ultimate load observed in the column reinforced with ties instead of spiral reinforcement can be attributed to the difference in confinement efficiency provided by the two configurations. Spiral reinforcement offers continuous and uniform confinement to the concrete core, which enhances ductility, delays spalling, and improves load-carrying capacity. In contrast, ties provide discrete confinement, with potential stress concentrations at corners and reduced confinement effectiveness between ties. As a result, the concrete core in the tied column experiences earlier cracking and spalling under axial loading, leading to a lower ultimate load compared to the spirally confined counterpart.

Chapter Six: Conclusions and Recommendations

6.1 General

Based on the results of laboratory tests and structural analysis of concrete columns reinforced with micro-admixtures, a set of conclusions was reached that illustrates the impact of these materials on concrete performance in a corrosion marine environment. These evaluations included the materials' effectiveness in improving mechanical properties, reducing permeability, and limiting reinforcing steel corrosion. This chapter presents the most important conclusions, followed by practical recommendations aimed at improving the design and implementation of sustainable concrete in aggressive environments.

6.2 Conclusions

After careful analysis of the results and comparison of the performance of different concrete mixes in terms of mechanical and durability properties, the following important conclusions were reached:

1. Fine admixtures have proven effective in enhancing the properties of concrete exposed to harsh marine environments. They have demonstrated their ability to improve density and reduce internal porosity, positively impacting both structural performance and resistance to environmental factors.
2. The mixture containing 0.5% graphite powder exhibited outstanding structural performance, as the ultimate load of the corresponding column increased by 11.69% compared to the reference mix. Upon exposure to corrosion, the load dropped by only 3.6%, while the reference column experienced a reduction of 19.6%, indicating excellent retention of load-bearing capacity after degradation. This mix also showed the lowest pressure permeability, decreasing by 33%, and

the lowest chloride penetration, with a reduction of 76.27% compared to the reference, reflecting strong resistance to aggressive agents causing corrosion.

3. The mix with 0.5% carbon black powder demonstrated significant enhancement in structural performance, achieving an 8.93% increase in ultimate load relative to the reference mix. After corrosion exposure, the load decreased by only 3.73%, compared to 19.6% in the reference mix, confirming its durability against degradation. Additionally, the pressure permeability decreased by 24.62%, and chloride penetration was reduced by 45.76%, indicating improved protection against corrosive environments.
4. The mix containing 15% ceramic powder achieved the highest improvement in ultimate load, with a 19.16% increase over the reference mix. After corrosion, the load dropped by 18.64%, which is slightly better than the 19.6% reduction in the reference mix, indicating a reasonable retention of structural capacity. Furthermore, pressure permeability was reduced by 68.46%, and chloride penetration decreased by 34.58%, showing significant improvement in resistance to environmental deterioration.
5. The mix incorporating 10% marble powder showed an 11.36% increase in ultimate load compared to the reference column. Post-corrosion, the load decreased by 12.39%, which is noticeably lower than the 19.6% drop recorded in the reference. Moreover, pressure permeability dropped by 31.54%, and chloride penetration by 33.05%, suggesting a considerable enhancement in durability against aggressive agents.
6. The concrete mix containing 10% glass powder achieved a 17.69% increase in ultimate load relative to the reference mix. After exposure

to corrosion, the load was reduced by 16.69%, still performing better than the reference mix. The mix also recorded the greatest reduction in pressure permeability at 76.92%, and a 30.51% decrease in chloride penetration, reflecting effective resistance against environmental factors that promote steel corrosion.

7. The 10% of glass and 15% of ceramic blends demonstrated the highest combined performance, showing the highest ultimate load values, the lowest chloride ion penetration depths, and the lowest permeability levels under pressure, in addition to significantly lower half-cell potential values, demonstrating high corrosion resistance and excellent durability in marine environments.
8. The 1.5% of graphite and carbon black mixtures showed a significant decrease in structural performance due to the agglomeration of fine particles, which led to increased permeability and ion penetration, increasing the potential for reinforcing steel corrosion.
9. The marble powder demonstrated relatively stable behavior, with moderate improvements in compressive strength and chloride penetration. However, its effect was limited due to the weak of pozzolanic interaction, making it more of a filler than a chemical strength enhancer.
10. The results of the half-cell stress test were consistent with the permeability and chloride penetration tests, enhancing the reliability of this test as an indicator for assessing the potential for reinforcing steel corrosion in chloride-saturated environments.
11. Structural tests of columns after corrosion showed a relative decrease in load-bearing capacity, which varied depending on the type of admixture. Admixtures with low chloride penetration and lower

porosity were better able to retain their structural efficiency after corrosion.

12. After modelling the studied reinforced concrete columns in Abaqus, a comparative analysis was conducted to evaluate the effect of replacing spiral reinforcement with conventional tie reinforcement on the structural behavior of the columns. The simulation results showed that this replacement led to a reduction in the ultimate load capacity of the columns; however, the reduction was minor and did not exceed 5% in all cases. This slight decrease is attributed to the higher confinement efficiency provided by spiral reinforcement compared to closed ties, which enhances the axial load capacity and post-cracking behavior of the concrete, particularly under deteriorating conditions.

6.3 Recommendations

Based on the results obtained from the experimental and structural analysis of concrete mixes and considering the performance of admixtures and their effect on chloride resistance, corrosion resistance, and load-bearing capacity, the following recommendations are made to ensure the design of more sustainable and efficient concrete mixes in harsh marine environments:

1. It is recommended to use 10% of glass powder or 15% of ceramic as partial cement replacement sustained materials in coastal constructions due to their positive impact on chloride resistance and improved structural performance.
2. Care should be exercised when using carbon black or graphite at concentrations exceeding 1% unless uniform particle distribution is ensured to avoid deterioration in permeability and increased corrosion potential.

3. Marble powder can be used as a partial cement replacement sustained materials at 5–10% in applications that do not require high penetration or corrosion resistance due to its good filler effect while maintaining stable mechanical properties.
4. A durability-based design approach is recommended, taking into account the physical, electrical, and chemical properties of the concrete mix, along with mechanical properties, to ensure long-term performance in aggressive environments.
5. The study recommends expanding the scope of research to include the long-term interaction of additives with hydration products through microscopic analysis and absorption and permeability tests after repeated cycles of wetting and drying or exposure to sulfates.
6. Eco-economic studies should be conducted on the use of these secondary materials to determine the overall feasibility of their use as sustainable alternatives to cement, enhancing environmental sustainability and reducing the carbon footprint in the construction sector.

References

Ahmad, S. (2003). Reinforcement corrosion in concrete structures, its monitoring and service life prediction—a review. *Cement and Concrete Composites*, *25*(4–5), 459–471. https://doi.org/10.1016/S0958-9465(02)00086-0

Ahmad, S. (2009). Techniques for inducing accelerated corrosion of steel in concrete. *Arabian Journal for Science and Engineering*, *34*(2), 95.

Ahmad, Z. (2006a). INTRODUCTION TO CORROSION. In *Principles of Corrosion Engineering and Corrosion Control* (pp. 1–8). Elsevier. https://doi.org/10.1016/B978-075065924-6/50002-7

Ahmad, Z. (2006b). *Principles of corrosion engineering and corrosion control*. Elsevier.

Ahmed Sbia, L., Peyvandi, A., Soroushian, P., Balachandra, A. M., & Sobolev, K. (2015a). Evaluation of modified-graphite nanomaterials in concrete nanocomposite based on packing density principles. *Construction and Building Materials*, *76*, 413–422. https://doi.org/10.1016/j.conbuildmat.2014.12.019

Ahmed Sbia, L., Peyvandi, A., Soroushian, P., Balachandra, A. M., & Sobolev, K. (2015b). Evaluation of modified-graphite nanomaterials in concrete nanocomposite based on packing density principles. *Construction and Building Materials*, *76*, 413–422. https://doi.org/10.1016/j.conbuildmat.2014.12.019

Ahn, N. (2005). Effects of C3A and Mineral Admixtures on the Sulfate Attack Using ASTM C 1012. *Journal of ASTM International*, *2*(2), 1–20. https://doi.org/10.1520/JAI12472

Aïtcin, P.-C. (2007). *Binders for durable and sustainable concrete*. CRC

Press.

Akadiri, P. O., Olomolaiye, P. O., & Chinyio, E. A. (2013). Multi-criteria evaluation model for the selection of sustainable materials for building projects. *Automation in Construction*, *30*, 113–125. https://doi.org/10.1016/j.autcon.2012.10.004

Al-Bayati, A. J., Butrouna, K. H., Steffen, R. E., Salman, B., & Al-Qaralleh, M. (2020). Utilizing Graphite Powder to Improve Concrete Conductivity, Compressive Strength, and Workability. *Construction Research Congress 2020*, 881–888. https://doi.org/10.1061/9780784482889.093

Ali, M. F., Memon, N. A., Memon, B. A., Memon, M. A., & Memon, A. N. (2019). The effect of textile on compressive strength of concrete. *Quest Research Journal*, *17*(2).

Aliabdo, A. A., Abd Elmoaty, A. E. M., & Auda, E. M. (2014a). Re-use of waste marble dust in the production of cement and concrete. *Construction and Building Materials*, *50*, 28–41. https://doi.org/10.1016/j.conbuildmat.2013.09.005

Aliabdo, A. A., Abd Elmoaty, A. E. M., & Auda, E. M. (2014b). Re-use of waste marble dust in the production of cement and concrete. *Construction and Building Materials*, *50*, 28–41. https://doi.org/10.1016/j.conbuildmat.2013.09.005

Angst, U., Elsener, B., Larsen, C. K., & Vennesland, Ø. (2009). Critical chloride content in reinforced concrete — A review. *Cement and Concrete Research*, *39*(12), 1122–1138. https://doi.org/10.1016/j.cemconres.2009.08.006

Ann, K. Y., & Song, H.-W. (2007). Chloride threshold level for corrosion of steel in concrete. *Corrosion Science*, *49*(11), 4113–4133. https://doi.org/10.1016/j.corsci.2007.05.007

Aprianti, E., Shafigh, P., Bahri, S., & Farahani, J. N. (2015). Supplementary cementitious materials origin from agricultural wastes – A review. *Construction and Building Materials*, *74*, 176–187. https://doi.org/10.1016/j.conbuildmat.2014.10.010

Arbili, M. M., Qaidi, S. M. A., Ghaffoori, F. K., Alzeebaree, R., & Awlla, H. A. (2022). Utilization waste granulated blast furnace slag to improve the properties of polluted soil with crude oil. *4TH INTERNATIONAL CONFERENCE ON MATERIALS ENGINEERING & SCIENCE: Insight on the Current Research in Materials Engineering and Science*, 020116. https://doi.org/10.1063/5.0107724

Arya, C., Buenfeld, N. R., & Newman, J. B. (1987). Assessment of simple methods of determining the free chloride ion content of cement paste. *Cement and Concrete Research*, *17*(6), 907–918. https://doi.org/10.1016/0008-8846(87)90079-2

Ashish, D. K. (2018). Feasibility of waste marble powder in concrete as partial substitution of cement and sand amalgam for sustainable growth. *Journal of Building Engineering*, *15*, 236–242. https://doi.org/10.1016/j.jobe.2017.11.024

ASTM C1152/C1152M-20. (2020). *ASTM C1152/C1152M-20 Standard Test Method for Acid-Soluble Chloride in Mortar and Concrete*. https://doi.org/10.1520/C1152_C1152M-20

Awoyera, P. O., Akinmusuru, J. O., & Moncea, A. (2017). Hydration mechanism and strength properties of recycled aggregate concrete made using ceramic blended cement. *Cogent Engineering*, *4*(1), 1282667. https://doi.org/10.1080/23311916.2017.1282667

Awoyera, P. O., Dawson, A. R., Thom, N. H., & Akinmusuru, J. O. (2017). Suitability of mortars produced using laterite and ceramic wastes:

Mechanical and microscale analysis. *Construction and Building Materials*, *148*, 195–203. https://doi.org/10.1016/j.conbuildmat.2017.05.031

Awoyera, P. O., & Okoro, U. C. (2019). Filler-Ability of Highly Active Metakaolin for Improving Morphology and Strength Characteristics of Recycled Aggregate Concrete. *Silicon*, *11*(4), 1971–1978. https://doi.org/10.1007/s12633-018-0017-8

Ayub, M., Othman, M. H. D., Khan, I. U., Hubadillah, S. K., Kurniawan, T. A., Ismail, A. F., Rahman, M. A., & Jaafar, J. (2021). Promoting sustainable cleaner production paradigms in palm oil fuel ash as an eco-friendly cementitious material: A critical analysis. *Journal of Cleaner Production*, *295*, 126296. https://doi.org/10.1016/j.jclepro.2021.126296

Azmi, N. B., Khalid, F. S., Irwan, J. M., Anting, N., & Mazenan, P. N. (2017). A study on the performance of concrete containing recycled aggregates and ceramic as materials replacement. *IOP Conference Series: Materials Science and Engineering*, *271*, 012081. https://doi.org/10.1088/1757-899X/271/1/012081

Baboo, R., Khan, H. N., Kr, A., Rushad, S. T., & Duggal, S. K. (2011). Influence of Marble powder/granules in Concrete mix. *International Journal of Civil & Structural Engineering*, *1*(4), 827–834.

Balestra, C. E. T., Lima, M. G., Silva, A. R., & Medeiros-Junior, R. A. (2016). Corrosion Degree Effect on Nominal and Effective Strengths of Naturally Corroded Reinforcement. *Journal of Materials in Civil Engineering*, *28*(10). https://doi.org/10.1061/(ASCE)MT.1943-5533.0001599

Balestra, C. E. T., Nakano, A. Y., Savaris, G., & Medeiros-Junior, R. A. (2019). Reinforcement corrosion risk of marine concrete structures evaluated through electrical resistivity: Proposal of parameters based on

field structures. *Ocean Engineering*, *187*, 106167. https://doi.org/10.1016/j.oceaneng.2019.106167

Balestra, C. E. T., Reichert, T. A., & Savaris, G. (2019). Contribution for durability studies based on chloride profiles analysis of real marine structures in different marine aggressive zones. *Construction and Building Materials*, *206*, 140–150. https://doi.org/10.1016/j.conbuildmat.2019.02.067

Başaran, B., Aksoylu, C., Özkılıç, Y. O., Karalar, M., & Hakamy, A. (2023). Shear behaviour of reinforced concrete beams utilizing waste marble powder. *Structures*, *54*, 1090–1100. https://doi.org/10.1016/j.istruc.2023.05.093

Bastidas-Arteaga, E., Chateauneuf, A., Sánchez-Silva, M., Bressolette, P., & Schoefs, F. (2011). A comprehensive probabilistic model of chloride ingress in unsaturated concrete. *Engineering Structures*, *33*(3), 720–730. https://doi.org/10.1016/j.engstruct.2010.11.008

Beeby, A. W. (1978). Corrosion of reinforcing steel in concrete and its relation to cracking. *Structural Engineer*, *56*(3), 77–81. https://trid.trb.org/View/78946

Berke, N. S. (1990). *Corrosion rates of steel in concrete* (Issue 1065). ASTM International.

Berkeley, K. G. C., & Pathmanaban, S. (1990). *Cathodic protection of reinforcement steel in concrete*. Butterworths and Company Publishers. http://worldcat.org/isbn/0408032731

Berrocal, C. G., Lundgren, K., & Löfgren, I. (2016). Corrosion of steel bars embedded in fibre reinforced concrete under chloride attack: State of the art. *Cement and Concrete Research*, *80*, 69–85. https://doi.org/10.1016/j.cemconres.2015.10.006

Bertolini, L., Elsener, B., Pedeferri, P., Redaelli, E., & Polder, R. B. (2013). *Corrosion of steel in concrete: prevention, diagnosis, repair*. John Wiley & Sons.

Biczok, I., & Blasovszky, N. (1964). *Concrete corrosion and concrete protection*.

Bogue, R. H. (1955). *The chemistry of Portland cement* (Vol. 79, Issue 4). LWW.

Bostanci, S. C. (2020). Use of waste marble dust and recycled glass for sustainable concrete production. *Journal of Cleaner Production*, *251*, 119785. https://doi.org/10.1016/j.jclepro.2019.119785

Broomfield, J. P. (2023). *Corrosion of steel in concrete: understanding, investigation and repair*. Crc Press.

Butler, W. B., Janssen, D. J., Schell, H. C., Cabrera, J. G., Keck, R. H., Schmitt, J. W., Carrasquillo, R. L., Khan, M. S., Scholer, C. F., & Ellis Jr, W. E. (2001). Guide to Durable Concrete. *ACI: Montreal, QC, Canada*.

CAHYADI, J. H., & UOMOTO, T. (1993). Effect of Environmental Relative Humidity on Carbonation of Concrete. 生産研究, *45*(3), 218–221. https://repository.dl.itc.u-tokyo.ac.jp/records/18893

Callejas, I. J. A., Durante, L. C., & Oliveira, A. S. de. (2017). Thermal resistance and conductivity of recycled construction and demolition waste (RCDW) concrete blocks. *REM - International Engineering Journal*, *70*(2), 167–173. https://doi.org/10.1590/0370-44672015700048

Chen, H.-P. (2018). Residual Flexural Capacity and Performance Assessment of Corroded Reinforced Concrete Beams. *Journal of Structural Engineering*, *144*(12). https://doi.org/10.1061/(ASCE)ST.1943-541X.0002144

Chen, H.-P., & Alani, A. M. (2013). Optimized maintenance strategy for concrete structures affected by cracking due to reinforcement corrosion. *ACI Structural Journal*, *110*(2), 229.

Chikhalikar, S. M., & Tande, S. N. (2012). An experimental investigation on characteristics properties of fibre reinforced concrete containing waste glass powder as pozzolona. *37th Conference on Our World in Concrete and Structures*.

Chousidis, N., Ioannou, I., Rakanta, E., Koutsodontis, C., & Batis, G. (2016). Effect of fly ash chemical composition on the reinforcement corrosion, thermal diffusion and strength of blended cement concretes. *Construction and Building Materials*, *126*, 86–97. https://doi.org/10.1016/j.conbuildmat.2016.09.024

Chung, D. D. . (2001). Electromagnetic interference shielding effectiveness of carbon materials. *Carbon*, *39*(2), 279–285. https://doi.org/10.1016/S0008-6223(00)00184-6

Coccia, S., Imperatore, S., & Rinaldi, Z. (2016). Influence of corrosion on the bond strength of steel rebars in concrete. *Materials and Structures*, *49*(1–2), 537–551. https://doi.org/10.1617/s11527-014-0518-x

Cordon, W. A., & Gillespie, H. A. (1963). Variables in Concrete Aggregates and Portland Cement Paste which Influence the Strength of Concrete. *ACI Journal Proceedings*, *60*(8), 1029–1052. https://doi.org/10.14359/7889

Dakhil, F. H., Al-Gahrani, A. S., Al-Saadoun, S. S., & Bader, M. A. (1990). Influence of Cement Composition on the Corrosion of Reinforcement and Sulfate Resistance of Concrete. *ACI Materials Journal*, *87*(2), 114–122. https://doi.org/10.14359/1908

Dali, J. S., & Tande, S. N. (2012). Performance of concrete containing mineral admixtures subjected to high temperature. *37th Conference on Our World*

in Concrete and Structures, Singapore, August.

Demirel, B. (2010). The effect of the using waste marble dust as fine sand on the mechanical properties of the concrete. *International Journal of the Physical Sciences*, *5*(9), 1372–1380. https://academicjournals.org/article/article1380805861_Demirel.pdf

Diao, B., Sun, Y., Cheng, S., & Ye, Y. (2011). Effects of Mixed Corrosion, Freeze-Thaw Cycles, and Persistent Loads on Behavior of Reinforced Concrete Beams. *Journal of Cold Regions Engineering*, *25*(1), 37–52. https://doi.org/10.1061/(ASCE)CR.1943-5495.0000019

Ding, Y., Chen, Z., Han, Z., Zhang, Y., & Pacheco-Torgal, F. (2013). Nano-carbon black and carbon fiber as conductive materials for the diagnosing of the damage of concrete beam. *Construction and Building Materials*, *43*, 233–241. https://doi.org/10.1016/j.conbuildmat.2013.02.010

Donatello, S., Tyrer, M., & Cheeseman, C. R. (2010). Comparison of test methods to assess pozzolanic activity. *Cement and Concrete Composites*, *32*(2), 121–127. https://doi.org/10.1016/j.cemconcomp.2009.10.008

Du, H., Gao, H. J., & Pang, S. D. (2016). Improvement in concrete resistance against water and chloride ingress by adding graphene nanoplatelet. *Cement and Concrete Research*, *83*, 114–123. https://doi.org/10.1016/j.cemconres.2016.02.005

Ebell, G., Burkert, A., Fischer, J., Lehmann, J., Müller, T., Meinel, D., & Paetsch, O. (2016). Investigation of chloride-induced pitting corrosion of steel in concrete with innovative methods. *Materials and Corrosion*, *67*(6), 583–590. https://doi.org/10.1002/maco.201608969

Elaqra, H. A., Haloub, M. A. A., & Rustom, R. N. (2019). Effect of new mixing method of glass powder as cement replacement on mechanical behavior of concrete. *Construction and Building Materials*, *203*, 75–82.

https://doi.org/10.1016/j.conbuildmat.2019.01.077

Ergün, A. (2011). Effects of the usage of diatomite and waste marble powder as partial replacement of cement on the mechanical properties of concrete. *Construction and Building Materials*, *25*(2), 806–812. https://doi.org/10.1016/j.conbuildmat.2010.07.002

Ericsson, M. (2019). XXIX World Marble and Stones Report 2018 by Carlo Montani. *Mineral Economics*, *32*(2), 255–256. https://doi.org/10.1007/s13563-019-00183-6

Fakhri, H., Fishman, K. L., & Ranade, R. (2020). A novel experimental method to determine the critical chloride content in cement-based composites. *Construction and Building Materials*, *263*, 120101. https://doi.org/10.1016/j.conbuildmat.2020.120101

Fayaz, D., Malik, A., Zakir, M., & Malik, T. A. (2018). Effects on the Properties of Concrete by Partial Replacement of Cement with Carbon Black and Natural Fine Aggregate with Robo Sand. *International Journal of Technical Innovation in Modern Engineering and Science*, *4*(6), 1–8.

Federico, L. M., & Chidiac, S. E. (2009). Waste glass as a supplementary cementitious material in concrete – Critical review of treatment methods. *Cement and Concrete Composites*, *31*(8), 606–610. https://doi.org/10.1016/j.cemconcomp.2009.02.001

Feng, W., Tarakbay, A., Ali Memon, S., Tang, W., & Cui, H. (2021). Methods of accelerating chloride-induced corrosion in steel-reinforced concrete: A comparative review. *Construction and Building Materials*, *289*, 123165. https://doi.org/10.1016/j.conbuildmat.2021.123165

Geng, C., Xu, Y., & Weng, D. (2008). A new method to quickly assess the inhibitor efficiency. *Journal of Wuhan University of Technology-Mater. Sci. Ed.*, *23*(6), 950–954. https://doi.org/10.1007/s11595-007-6950-9

Ghahari, S. A., Mohammadi, A., & Ramezanianpour, A. A. (2017). Performance assessment of natural pozzolan roller compacted concrete pavements. *Case Studies in Construction Materials*, *7*, 82–90. https://doi.org/10.1016/j.cscm.2017.03.004

Goncalves, J. R. A., Boluk, Y., & Bindiganavile, V. (2018). Crack growth resistance in fibre reinforced alkali-activated fly ash concrete exposed to extreme temperatures. *Materials and Structures*, *51*(2), 42. https://doi.org/10.1617/s11527-018-1163-6

Gonzalez-Corominas, A., & Etxeberria, M. (2014). Properties of high performance concrete made with recycled fine ceramic and coarse mixed aggregates. *Construction and Building Materials*, *68*, 618–626. https://doi.org/10.1016/j.conbuildmat.2014.07.016

Gopalakrishnan, R., & Govindarajan, D. (2011). Compressive Strength and Electron Paramagnetic Resonance Studies on Waste Glass Admixtured Cement. *New Journal of Glass and Ceramics*, *01*(03), 119–124. https://doi.org/10.4236/njgc.2011.13017

Goyal, A., Pouya, H. S., Ganjian, E., & Claisse, P. (2018). A Review of Corrosion and Protection of Steel in Concrete. *Arabian Journal for Science and Engineering*, *43*(10), 5035–5055. https://doi.org/10.1007/s13369-018-3303-2

Guo, Z., Kong, X., Zhang, J., Sun, Y., Tu, A., & Jiang, T. (2020). Life-cycle assessment of concrete building blocks incorporating recycled concrete aggregates—A case study in China. In *Advances in Construction and Demolition Waste Recycling* (pp. 515–535). Elsevier. https://doi.org/10.1016/B978-0-12-819055-5.00025-5

Gupta, A. K. (1988). Corrosion of Reinforced Concrete Structures and their Rehabilitation. *Indian Concrete Bulletin*, *23*, 19–32.

Hamada, H., Tayeh, B., Yahaya, F., Muthusamy, K., & Al-Attar, A. (2020). Effects of nano-palm oil fuel ash and nano-eggshell powder on concrete. *Construction and Building Materials*, *261*, 119790. https://doi.org/10.1016/j.conbuildmat.2020.119790

Hansson, C. M. (1984). Comments on electrochemical measurements of the rate of corrosion of steel in concrete. *Cement and Concrete Research*, *14*(4), 574–584. https://doi.org/10.1016/0008-8846(84)90135-2

He, Y., Lu, L., Jin, S., & Hu, S. (2014). Conductive aggregate prepared using graphite and clay and its use in conductive mortar. *Construction and Building Materials*, *53*, 131–137. https://doi.org/10.1016/j.conbuildmat.2013.11.085

Heidari, A., & Tavakoli, D. (2013). A study of the mechanical properties of ground ceramic powder concrete incorporating nano-SiO2 particles. *Construction and Building Materials*, *38*, 255–264. https://doi.org/10.1016/j.conbuildmat.2012.07.110

Higashiyama, H., Yagishita, F., Sano, M., & Takahashi, O. (2012). Compressive strength and resistance to chloride penetration of mortars using ceramic waste as fine aggregate. *Construction and Building Materials*, *26*(1), 96–101. https://doi.org/10.1016/j.conbuildmat.2011.05.008

Ho, D. W. S., & Lewis, R. K. (1987). Carbonation of concrete and its prediction. *Cement and Concrete Research*, *17*(3), 489–504. https://doi.org/10.1016/0008-8846(87)90012-3

Hooton, R., & Khaloo, A. (1995). Crushed Tile Coarse Aggregate Concrete. *Cement, Concrete and Aggregates*, *17*(2), 119. https://doi.org/10.1520/CCA10137J

Ikotun, J., Adedeji, P., Babafemi, A., & Otieno, M. (2025). Use of Ceramic

Waste Powder as a Partial Cement Replacement in Concrete—A Review of Microstructure and Durability Properties. In H. Beushausen, J. Ndawula, M. Alexander, F. Dehn, & P. Moyo (Eds.), *Proceedings of the 7th International Conference on Concrete Repair, Rehabilitation and Retrofitting. ICCRRR 2024. RILEM Bookseries, vol 59. Springer* (Vol. 59, pp. 505–519). Springer Nature Switzerland. https://doi.org/10.1007/978-3-031-75507-1_49

Ip, B. B. H., & C., A. K. (1987). Chloride Corrosion Threshold in Concrete. *ACI Materials Journal*, *84*(4). https://doi.org/10.14359/1617

Islam, M., & Arifuzzaman, A. K. (2012). Deterioration of concrete in ambient marine environment (RESEARCH NOTE). *International Journal of Engineering*, *25*(4), 289–302.

Islam, M. M., Islam, M. S., Mondal, B. C., & Das, A. (2009). Strength behavior of mortar using slag with cement in sea water environment. *J Civ Eng-IEB*, *37*(2), 111–122.

Islam, M. S., Islam, M. M., & Mondal, B. C. (2010). Effect of freeze-thaw action on physical and mechanical behavior of marine concrete. *J Inst Eng Malaysia*, *71*(1), 53–64.

Islam, M. S., Kaushik, S. K., & Islam, M. M. (2005). Physical and mechanical behavior of concrete in seawater under high hydrostatic pressure. *J. Inst. Eng. Malaysia*, *66*, 46–52.

Jaegermann, C. (1990). Effect of water-cement ratio and curing on chloride penetration into concrete exposed to Mediterranean sea climate. *Materials Journal*, *87*(4), 333–339.

Jatoi, M. A., Solangi, G. S., Shaikh, F. A., & Rajput, S. (2019). Effect of Lakhra fly ash as partial replacement of cement in traditional concrete. *Mehran University Research Journal of Engineering & Technology*,

38(4), 1045–1056. https://doi.org/10.3316/INFORMIT.729989619333426

Jokhio, G. A., Hamada, H. M., Humada, A. M., Gul, Y., & Abu-Tair, A. (2020). Environmental benefits of incorporating palm oil fuel ash in cement concrete and cement mortar. *E3S Web of Conferences*, *158*, 03005. https://doi.org/10.1051/e3sconf/202015803005

Jones, A. E. K. (1997). *Development of an holistic approach to ensure the durability of new concrete construction*. British Cement Association.

Kannan, D. M., Aboubakr, S. H., EL-Dieb, A. S., & Reda Taha, M. M. (2017). High performance concrete incorporating ceramic waste powder as large partial replacement of Portland cement. *Construction and Building Materials*, *144*, 35–41. https://doi.org/10.1016/j.conbuildmat.2017.03.115

Khan, I., François, R., & Castel, A. (2014). Prediction of reinforcement corrosion using corrosion induced cracks width in corroded reinforced concrete beams. *Cement and Concrete Research*, *56*, 84–96. https://doi.org/10.1016/j.cemconres.2013.11.006

Kim, K.-S., Park, K.-T., & Park, C. (2022). Structural behavior of expanded rib steel bars used in reinforced concrete beams. *Results in Engineering*, *14*, 100455. https://doi.org/10.1016/j.rineng.2022.100455

Kobayashi, K., & Shuttoh, K. (1991). Oxygen diffusivity of various cementitious materials. *Cement and Concrete Research*, *21*(2–3), 273–284. https://doi.org/10.1016/0008-8846(91)90009-7

Konsta-Gdoutos, M. S., Metaxa, Z. S., & Shah, S. P. (2010). Multi-scale mechanical and fracture characteristics and early-age strain capacity of high performance carbon nanotube/cement nanocomposites. *Cement and Concrete Composites*, *32*(2), 110–115.

https://doi.org/10.1016/j.cemconcomp.2009.10.007

Kumarappan, N. (2013). Partial replacement cement in concrete using waste glass. *International Journal of Engineering Research and Technology*, *2*(10), 1880–1883.

Kurdowski, W. (2002). Chloride corrosion in cementitious system. *W Structure and Performance of Cements, 2nd Ed., Spon Press, London & NY*, 295–309.

Levy, S. M., & Helene, P. (2004). Durability of recycled aggregates concrete: a safe way to sustainable development. *Cement and Concrete Research*, *34*(11), 1975–1980. https://doi.org/10.1016/j.cemconres.2004.02.009

Li, C., & Li, K. (2010). Chloride ion transport in cover concrete under drying-wetting cycles: theory, experiment and modeling. *Kuei Suan Jen Hsueh Pao*, *38*(4), 581–589.

Li, F., & Yuan, Y. (2013). Effects of corrosion on bond behavior between steel strand and concrete. *Construction and Building Materials*, *38*, 413–422. https://doi.org/10.1016/j.conbuildmat.2012.08.008

Li, X., Korayem, A. H., Li, C., Liu, Y., He, H., Sanjayan, J. G., & Duan, W. H. (2016). Incorporation of graphene oxide and silica fume into cement paste: A study of dispersion and compressive strength. *Construction and Building Materials*, *123*, 327–335. https://doi.org/10.1016/j.conbuildmat.2016.07.022

Lindahl, A. M. L. (2009). *Sources of pesticide losses to surface waters and groundwater at field and landscape scales*. Department of Soil and Environment, Swedish University of Agricultural Sciences.

Litvan, G. G., & Bickley, J. A. (1987). *Durability of parking structures: analysis of field survey*. Citeseer.

Liu, H., Xue, J., Li, B., Wang, J., Lv, X., & Zhang, J. (2022). Effect of graphite

tailings as substitute sand on mechanical properties of concrete. *European Journal of Environmental and Civil Engineering*, *26*(7), 2635–2653. https://doi.org/10.1080/19648189.2020.1763476

Lu, J.-X., & Poon, C. S. (2019). Recycling of waste glass in construction materials. In *New Trends in Eco-efficient and Recycled Concrete* (pp. 153–167) Elsevier https://doi.org/10.1016/B978-0-08-102480-5.00006-3

Luo, W., Sandanayake, M., & Zhang, G. (2019). Direct and indirect carbon emissions in foundation construction – Two case studies of driven precast and cast-in-situ piles. *Journal of Cleaner Production*, *211*, 1517–1526. https://doi.org/10.1016/j.jclepro.2018.11.244

Madandoust, R., & Ghavidel, R. (2013). Mechanical properties of concrete containing waste glass powder and rice husk ash. *Biosystems Engineering*, *116*(2), 113–119. https://doi.org/10.1016/j.biosystemseng.2013.07.006

Malumbela, G., Moyo, P., & Alexander, M. (2012). A step towards standardising accelerated corrosion tests on laboratory reinforced concrete specimens. *Journal of the South African Institution of Civil Engineering= Joernaal van Die Suid-Afrikaanse Instituut van Siviele Ingenieurswese*, *54*(2), 78–85.

Mangi, S. A., Ibrahim, M. H. W., Jamaluddin, N., Arshad, M. F., Memon, F. A., Jaya, R. P., & Shahidan, S. (2018). A review on potential use of coal bottom ash as a supplementary cementing material in sustainable concrete construction. *International Journal of Integrated Engineering*, *10*(9).

Mangi, S. A., Ibrahim, M. H. W., Jamaluddin, N., Arshad, M. F., & Ramadhansyah, P. J. (2019). Effects of ground coal bottom ash on the properties of concrete. *Journal of Engineering Science and Technology*, *14*(1), 338–350.

Medeiros-Junior, R. A., & Lima, M. G. (2016). Electrical resistivity of unsaturated concrete using different types of cement. *Construction and Building Materials*, *107*, 11–16. https://doi.org/10.1016/j.conbuildmat.2015.12.168

Mehta, P. K. (1980). Durability of concrete in marine environment--A review. *Special Publication*, *65*, 1–20. https://doi.org/https://doi.org/10.14359/6343

Mehta, P. K., & Monteiro, P. J. (2006). Concrete: microstructure, properties, and materials. *McGraw-Hill New York*, *3*.

Mehta, P. K., & Monteiro, P. J. M. (2005). Concrete: Microstructure, Properties, and Materials 4th Edition. In *McGraw-Hill Education* (Third Edit). McGraw-Hill Education; 4 edition. http://booksdescr.org/item/index.php?md5=C2193133AAF5C6ACB8D2F2576D9064BA

Melchers, R. E. (2020). Long-Term Durability of Marine Reinforced Concrete Structures. *Journal of Marine Science and Engineering*, *8*(4), 290. https://doi.org/10.3390/jmse8040290

Melchers, R. E., & Chaves, I. A. (2017). A comparative study of chlorides and longer-term reinforcement corrosion. *Materials and Corrosion*, *68*(6), 613–621. https://doi.org/10.1002/maco.201609310

Meyer, C. (2009). The greening of the concrete industry. *Cement and Concrete Composites*, *31*(8), 601–605. https://doi.org/10.1016/j.cemconcomp.2008.12.010

Mh, W. I., Hamzah, A. F., Jamaluddin, N., Mangi, S. A., & Ramadhansyah, P. J. (2020). Influence of bottom ash as a sand replacement material on durability of self-compacting concrete exposed to seawater. *Journal of Engineering Science and Technology*, *15*(1), 555–571.

Michel, A., Otieno, M., Stang, H., & Geiker, M. R. (2016). Propagation of steel corrosion in concrete: Experimental and numerical investigations. *Cement and Concrete Composites*, *70*, 171–182. https://doi.org/10.1016/j.cemconcomp.2016.04.007

Mingqing, S., Xinying, M., Xiaoying, W., Zuofu, H., & Zhuoqiu, L. (2008). Experimental studies on the indoor electrical floor heating system with carbon black mortar slabs. *Energy and Buildings*, *40*(6), 1094–1100. https://doi.org/10.1016/j.enbuild.2007.10.009

Monteiro, A. O., Loredo, A., Costa, P. M. F. J., Oeser, M., & Cachim, P. B. (2017). A pressure-sensitive carbon black cement composite for traffic monitoring. *Construction and Building Materials*, *154*, 1079–1086. https://doi.org/10.1016/j.conbuildmat.2017.08.053

Moosberg-Bustnes, H., Lagerblad, B., & Forssberg, E. (2004). The function of fillers in concrete. *Materials and Structures*, *37*(2), 74–81. https://doi.org/10.1007/BF02486602

Morcillo, M., Chico, B., Mariaca, L., & Otero, E. (2000). Salinity in marine atmospheric corrosion: its dependence on the wind regime existing in the site. *Corrosion Science*, *42*(1), 91–104. https://doi.org/10.1016/S0010-938X(99)00048-7

Moser, R., Holland, B., Kahn, L., Singh, P., & Kurtis, K. (2011). Durability of Precast Prestressed Concrete Piles in Marine Environment : Reinforcement Corrosion and Mitigation – Part 1. *GDOT Research Project No. 07-30*, *07*, 92.

Mozer, J. D., Bianchini, A. C., & Kesler, C. E. (1965). Corrosion of Reinforcing Bars in Concrete. *ACI Journal Proceedings*, *62*(8), 909–932. https://doi.org/10.14359/7729

Nagarajan, V. K., Devi, S. A., Manohari, S. P., & Santha, M. M. (2014).

Experimental study on partial replacement of cement with coconut shell ash in concrete. *International Journal of Science and Research*, *3*(3), 651–661.

Neville, A. (1995). Chloride attack of reinforced concrete: an overview. *Materials and Structures*, *28*(2), 63–70. https://doi.org/10.1007/BF02473172

Neville, A. M. (1995). *Properties of concrete*. Longman.

Nguyen, P. T., Bastidas-Arteaga, E., Amiri, O., & El Soueidy, C.-P. (2017). An Efficient Chloride Ingress Model for Long-Term Lifetime Assessment of Reinforced Concrete Structures Under Realistic Climate and Exposure Conditions. *International Journal of Concrete Structures and Materials*, *11*(2), 199–213. https://doi.org/10.1007/s40069-017-0185-8

O'Neill Iqbal, P., & Ishida, T. (2009). Modeling of chloride transport coupled with enhanced moisture conductivity in concrete exposed to marine environment. *Cement and Concrete Research*, *39*(4), 329–339. https://doi.org/10.1016/j.cemconres.2009.01.001

Patil, D. M., & Sangle, K. K. (2013). Experimental investigation of waste glass powder as partial replacement of cement in concrete. *Int. J. Adv. Technol. Civ. Eng*, *2*(1), 112–117.

Peyvandi, A., Sbia, L. A., Soroushian, P., & Sobolev, K. (2013). Effect of the cementitious paste density on the performance efficiency of carbon nanofiber in concrete nanocomposite. *Construction and Building Materials*, *48*, 265–269. https://doi.org/10.1016/j.conbuildmat.2013.06.094

Popov, B. N. (2015). *Corrosion engineering: principles and solved problems*. Elsevier.

Pourakbar, S., & Huat, B. K. (2016). A review of alternatives traditional cementitious binders for engineering improvement of soils. *International Journal of Geotechnical Engineering*, 1–11. https://doi.org/10.1080/19386362.2016.1207042

Puertas, F., García-Díaz, I., Barba, A., Gazulla, M. F., Palacios, M., Gómez, M. P., & Martínez-Ramírez, S. (2008). Ceramic wastes as alternative raw materials for Portland cement clinker production. *Cement and Concrete Composites*, *30*(9), 798–805. https://doi.org/10.1016/j.cemconcomp.2008.06.003

Rasheeduzzafar, A. S. Al-Gahtani, and S. S. A.-S. (1989). Influence of Construction Practices on Concrete Durability. *ACI Materials Journal*, *86*(6), 566–575. https://doi.org/10.14359/2219

Rasheeduzzafar. (1992). Influence of cement composition on concrete durability. *ACI Materials Journal*, *89*(6), 574–586.

Raval, A. D., Patel, D. I. N., & Pitroda, J. (2013). Ceramic waste: Effective replacement of cement for establishing sustainable concrete. *International Journal of Engineering Trends and Technology (IJETT)*, *4*(6), 2324–2329.

Razaqpur, A. G., & Isgor, O. B. (2009). Prediction of reinforcement corrosion in concrete structures. *Front. Technol. Infrastructures Eng. Struct. Infrastructures*, *4*, 45–69.

Revie, R. W. (2008). *Corrosion and corrosion control: an introduction to corrosion science and engineering*. John Wiley & Sons.

Rodrigues, S., Marques, M., Suárez-Ruiz, I., Camean, I., Flores, D., & Kwiecinska, B. (2013). Microstructural investigations of natural and synthetic graphites and semi-graphites. *International Journal of Coal Geology*, *111*, 67–79. https://doi.org/10.1016/j.coal.2012.06.013

Safehian, M., & Ramezanianpour, A. A. (2013). Assessment of service life models for determination of chloride penetration into silica fume concrete in the severe marine environmental condition. *Construction and Building Materials*, *48*, 287–294. https://doi.org/10.1016/j.conbuildmat.2013.07.006

Şahan Arel, H. (2016). Recyclability of waste marble in concrete production. *Journal of Cleaner Production*, *131*, 179–188. https://doi.org/10.1016/j.jclepro.2016.05.052

Sánchez de Rojas Gómez, M. I., & Frías Rojas, M. (2013). Natural pozzolans in eco-efficient concrete. In *Eco-Efficient Concrete* (pp. 83–104). Elsevier. https://doi.org/10.1533/9780857098993.2.83

Sandanayake, M., Bouras, Y., Haigh, R., & Vrcelj, Z. (2020). Current Sustainable Trends of Using Waste Materials in Concrete—A Decade Review. *Sustainability*, *12*(22), 9622. https://doi.org/10.3390/su12229622

Sandanayake, M., Gunasekara, C., Law, D., Zhang, G., Setunge, S., & Wanijuru, D. (2020). Sustainable criterion selection framework for green building materials – An optimisation based study of fly-ash Geopolymer concrete. *Sustainable Materials and Technologies*, *25*, e00178. https://doi.org/10.1016/j.susmat.2020.e00178

Sandanayake, M., Zhang, G., & Setunge, S. (2019). Estimation of environmental emissions and impacts of building construction – A decision making tool for contractors. *Journal of Building Engineering*, *21*, 173–185. https://doi.org/10.1016/j.jobe.2018.10.023

Sargam, Y., Wang, K., & Alleman, J. E. (2020). Effects of Modern Concrete Materials on Thermal Conductivity. *Journal of Materials in Civil Engineering*, *32*(4). https://doi.org/10.1061/(ASCE)MT.1943-

5533.0003026

Schiessl, P. (1975). Admissible Crack Widths in Reinforced Concrete Structures. In *Behaviour in Service of Concrete Structures*. Liege.

Shaikh, F. U. A. (2018). Effect of Cracking on Corrosion of Steel in Concrete. *International Journal of Concrete Structures and Materials*, *12*(1), 3. https://doi.org/10.1186/s40069-018-0234-y

Shi, C., Wu, Y., Riefler, C., & Wang, H. (2005). Characteristics and pozzolanic reactivity of glass powders. *Cement and Concrete Research*, *35*(5), 987–993. https://doi.org/10.1016/j.cemconres.2004.05.015

Standard, A. A. (2011). Building code requirements for structural concrete (ACI 318-11). *American Concrete Institute*.

Stanish, K. D., Hooton, R. D., & Thomas, M. D. A. (2000). *Testing the chloride penetration resistance of concrete: a literature review*. Department of Civil Engineering, University of Toronto.

Tapan, M., & Aboutaha, R. S. (2011). Effect of steel corrosion and loss of concrete cover on strength of deteriorated RC columns. *Construction and Building Materials*, *25*(5), 2596–2603. https://doi.org/10.1016/j.conbuildmat.2010.12.003

Tayeh, B. A., Hasaniyah, M. W., Zeyad, A. M., & Yusuf, M. O. (2019). Properties of concrete containing recycled seashells as cement partial replacement: A review. *Journal of Cleaner Production*, *237*, 117723. https://doi.org/10.1016/j.jclepro.2019.117723

Thangavel, K., Balasubramanian, T. M., & Rengaswamy, N. S. (2000). Fixing of chloride in concrete using admixtures. *Indian Concrete Journal*, *74*(04), 203–207.

Topçu, İ. B., & Canbaz, M. (2007). Effect of different fibers on the mechanical properties of concrete containing fly ash. *Construction and Building*

Materials, *21*(7), 1486–1491. https://doi.org/10.1016/j.conbuildmat.2006.06.026

Toubal Seghir, N., Mellas, M., Sadowski, Ł., Krolicka, A., Żak, A., & Ostrowski, K. (2019). The Utilization of Waste Marble Dust as a Cement Replacement in Air-Cured Mortar. *Sustainability*, *11*(8), 2215. https://doi.org/10.3390/su11082215

Tugrul Tunc, E. (2019). Recycling of marble waste: A review based on strength of concrete containing marble waste. *Journal of Environmental Management*, *231*, 86–97. https://doi.org/10.1016/j.jenvman.2018.10.034

Tumidajski, P. J., Chan, G. W., & Philipose, K. E. (1995). An effective diffusivity for sulfate transport into concrete. *Cement and Concrete Research*, *25*(6), 1159–1163. https://doi.org/10.1016/0008-8846(95)00108-O

Tuutti, K. (1982). *Corrosion of steel in concrete*.

Ueda, T., & Takewaka, K. (2007). Performance-based Standard Specifications for Maintenance and Repair of Concrete Structures in Japan. *Structural Engineering International*, *17*(4), 359–366. https://doi.org/10.2749/101686607782359119

Uhlig, H. H., & Revie, R. W. (1985). *Corrosion and corrosion control*.

Val, D. V., & Stewart, M. G. (2003). Life-cycle cost analysis of reinforced concrete structures in marine environments. *Structural Safety*, *25*(4), 343–362. https://doi.org/10.1016/S0167-4730(03)00014-6

Vandhiyan, R., Ramkumar, K., & Ramya, R. (2013). Experimental study on replacement of cement by glass powder. *Int. J. Eng. Res. Technol*, *2*(5), 234–238.

Vasudevan, G., & Pillay, S. G. K. (2013). Performance of using waste glass

powder in concrete as replacement of cement. *Am. J. Eng. Res*, *2*(12), 175–181.

Vijayakumar, G. (2013). Studies on mechanical properties of concrete containing waste glass powder as a partial replacement of cement in concrete. *Cement and Concrete Research*, *3*(2), 153–157.

Virtanen, S. (2009). ELECTROCHEMICAL THEORY | Corrosion. In *Encyclopedia of Electrochemical Power Sources* (pp. 56–63). Elsevier. https://doi.org/10.1016/B978-044452745-5.00026-5

Wang, S. N., Li, K. F., Fan, Z. H., Su, Q. K., & Xiong, J. B. (2015). Durability strategy for main concrete structure of Hong Kong-Zhuhai-Macao bridge with designed service life of 120 years. *Port Waterw. Eng.*, *3*(78–84), 92.

Wee, T. H., Suryavanshi, A. K., Wong, S. F., & Rahman, A. K. M. A. (2000). Sulfate Resistance of Concrete Containing Mineral Admixtures. *ACI Materials Journal*, *97*(5), 536–549. https://doi.org/10.14359/9286

Wen, S., & Chung, D. D. L. (2007). Partial replacement of carbon fiber by carbon black in multifunctional cement–matrix composites. *Carbon*, *45*(3), 505–513. https://doi.org/10.1016/j.carbon.2006.10.024

Whitmore, D. (2018). Corrosion Protection of Reinforced Concrete Columns and Piles in a Marine Environment. In *CORROSION 2018* (p. NACE-2018-10558).

Xu, R., & Zhao, S. (1994). Identification of an k B-like motif at the 5′ upstream region of human lymphotoxin gene. *Cell Research*, *4*(1), 1–7.

Yang, L. F., Cai, R., & Yu, B. (2017). Investigation of computational model for surface chloride concentration of concrete in marine atmosphere zone. *Ocean Engineering*, *138*, 105–111. https://doi.org/10.1016/j.oceaneng.2017.04.024

Yıldırım, G., Öztürk, O., Al-Dahawi, A., Afşın Ulu, A., & Şahmaran, M.

(2020). Self-sensing capability of Engineered Cementitious Composites: Effects of aging and loading conditions. *Construction and Building Materials*, *231*, 117132. https://doi.org/10.1016/j.conbuildmat.2019.117132

Yu, H., Da, B., Ma, H., Zhu, H., Yu, Q., Ye, H., & Jing, X. (2017). Durability of concrete structures in tropical atoll environment. *Ocean Engineering*, *135*, 1–10. https://doi.org/10.1016/j.oceaneng.2017.02.020

Yu, L., François, R., Dang, V. H., L'Hostis, V., & Gagné, R. (2015). Structural performance of RC beams damaged by natural corrosion under sustained loading in a chloride environment. *Engineering Structures*, *96*, 30–40. https://doi.org/10.1016/j.engstruct.2015.04.001

Yuan, H.-W., Lu, C.-H., Xu, Z.-Z., Ni, Y.-R., & Lan, X.-H. (2012). Mechanical and thermal properties of cement composite graphite for solar thermal storage materials. *Solar Energy*, *86*(11), 3227–3233. https://doi.org/10.1016/j.solener.2012.08.011

Zeyad, A. M., Megat Johari, M. A., Tayeh, B. A., & Yusuf, M. O. (2017). Pozzolanic reactivity of ultrafine palm oil fuel ash waste on strength and durability performances of high strength concrete. *Journal of Cleaner Production*, *144*, 511–522. https://doi.org/10.1016/j.jclepro.2016.12.121

Zhang, K., Xiao, J., Zhao, Y., & Zhang, Q. (2019). Analytical model for critical corrosion level of reinforcements to cause the cracking of concrete cover. *Construction and Building Materials*, *223*, 185–197. https://doi.org/10.1016/j.conbuildmat.2019.06.210

Zhang, Q., Luan, C., Yu, C., Huang, Y., & Zhou, Z. (2022). Mechanisms of carbon black in multifunctional cement matrix: Hydration and microstructure perspectives. *Construction and Building Materials*, *346*, 128455. https://doi.org/10.1016/j.conbuildmat.2022.128455

الخلاصة

تواجه المنشآت الخرسانية المسلحة في البيئات البحرية تحديات بيئية شديدة نتيجة التعرض المستمر لأيونات الكلوريد والكبريتات الموجودة في مياه البحر، مما يساهم في تدهور الخرسانة وتسريع تآكل حديد التسليح، الأمر الذي يؤدي إلى تقليص عمر الخدمة وزيادة تكاليف الصيانة. ولمعالجة هذه المشكلة، توجّهت الأبحاث نحو تطوير خلطات خرسانية مستدامة باستخدام مواد مضافة دقيقة مثل المساحيق المعدنية والمواد البوزولانية، لما لها من دور في تحسين الكثافة وتقليل النفاذية ومقاومة التفاعلات الكيميائية الضارة.

يهدف هذا البحث إلى تقييم أداء الأعمدة الخرسانية المسلحة المصنّعة من خلطات تحتوي على مواد ثانوية بديلة جزئيًا عن الأسمنت، مثل مسحوق الزجاج، مسحوق السيراميك، ومسحوق المرمر ومواد مضافة للأسمنت مثل مسحوق الكربون الأسود، مسحوق الجرافيت.

وقد تم دمج هذه المواد في الخلطات الخرسانية إما كمضافات، تحديدًا مسحوق الكربون الأسود ومسحوق الجرافيت بنسبة ٠,٥٪، ١٪، و١,٥٪ من وزن الأسمنت، أو كبدائل جزئية عن الأسمنت مثل مساحيق الزجاج، السيراميك، والمرمر بنسب استبدال ٥٪، ١٠٪، و١٥٪. تم في هذه الدراسة فحص ١٦ خلطة خرسانية، تضمنت خمسة أنواع من المساحيق البديلة للأسمنت، كل منها اختُبر بثلاث نسب استبدال أو إضافة، بالإضافة إلى خلطة مرجعية بدون أي مواد مضافة.

خضعت النماذج المفحوصة إلى برنامج تجريبي شامل شمل تقييمات ميكانيكية وإنشائية وديمومية. شملت الاختبارات الميكانيكية مقاومة الانضغاط، مقاومة الشد بالانشطار، والكثافة. وتم تقييم السلوك الإنشائي من خلال سعة الحمل الأقصى، والليونة، ومؤشرات المتانة. أما التقييم الديمومي فقد تضمّن اختبار اختراق أيونات الكلوريد، ونفاذية الماء تحت الضغط، وقياس جهد نصف الخلية لتحديد احتمالية تآكل حديد التسليح. أُجريت الفحوصات الإنشائية على مجموعتين من النماذج: الأولى لم تتعرض للتآكل، بينما خضعت الثانية لتآكل مسرّع باستخدام تيار كهربائي.

أظهرت الخلطات المحسّنة باستخدام المساحيق الدقيقة تحسنًا ملحوظًا في القدرة الإنشائية للأعمدة الخرسانية. وسجلت الخلطة التي تحتوي على ١٥٪ من مسحوق السيراميك أعلى زيادة في الحمل الأقصى بنسبة ١٩,١٦٪ مقارنة بالخلطة المرجعية، تلتها خلطة مسحوق الزجاج بنسبة ١٠٪ بزيادة ١٧,٦٩٪، ثم مسحوق الجرافيت ٠,٥٪ بنسبة ١١,٦٩٪، ومسحوق المرمر ١٠٪ بنسبة ١١,٣٦٪، وأخيرًا مسحوق الكربون الأسود ٠,٥٪ بنسبة ٨,٩٣٪. وتعكس هذه النتائج التأثير الإيجابي للمساحيق المضافة في تعزيز مقاومة الحمل المحوري وتحسين التماسك الداخلي للخرسانة.

تحت ظروف التآكل المسرّع، أظهرت عدة خلطات محسّنة انخفاضًا أقل في الحمل الأقصى مقارنة بالخلطة المرجعية التي فقدت ١٩,٦٪ من سعتها الإنشائية. وحققت خلطة مسحوق الجرافيت ٠,٥٪ أفضل أداء من حيث الديمومة، حيث بلغ الانخفاض في سعة التحمل ٣,٦٪ فقط، تلتها خلطة مسحوق الكربون الأسود ٠,٥٪ بنسبة ٣,٧٣٪، ثم مسحوق المرمر ١٠٪ بنسبة ١٢,٣٩٪، ومسحوق الزجاج ١٠٪ بنسبة ١٦,٦٩٪، وأخيرًا مسحوق السيراميك ١٥٪ بنسبة ١٨,٦٤٪. وتبرز هذه النتائج فعالية بعض المساحيق، خصوصًا الجرافيت والكربون الأسود، في الحد من تأثيرات التآكل السلبية على السلوك الإنشائي.

كما أظهرت عدة خلطات محسّنة انخفاضًا في نفاذية الماء تحت الضغط مقارنة بالخلطة المرجعية، مما يدل على مقاومة أفضل لاختراق السوائل والملوثات. وسجلت خلطة مسحوق الزجاج ١٠٪ أعلى انخفاض بنسبة ٧٦,٩٢٪، تلتها خلطة السيراميك ١٥٪ بنسبة ٦٨,٤٦٪، ومسحوق الجرافيت ٠,٥٪ بنسبة ٣٣٪، ومسحوق المرمر ١٠٪ بنسبة ٣١,٥٤٪، وأخيرًا مسحوق الكربون الأسود ٠,٥٪ بنسبة ٢٤,٦٢٪. ويُعزى هذا التحسن إلى الدورين الفيزيائي والكيميائي للمساحيق في تقليل المسامية وتحسين ترابط الجزيئات.

وبشأن مقاومة اختراق أيونات الكلوريد، فقد تفوقت جميع الخلطات على الخلطة المرجعية، مما يعكس تأثيرًا إيجابيًا على مقاومة التآكل. وحققت خلطة مسحوق الجرافيت ٠,٥٪ أعلى تقليل في اختراق الكلوريد بنسبة ٧٦,٢٧٪، تلتها خلطة الكربون الأسود ٠,٥٪ بنسبة ٤٥,٧٦٪، ومسحوق السيراميك ١٥٪ بنسبة ٣٤,٥٨٪، ومسحوق المرمر ١٠٪ بنسبة ٣٣,٠٥٪، وأخيرًا مسحوق الزجاج ١٠٪ بنسبة ٣٠,٥١٪. وتدل هذه النتائج على أن المساحيق، وخصوصًا مسحوق الجرافيت، تُحسن من حماية حديد التسليح في البيئات الغنية بالكلوريد.

إن عدم عرض باقي الخلطات لا يعني أنها أظهرت أداءً ضعيفًا، بل إن الخلطات المعروضة قد أظهرت تحسنًا في جميع الفحوصات، على عكس بعض الخلطات الأخرى التي سجلت انخفاضًا طفيفًا أو تحسنًا هامشيًا في بعض الجوانب.

يوصي البحث باختيار نسب الإضافة بدقة وبشكل مدروس استنادًا إلى الخصائص الفيزيائية والكيميائية للمواد، مع تجنب الإفراط في استخدام المواد ذات التوصيلية العالية حتى يتم ضمان توزيعها المتجانس. كما يؤكد على أهمية إجراء تقييم شامل للخصائص الميكانيكية والإنشائية عند تصميم خلطات خرسانية مخصصة للبيئات القاسية لضمان استدامة الأداء على المدى الطويل.

جمهورية العراق

وزارة التعليم العالي و البحث العلمي

جامعة كربلاء

كلية الهندسة

قسم الهندسة المدنية

خصائص الأعمدة الدائرية الخرسانية المسلحة المستدامة المعرضة لمياه البحر

اطروحة مقدمة الى مجلس كلية الهندسة / جامعة كربلاء وهي جزء من متطلبات نيل درجة الدكتوراه في علوم الهندسة المدنية

كتبت بواسطة:

عبدالرسول ثامر عبدالرسول قنديل

باشراف :

أ.د. ليث شاكر رشيد القرعاوي

أ.م.د. ايمن جميل كاظم السعد

محرّم - ١٤٤٧ تموز - ٢٠٢٥